The Metabolomics of Chronic Stress

by

Constance Ananta Sobsey
BA, University of Alberta, 2007

A Thesis Submitted in Partial Fulfillment
of the Requirements for the Degree of

MASTER OF SCIENCE

in the Department of Biochemistry & Microbiology

Supervisory Committee

The Metabolomics of Chronic Stress

by

Constance Ananta Sobsey
BA, University of Alberta, 2007

Supervisory Committee

Dr. Christoph Borchers, Department of Biochemistry & Microbiology
Supervisor

Dr. Caren Helbing, Department of Biochemistry & Microbiology
Departmental Member

Dr. Scott McIndoe, Department of Chemistry
Outside Member

Abstract

Supervisory Committee
Dr. Christoph Borchers, Department of Biochemistry & Microbiology
Supervisor
Dr. Caren Helbing, Department of Biochemistry & Microbiology
Departmental Member
Dr. Scott McIndoe, Department of Chemistry
Outside Member

The World Health Organization has called stress-related illness *"the* health epidemic of the 21st century." While the biochemical pathways associated with the acute stress response are well-characterized, many of the pathways behave differently under conditions of chronic stress. The purpose of this project is to apply high-sensitivity mass spectrometry (MS)-based targeted and untargeted metabolomics approaches to generate new insights into the biochemical processes and pathways associated with the chronic stress response, and potential mechanisms by which chronic stress produces adverse health effects.

Chapter 1 describes the application of sets of targeted and untargeted metabolomics approaches to analyze serum samples from a human epigenetic model of chronic stress in order to identify potential targets for further analysis. To test the resulting hypothesis that oxidative stress is a key feature of chronic stress, a new targeted multiple reaction monitoring (MRM)-MS assay was developed for the accurate quantitation of aldehyde products of lipid peroxidation, as described in Chapter 2. In Chapter 3, the validated method for quantitation of malondialdehyde (MDA) was t applied to mouse plasma samples from a model of chronic social defeat stress to determine whether animals exposed to psychosocial stress show increases in oxidative stress. Mouse plasma samples from this model were also analyzed by untargeted metabolomics using Fourier-transform (FT)-MS to identify other important metabolite features, particularly those that overlap with metabolites identified in the human epigenetic model.

Analysis of metabolomic data from two very different models of chronic stress supports the consistent detection of a metabolomic phenotype for chronic stress that is characterized by the dysregulation of energy metabolism associated with decreased concentrations of diacyl-phospholipids in blood. Increased blood concentrations of fatty acids, carnitines, acylcarnitines, and ether phospholipids were also observed. In addition to metabolites associated with energy metabolism, chronic stress also significantly influenced metabolites associated with amino acid metabolism and cell death. This characteristic pattern of differences in metabolite concentrations was observed in the plasma of mice exposed to chronic social defeat stress, irrespective of whether or not they displayed outward signs of a chronic stress response; In fact, mice that were "resilient" to the behavioural effects of chronic social defeat stress displayed an exaggerated phenotype over mice that showed depressive-like symptoms following chronic stress exposure. This may suggest that the observed changes in fatty acid composition are protective against stress. However, changes in fatty acid composition are also known to be associated with a wide variety of pathologies including heart disease, neurodegenerative diseases, and mood disorders, so the lipidomic changes associated with chronic stress may also contribute to its health impact. Overall, the results provide further evidence that changes in energy metabolism are a central part of allostatic adaptation to chronic stress.

Table of Contents

Supervisory Committee ii
Abstract iii
Table of Contents v
List of Abbreviations vii
List of Tables i
List of Figures ii
Acknowledgments iii
Dedication iv

Introduction 1
Why study chronic stress? 1
Global health impacts of chronic stress 1
The unique physiology of chronic stress 2
Challenges in studying chronic stress 6
Project Purpose 7
Metabolomics for studying chronic stress 8
Background on metabolomics 8
Metabolomics technologies 9
Application of metabolomics in the study of chronic stress 13
Published models and markers of chronic stress 16
Models employing psychosocial stressors 16
Animal models of chronic stress 17
Human models of chronic stress 20
Published markers of chronic stress 20
Limitations of previous studies 24
Hypothesis, Objectives & Approach 24

Chapter 1: Metabolomics of Chronic Stress in a Human Epigenetic Model 26
Chapter Summary 26
Introduction 27
An epigenetic model of chronic stress 27
Materials & Methods 29
Human plasma samples & sample metadata 29
Standards & Reagents 31
Methods for targeted metabolomics 31
Methods for untargeted metabolomics 34
Results 37
Analysis of sample metadata & grouping based on epigenetic model 37
Targeted metabolomics results 40
Results of untargeted metabolomics analysis 47
Discussion 49
Phosphatidylcholines and other phospholipids in chronic stress 49
Important caveats 53
Next steps 55

Chapter 2: Development of Methods to Analyze Aldehyde Markers of Oxidative Stress as a Potential Feature of Chronic Stress 56
Chapter Summary 56
Introduction 57
Oxidative stress as a potential feature of chronic stress 57
Methods for quantifying oxidative stress 58
Materials & Methods 60
Standards & Reagents 60
Human plasma samples 62
Testing of Chemical Derivatization Reagents 62
Mass spectrometry for screening of derivatization products 64
Optimization of Chemical Derivatization of MDA with 3NPH 65
Mass spectrometry (LC/MRM-MS) 66
Preparation of human plasma samples for MDA quantitation 67
3NPH-MDA Assay Performance Testing 68
Quantitation of MDA with 2,4-DNPH Derivatization - LC-UV 69
Results 69
Assay Development 69
Assay performance 77
Quantitation of MDA in human plasma samples 79
Application of MDA quantitation to a clinical study of MDD-s 80
Discussion 82

Chapter 3: Assessment of Mouse Plasma MDA and Lipid Profiles in a Model of Chronic Social Defeat Stress 85
Chapter Summary 85
Introduction 86
Mouse model of chronic social defeat stress 86
Materials & Methods 88
Targeted quantitation of MDA 89
Untargeted lipid profiling using UPLC-FT-MS 90
Results 93
MDA analysis 93
Lipid Profiling 94
Discussion 103

Conclusions & Outlook 106
Major outcomes 106
Metabolomics-derived insights into chronic stress 108
Direct extensions 109
Additional directions in chronic stress research 109

Bibliography 111
Appendix I 128

List of Abbreviations

ACTH - Adrenocorticotropic Hormone
ANOVA – Analysis Of Variance
BMI – Body Mass Index
CE-MS – Capillary Electrophoresis-MS
CID – Collision-Induced Dissociation
CRH - Corticotropin-Releasing Hormone
CRP – C-Reactive Protein
CSF – Cerebrospinal Fluid
CUMS – Chronic Unpredictable Mild Stressors model
CV – Coefficient Of Variation
CVD – Cardiovascular Disease
DI-MS – Direct Injection-MS
ELSD – Evaporative Light Scattering Detector
ESI – Electrospray Ionization
FC – Fold Change
FD – Fluorescence Detection
FDR – False Discovery Rate
FIA – Flow Injection Analysis
FT-MS – Fourier Transform -MS
GC-MS – Gas Chromatography - MS
GR - Glucocorticoid Receptor
HCD – High-Energy Collision Dissociation
HDL – High Density Lipoprotein
HILIC - Hydrophilic Interaction Liquid Chromatography
HMDB – the Human Metabolome Database
HPA – Hypothalamic-Pituitary-Adrenal axis
HPLC – High Pressure Liquid Chromatography
IPV – Inter-Partner Violence
IS – Internal Standard
LC - Liquid Chromatography
LDL – Low Density Lipoprotein
LLOD – Lower Limit Of Detection
LLOQ – Lower Limit Of Quantitation
m/z – mass-to-charge ratio
MDA – Malondialdhyde
MDD-s – Major Depressive Disorder with seasonal-type pattern
MRM – Multiple Reaction Monitoring
MS – Mass Spectrometry (*also used in place of mass spectrometer*)
MS/MS – Tandem MS
NMR – Nuclear Magnetic Resonance
PA – Phosphatidic Acid
PC - Phosphatidylcholine
PC1, PC2, PC3 – Principle Components
PCA – Principal Components Analysis
PE - Phosphatidylethanolamine
PI - Phosphatidylinositol
PLS-DA – Partial Least Squares Discriminant Analysis
PS - Phosphatidylserine
PTSD – Post-Traumatic Stress Disorder
Q1 / Q3 –Quadruople 1 / Quadrupole 3
QC – Quality Control
QTOF – Quadrupole Time-of-Flight
ROS – Reactive Oxygen Species
RPLC – Reversed Phase Liquid Chromatography
SD – Standard Deviation
SM - Sphingomyelin
HODE - Hydroxyoctadecadienoic acid
HHE – 4-Hydroxyhexenal
HNE – 4-Hydroxynonenal
SMPDB – Small Molecule Pathway Database
SPE – Solid Phase Extraction
TBARS – Thiobarbituric Acid Reactive Substances
TIC – Total Ion Chromatogram
ULOQ – Upper Limit Of Quantitation
UPLC – Ultrahigh Pressure Liquid Chromatography
UV – Ultraviolet
VIP - Variable Importance in Projection score
XIC – Extracted Ion Chromatogram

Abbreviations of chemical reagent names:

ACN - Acetonitrile
AEC – 3-Amino-9-Ethylcarbazole
DH – Dansyl Hydrazine
DNPH – 2,4-Dinitrophenylhydrazine
EDC - N-(3-Dimethylaminopropyl)-N′-Ethylcarbodiimide Hydrochloride
FA – Formic Acid
GRP - Girard's Reagent P
GRT - Girard's Reagent T
ISP - Isopropanol
MeOH – Methanol
NaOH – Sodium Hydroxide
NPH – Nitrophenylhydrazine
PBS – Phosphate-Buffered Saline
PITC – Phenylisothiocyanate
PSC - 4-Phenylsemicarbazide Hydrochloride
TBA - Thiobarbituric Acid
TCA – Trichloroacetic Acid
TFA – Trifluoroacetic Acid

List of Tables

Table 1. Published metabolomics biomarkers of chronic stress in human models 22
Table 2. Published metabolomics biomarkers of chronic stress in murine models 23
Table 3. Methylation sites spanning the GR gene associated with early life stress 38
Table 4. Significant features identified by Untargeted metabolomics analysis 47
Table 5. Putative Metabolite IDs.....48
Table 6. Reaction conditions used in screening derivatizing reagents 63
Table 7. MRM-MS transitions for aldehyde derivatives 72
Table 8. Intra- and inter-run CVs for Quantitation of 3NPH-MDA.....78
Table 9. Comparison of two methods for quantifying MDA in human plasma. 80
Table 10. Summary of features identified in UPLC-FTMS and UPLC-MS/MS lipid profiling of mouse plasma 98
Table 11. List of metabolite IDs obtained from lipidomic profiling of mouse plasma 98

List of Figures

Figure 1. Simplified schematic of the HPA axis in the acute stress response 3
Figure 2. Schematic of a multiple reaction monitoring (MRM) approach 12
Figure 3. Metabolite profiles observed in acute versus chronic stress 19
Figure 4. Overview of an epigenetic model of chronic stress 29
Figure 5. Workflow for untargeted metabolomics 34
Figure 6. Summary of grouping based on methylation percentages. 39
Figure 7. Data normalization with Metaboanalyst 41
Figure 8. Volcano plot of features with t-test p-value <0.01 and FC >1.5 for high and low methylation groups. 42
Figure 9. PCA and PLSDA plots of separation between the high and low methylation groups, with 15 most important Variables in Projection (VIP). 43
Figure 10. Pearson correlation analysis of compounds associated with a non-continuous measure of average methylation at promoter-associated sites. 44
Figure 11. Comparison of metabolite concentrations between low, medium, and high methylation groups. 45
Figure 12. PLS-DA of low, medium, and high methylation groups and important variables for separation. 46
Figure 13. Boxplots and extracted ion chromatogram for PC 32:1 49
Figure 14. Generic structure of a phosphatidylcholine 49
Figure 15. Proportion of total PC abundance accounted for by different subspecies. 51
Figure 16. Markers of oxidative stress. 58
Figure 17. Derivatization reaction of 3NPH with various aldehydes. 71
Figure 18. Effect of reaction conditions on the 3NPH derivatization of MDA 74
Figure 19. Comparison of sample preparation protocols and signal intensities for free vs. total MDA in human plasma 75
Figure 20. LC/MRM-MS chromatogram acquired from a pooled human plasma 76
Figure 21. Linearity of 3NPH-MDA in plasma and buffer. 78
Figure 22. Comparison of total plasma MDA concentrations for patients with low-normal BMI verus high BMI at the fall and winter timepoints. 81
Figure 23. Total plasma MDA concentration in mice subjected to chronic social defeat stress. 93
Figure 24. Example of stacked total ion chromatograms and corresponding PCA plots before and after outlier removal. 94
Figure 25. MS/MS spectra of putative phosphatidylcholine with fragments commonly observed for PCs 96
Figure 26. PLS-DA of MS peak intensities for control versus stressed mice 97

Acknowledgments

This research was made possible through Genome Canada and Genome BC funding for the Metabolomics Innovation Centre (TMIC). I also gratefully acknowledge scholarship support from the Leading Edge Endowment Fund (LEEF) Don and Eleanor Rix B.C. Leadership Chair in Biomedical and Environmental Proteomics and from the Faculty of Graduate Studies at the University of Victoria.

Thank you to my graduate supervisor, Dr. Christoph Borchers, for his support to complete this project, for his ongoing encouragement, and most of all for providing the impetus to undertake a graduate program in Biochemistry. I also wish to thank my committee members, Dr. Caren Helbing and Dr. J. Scott McIndoe, for their engagement, insightful suggestions, and active participation in committee meetings. Thanks to Dr. Carol Parker for her meticulous review of my thesis and valuable editorial suggestions.

I thank my collaborators without whom this work would not have been possible: Dr. David Wishart for providing laboratory access and supplies to run Biocrates analysis, as well as project advice, especially in the early stages of the project; Dr. Rupasri Mandal for providing assistance with analysis of Biocrates data; Drs. Thomas Elbert, Clemens Kirschbaum, and Karl Radtke for providing access to samples, sample metadata, biochemical data in relation to a human epigenetic model of chronic stress; Drs. Walter Swardfager and Anthony Levitt for providing patient samples and metadata for the proof-of-principle project to quantify malondialdehyde in human plasma; and Dr. Michael Meaney for providing plasma samples from a mouse model of chronic social defeat stress.

Finally, I am extremely thankful to Dr. Jun Han for all of his contributions to this project and to my graduate education. I offer my unending thanks to Jun for introducing me to the techniques and equipment required for this work, for his assistance with experimental design and tireless aid with troubleshooting, for sharing his astonishingly vast expertise and knowledge with me and with all of the trainees in our lab, for his boundless enthusiasm for research, and for ultimately investing so much time and energy to provide me with guidance and training of the highest quality, which was absolutely essential for completing this work.

Dedication

I dedicate my thesis to Dr. Dick Sobsey. Thank you for endowing me with your earnest curiosity, your genuine love of learning, and your endless desire to contemplate the world around us, including those things at the very edge of our understanding. You were the first person to set me to work on a research project and you were the first person to introduce me to many of the interesting concepts that would eventually become the foundation for this project. I am grateful for your wisdom, and more importantly, for your friendship. I'm so lucky that you are my dad.

I also dedicate this work to Dr. David Wishart. The mentorship, training, advice, and opportunities you have offered me over the past 9 years continue to be absolutely invaluable. I am endlessly thankful for your influence on my professional development, your encouragement, and for the skills and expertise I was able to cultivate in your lab. I am inspired by your outstanding example of scientific leadership and professional excellence, your efforts to communicate complex material in a way that is accessible to a wide audience, your focus on building publically-available resources to foster research across the whole community, and your genuine kindness.

I also extend my thanks and appreciation to my colleagues at the Proteomics Centre, my supports in the department – especially Melinda Powell and Dr. Steve Evans, and my family and friends near and far -- especially Alisha Brown, Tamara Lim, Nicole Sessler, Andre Leblanc. Thank you for helping me get through the past few years of graduate school in more or less one piece.

Introduction

Why study chronic stress?

Global health impacts of chronic stress

Chronic stress is an extremely widespread problem that results from the adverse events or simply the pressure of daily life. It affects people around the world and across many segments of society. While stress is not a disease in itself, it does affect our health in very significant ways. In fact, the World Health Organization recently called stress-related illness *"the* health epidemic of the 21st century." In terms of global health, chronic stress may be one of the most overlooked causes of health disparities in socioeconomically disadvantaged portions of the population [1], and some studies have suggested that chronic stress may be responsible for a significant portion of harmful health outcomes associated with low socioeconomic status [2]. The American Psychological Society (2012) has found that approximately >30% of all days of work absence can be attributed to consequences of stress exposure with an estimated economic impact of $300 billion per year in the USA.

The health impacts of chronic stress are serious and highly multi-dimensional. Unsurprisingly, chronic stress contributes to a variety of psychological health risks including mood disorders (clinical anxiety, depression, bipolar depression), sleep disturbances, addictions risk, cognitive impairment, memory loss, and fatigue [3-11] However, it is also associated with increased risk for numerous other health conditions including neurological risks (neurodegeneration, loss of hippocampal volume), cardiovascular disease (hypertension, coronary heart disease), metabolic syndrome and weight gain, diabetes risk, gastrointestinal problems (stomach, gut & bowel problems), reproductive and fertility issues, increased pain, immune dysfunction (inflammation, cytokine circulation, musculoskeletal disorders, impaired immune response, poor immune memory), and premature aging, including even telomere shortening in cells [5, 12-23]. In fact, several studies have found that high levels of chronic stress are

associated with increased 1-year, 2.5-year and 5-year risk of mortality, and stress reduction is associated with lower all-cause mortality risk [11, 24].

Through modern medicine, we have developed many new ways of preventing and treating many of the acute infections, diseases, injuries, deficiencies and toxicities that for a long time were responsible for a large proportion of deaths. However, as people live overall longer lives, we are increasingly burdened by the impact of serious long-term health conditions. In fact, it is now true that the most serious and common risks to our healthy aging are heart disease and stroke [25]; both risks are exacerbated by stress and stress is associated with poorer outcomes [26, 27]. For many of the conditions associated with chronic stress, the mechanism by which stress exerts an influence on disease risk or progression is not well understood. The slow progression and "chronic" nature of these health issues may make the insidious influence of chronic stress harder to assess. However, the extended course over which chronic stress exerts an influence also means that there is a significant opportunity to intervene before serious health effects arise.

The unique physiology of chronic stress

The physiology of chronic stress is distinct from that of acute stress. The acute stress response has been very well characterized, starting with the work of Dr. János Hugo Bruno "Hans" Selye in the 1930s [28]. Dr. Seyle was the first to coin the term "stress" and describe the role of the hypothalamic pituitary adrenal (HPA) axis in the stress response.

HPA activity in the acute stress response: The acute stress response revolves around the activity of the hypothalamic pituitary adrenal (HPA) axis, which mediates the response to stressors through a cascade of hormones, as shown in Figure 1 [29].

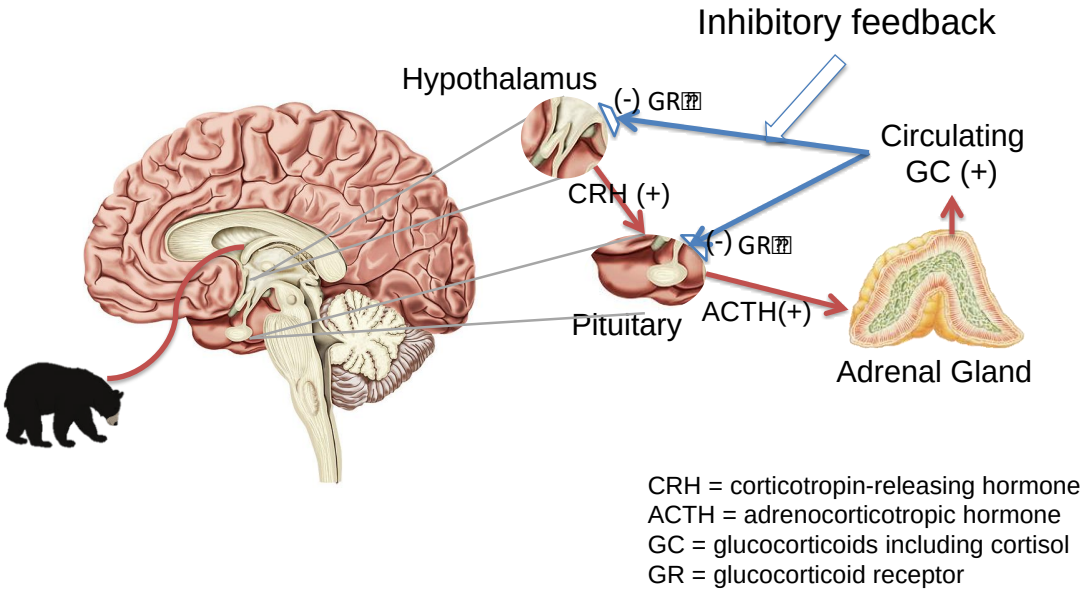

Figure 1. Simplified schematic of the HPA axis in the acute stress response.

When a life-threatening threat is detected in the environment, efferent visceral pathways relay information from the sensory system to specific mid-brain structures, including the amygdala, hippocampus, and septum [30]. This system offers a rapid response, since the midbrain structures receive information directly from the sensory channels, prior to interpretation by the pre-frontal cortex. The midbrain then signals the hypothalamus to initiate the stress response by secreting corticotropin-releasing hormone (CRH) onto the anterior pituitary gland, where it binds to CRH receptors, causing the pituitary to release adrenocorticotropic hormone (ACTH) into the bloodstream. ACTH in turn enters the adrenal glands, causing them to secrete glucocorticoids, such cortisol and other glucocorticoids. During the acute stress response, salivary cortisol concentrations may increase by 2- to 4-fold its baseline levels [31]. These circulating glucocorticoids bind to glucocorticoid receptors (GR), which are present in almost every cell in vertebrate animals, and act on peripheral target tissues and glands to create the physiological responses associated with the sympathetic nervous system. At the same time, excess circulating glucocorticoids bind to GR located in the hypothalamus and pituitary gland. Binding at GR in the hypothalamus and pituitary suppresses the production of CRH and ACTH, providing a negative feedback mechanism to automatically dampen the stress response once the necessary responses have been initiated.

The action of this large-scale signaling is complex and involves many hormones, genes, receptors, and transmitters that have specific effects on various organs and tissues throughout the body. This dramatic, and largely non-specific, response is geared for survival: it prepares each system for a flight-or-fight response, for example by increasing heart rate, liberating glucose into the blood stream, and sending blood to the extremities to enable rapid flight from threats, by constricting arteries to reduce potential blood loss, and by halting digestion so that energy can be redirected to more urgent processes [32]. It also primes the brain by enhancing mental acuity, suppressing pain signals, and facilitating learning [33, 34], as cognitive performance may prove invaluable for ensuring current and future survival. In this sense, a degree of stress is healthy and is important for optimal functioning [35]. However, the stress response system is ultimately intended as a short-term solution to a short-term problem. Under normal circumstances, the dampening effects of negative feedback from GR help to protect against over-activation of the stress response and the potential adverse effects of persistently high cortisol concentrations, such as loss of hippocampal volume and depression of the HPA axis [36, 37]. Regulation of this response is importance since when the acute stress response is excessively activated, the response is no longer functional.

HPA dysregulation in the chronic stress response: Given the role of the HPA in mediating the acute stress response, this system has been the focus of much of the research conducted into chronic stress. In acute stress, activation of the HPA axis results in peaks in cortisol, adrenocorticotropic hormone, and glucocorticoid levels. If the acute stress response were to be activated excessively, this could result in long-term exposure to high levels of these stress hormones, which is known to have harmful effects. It may therefore be tempting to attribute many of the health impacts of chronic stress to the cumulative downstream effects of an exaggerated or extended acute stress response. However, a growing body of evidence suggests that the physiology of chronic stress does not resemble acute stress and is not a consequence of long-term activation of the HPA. In fact, the relationship between chronic stress and HPA activity is currently unclear and the literature in this area is fraught with conflicting evidence.

Some studies show persistent increases in HPA activity in stress disorders and long-term stress [38]. Depression has also been associated with hypercortisolism even though its symptoms are more associated with low mood state and fatigue than with the acute experience of stress [38]. However, a significant body of data now shows that many stress-associated conditions, including anxiety disorder, post-traumatic stress disorder (PTSD), recurrent traumatization, and 'burnout', have also been associated with depressed cortisol levels despite the fact that their characteristic feature is an excess of perceived stress [39-41]. In chronic fatigue, cortisol levels are depressed, and show decreases and pattern changes months in advance of the onset of symptoms [42].

At first glance, the lowered baseline cortisol levels observed in some chronically stressed individuals might be superficially dismissed as physical habituation to stressors. This is perhaps implied by the observation that exposure to prior adversity may be associated with decreased cortisol response to traumatic events [43]. However, habituation (i.e., a diminished stress response to a repeated stimuli) is not an adequate explanation, as the same study found that individuals with prior interpersonal trauma showed higher ongoing psychological distress. In PTSD, decreases in baseline cortisol levels not only correlate with increasing severity of symptoms, but also predict symptom increases in response to new traumatic events [44]. Even when cortisol levels are depressed, both the psychological and physical symptoms of stress (e.g., increased heart rate) are still present [40].

The response of the HPA and glucocorticoid levels can vary widely in response to chronic stress: In some cases, depressed baseline cortisol in chronic stress may be accompanied by sensitization of the HPA axis causing exaggerated responses to acute stress [45]. In other cases, increases in baseline cortisol are associated with a flattening of the acute stress response [46]. The typical diurnal rhythms of circulating glucocorticoid concentrations may also be disrupted or suppressed [47]. Overall, a multitude of studies suggest a complex relationship between chronic stress and cortisol. It appears that chronic stress *dysregulates* the HPA as opposed to simply over-activating or suppressing it.

Challenges in studying chronic stress

While the body's response to acute stress is reasonably well characterized, research into the physiology of chronic stress is limited, in part because of challenges in the development or establishment of meaningful models. In many ways, chronic stress is a fundamentally human problem, but ethical issues prohibit imposing chronic stress on human participants, which limits opportunities for controlled experiments. As a result, the majority of human studies of chronic stress depend on estimating participants' prior/ongoing stress exposure. Accurately assessing the degree of stress experienced is paramount, since stress is not a binary condition *in vivo*; there is a spectrum of very little stress to very high stress, but there are no "stressed" versus "unstressed" conditions. This is not a simple task, however, as stress can be imposed by a wide variety of stimuli. Furthermore, stress is subjective and the product of opaque internal processes, which are influenced by many psychosocial factors (e.g., individual personality traits, social support) as well as biology (e.g., biological traits, illness), so even when the stressor can be measured, the stress experienced by individuals is subjective and highly variable [48-50]. This leads many chronic stress studies to depend on participants' self-reporting of their perceived stress exposure and intensity of stress experienced, but it is well known in the field of psychology that self-reports of symptoms may result in poor quality data due to frequent participant bias even when performed with well-validated psychological tools [51-53]. Clinical symptoms associated with chronic stress may help to identify chronically stressed individuals [54]. However, this approach is most useful for facilitating studies where significant health impacts have already occurred. The clinical presentation of stress-associated diseases may make it hard to distinguish the physiology specifically associated with chronic stress from that associated with its health impacts.

Animal models of chronic stress offer some advantages, such as the ability to systematically impose stressors, environmental control, and less biological variability, all of which make them more robust than human models. Furthermore, it is generally deemed unnecessary to try to account for psychological factors in most commonly-used animal models: the scientific imperative to avoid speculating on the mental processes of non-human experimental subjects (i.e., Skinner's black box) simplifies research questions

and the interpretation of results [55]. However, animal models of psychological conditions have their own set of drawbacks. In particular, it can be difficult to interpret whether signs and symptoms of stress in animals are fully analogous to those in humans. Much effort has been put into validating whether or not measurements of animals' behaviour or biology bear appropriate similarity to the signs and symptoms of psychological disorders in humans [56-58], but psychological conditions in humans are generally rife with subtleties that may or may not be captured in an animal model. Animal models are also generally optimized to generate the most dramatic behavioural or physical responses, which might only reflect the most severe presentations of a human disorder and not the most common ones. Equally importantly, even if an animal model can be considered meaningful and representative, humans' last common ancestor with mice occurred 100 million years ago, so biological findings in any these models often have only modest applicability to human health or fail to translate altogether [59, 60].

Project Purpose

The purpose of this project is to generate new insights into the biochemical processes and pathways associated with the chronic stress response, beyond the direct activity of the hard-to-study HPA. New insights into the chronic stress response will help develop a clearer picture of the physiological impacts of chronic stress and may help to elucidate the mechanisms by which chronic stress produces adverse health effects. A more developed characterization of the pathways affected by chronic stress could also support the identification of markers for the onset and progression of chronic stress that could be used in clinical monitoring to enable the more effective prediction, prevention, and/or treatment of disease associated with chronic stress. Moreover, a reliable biological measure to assess chronic stress could be used to reduce dependence on self-reports in humans and to provide additional validation measures for animal studies. New tools to objectively verify and quantify chronic stress independent of HPA activity would facilitate data analysis and interpretation, and would enable more meaningful comparisons between studies.

Metabolomics for studying chronic stress

Background on metabolomics

Metabolomics is the simultaneous study of a large number of metabolites in a given cell, tissue, or organism to gain insights into biological processes. It involves identifying and quantifying small molecules (usually <1500 Da) in complex biological samples. In humans, metabolites may include all sugars, nucelosides, organic acids, ketones, aldehydes, amines, amino acids, lipids, steroids, alkaloids, and even peptides that are present at a detectable concentration in biofluids or tissues (>1 pM). These chemicals may be endogenous in origin, or may be introduced from foods, pollutants, toxins, drugs, or microbes. Previous studies have quantified >4000 endogenous metabolites in the human serum metabolome [61], >400 in the human CSF metabolome [62] and >3000 in urine [63]. In contrast with a tightly-focused study of a single gene, protein, or metabolite, metabolomics looks at a wide range of targets to identify changes in certain compounds or pathways that are associated with a particular phenotype or condition.

Metabolomics presents a powerful tool for characterizing human health and disease status [64]. While genomics can be very useful for predicting disease risk, single nucleotide polymorphisms (SNPs) commonly account for a modest proportion (<10%) of phenotypic variability and relatively small increments in risk (<1.5 fold), except in a handful of inborn autosomal disorders [65, 66]. In many of these cases, metabolites are sensitive indicators of the presence of such a mutation: newborn screening tests identify genetic disorders (e.g., phenylketonuria) based on their dramatic effect on metabolites. A single change in nucleotide can lead to a 10,000-fold change in metabolite concentration [67].

On the other hand, since the genome stays relatively static over the course of an organism's lifetime, the genome does not generally reflect the influence of the environment. The epigenome, transcriptome, and proteome -- which vary over the course of hours to years -- all offer more up-to-date information about an organism's status that reflect the influence of both genes and the environment. Metabolites, however, can

respond even more rapidly to environmental changes, sometimes with dramatic changes in abundance.

In this sense, the metabolome provides a unique real-time picture of what is happening in the organism, body, or tissue that collectively represents the interplay of biology and the environment. For this reason, it has proven to be very effective for identifying high-sensitivity, high-specificity biomarker panels with extremely strong predictive or prognostic value (e.g., predicting diabetes 12 years before onset [68]), elucidating the mechanisms of disease pathology (e.g., identifying the combination of factors responsible for chronic inflammation leading to malnutrition in environmental enteropathy [69]), and informing the rational selection, design, and testing of treatment targets (e.g., by identifying metabolomic deficits in knock-out mice [70]) or potential interventions (e.g., choline supplementation to reduce risk of preeclampsia [71]).

Metabolomics technologies

A typical metabolomics workflow involves several steps. First, metabolites must be extracted from the biological samples to be analyzed. The extract can then be subjected to chemical analysis with specialized equipment (e.g., NMR, HPLC-UV, MS) that is intended to enable the rapid and simultaneous detection of a large number of analytes, from 10s to 1000s of compounds. Data from the chemical analysis is then analyzed to generate some type of metabolite measurement, either in the form of concentration values or relative quantities (as compared between two groups). The former approach – toward obtaining 'absolute' concentrations of specified metabolites – is often referred to as "targeted metabolomics", and the latter, as chemometric or 'untargeted metabolomics'

Targeted metabolomics with absolute quantitation has several advantages. Since assays are optimized for the accurate quantitation of the targeted compounds, the assay's performance characteristics (i.e., specificity, sensitivity, precision, linear range) are often better. Furthermore, because the data generated is made up of actual concentration values, it is possible to compare results within longitudinal studies and across independent studies. Reliable quantitation is therefore required for large clinical studies where the samples cannot all be run at one time in one experiment, or for clinical

implementation, which requires establishing reference ranges. However, a targeted approach does require prior knowledge in order to inform target selection, and optimizing one's analytical approach toward a small set of targeted analytes means that some important differences between groups may be missed. Targeted quantitative assays also require the use of standards (preferably internal standards) and rigorous validation prior to implementation in order to ensure reproducibility.

In contrast, the advantage of an untargeted approach is that it is possible to obtain a great deal of information even with limited prior knowledge of the systems involved. In an untargeted approach, samples from two (or more) groups can subjected to chemical analysis and compared to identify discriminating features. However, untargeted metabolomics studies are challenging to conduct because they require meticulous experimental design, generate a large amount of data, and are computationally intensive. They are also prone to errors associated with experimental bias, poor identification of analytes (low specificity), and statistical over-fitting due to the large number of variables, especially when group sizes are small. However, in many cases, untargeted or even broadly-targeted metabolomics studies are a useful first step for obtaining new information about the pathways involved in disease, and these findings may inform more carefully targeted follow-on studies.

A variety of platforms have been employed for metabolite analysis, primarily nuclear magnetic resonance (NMR) spectroscopy and mass spectrometry (MS). In the case of MS technologies, several different detection schemes have been developed: samples may be subject to direct infusion (DI), flow injection analysis (FIA), gas chromatography (GC), liquid chromatography (LC), capillary electrophoresis (CE) or combination approaches (e.g., reversed-phase LC x hydrophilic interaction liquid chromatography, GCxGC) prior to detection via MS or tandem MS (MS/MS). Additional methods using alternative combinations of separation and detection strategies have also been developed for specialized analysis of certain groups of compounds, e.g., HPLC with Evaporative Light Scattering Detector (ELSD) for lipidomics, HPLC with UV or Fluorescence Detection (FD) for analysis of aromatics and secondary metabolites found in plants and xenobiotics (e.g., polyphenols, flavonoids, etc.), and Inductively coupled plasma (ICP)-

MS for quantitation of metals. Each technique has its own merits and limitations in metabolite identification and quantification that determine its suitability for a specific application [61].

NMR analysis, for example, is highly accurate and does not require internal standards, but coverage is primarily limited to a maximum of about 50 water-soluble metabolites (e.g., amino acids, alcohols, amines, sugars, organic acids) that can be quantified. Limited sensitivity necessitates the use of larger sample volumes: the lowest concentrations that can reliably detected are in the 12-15 µM range and analysis typically requires 100 µL or more of serum. NMR analysis may also be slower than competing technologies: data acquisition times can range from 20-90 minutes per sample and extensive sample preparation is sometimes necessary to remove interfering salts from the sample. In the past, analysis of NMR data was also labour-intensive requiring hours of hands-on time by experts in order to identify and quantify metabolites, but new automated tools for NMR spectral analysis, such as Bayesil (www.bayesil.ca), have largely removed this bottleneck [72]. One of the enduring strengths of NMR is the reproducibility of spectral data. Acquired NMR spectra from untargeted experiments can be retained for decades and meaningfully compared to newly acquired spectra from similar instruments [73].

Mass spectrometry-based metabolomics: Different MS approaches also have specific strengths and weaknesses. GC-MS is compatible with quantitation of many volatile analytes that are difficult to quantify with other methods, but it sometimes requires higher sample volumes than LC- or DI-MS (30-50 µL versus 10-20 µL) and is typically less sensitive (<mM LODs as opposed to <nM). DI-MS can quantify a large number of hydrophobic metabolites (>180 in a single analysis) and is highly sensitive (LOD ~5 nM), but since it does not involve a front-end separation step, it can only be used with relatively simple biofluid samples such as serum and CSF.

LC-MS approaches the high sensitivity of DI-MS, but front-end separations enable the analysis of very complex samples and the targeting of a large number of metabolites with a variety of chemistries across a broad range of concentrations. This has made LC-MS,

particularly ultra-high performance liquid chromatography (UPLC) with high-resolution MS the most commonly-used analytical technique for untargeted metabolomic profiling of biological samples [74, 75]. The high resolution offered by modern MS instruments enables even co-eluting analytes in complex samples to be distinguished from one another on the basis of mass-to-charge ratios, while high accuracy m/z measurements facilitate identification of the compound [76]. However, the high sensitivity means that MS spectra are complex, and are highly affected by noise and trace contaminants. The detection of multiple isomers and adducts for each compound also makes data analysis more challenging. Moreover, much of the data acquired by untargeted LC-MS is currently not useful due to a lack of reference information needed to identify the associated compound; for many compounds, either no reference spectra has been acquired or the acquired spectra cannot be compared to the newly collected data. While the mass-to-charge ratio (m/z) used to identify a compound in MS may be highly accurate, the relative intensity of signals produced by metabolites in MS vary dramatically depending on instrument setup and ion suppression effects, so spectra cannot be easily compared between experiments. A targeted approach with high quality internal standards is required for positive compound identification by LC-MS and for accurate quantitation.

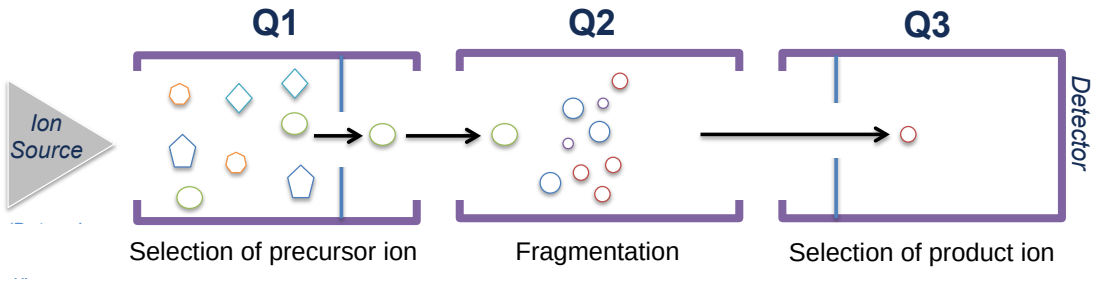

Figure 2. Schematic of a multiple reaction monitoring (MRM) approach using a triple quadrupole (QQQ) tandem mass spectrometer.

Multiple reaction monitoring (MRM) is an analytical approach that uses tandem mass spectrometry (MS/MS) to positively identify and quantify a target compound. MRM-MS is conducted on a triple-quadrupole mass spectrometer. As shown in Figure 2, the first

quadrupole selects for the precursor ion. Only those ions with an m/z ratio matching the target derivative are allowed to enter the second quadrupole, where the ions undergo collision with an inert gas and are fragmented into product ions. Each chemical species undergoes a unique pattern of breakages based on its specific bond strengths and produces a characteristic set of fragments. The fragments enter the third and final quadrupole, which scans through various m/z ranges and selects for those product ions with a m/z value matching the known signature for the target compound. This allows for the selective detection of fragments associated with specific precursor ions. MRM-MS approaches therefore offer exceptionally high specificity by confirming the identity of the measured ion based on the m/z of both the precursor and product ions, as well as the correct retention time. The use of ^{13}C or ^{15}N isotope-labeled internal standards enable accurate quantitation by MRM-MS, because the internal standard for a given compound will co-elute with, and can be simultaneously detected along with the endogenous metabolite. The peak intensity of the endogenous metabolite (unknown concentration) can then be compared to the peak intensity of the internal standard (fixed concentration), to achieve quantitation based on a standard curve for calibration.

The unparalleled specificity of the MRM-MS approach makes it compatible with high levels of multiplexing, so a large number of analytes can be targeted in a single analysis, particularly if scheduled MRM is used where precursor/product ion pairs are monitored in specific retention time windows. As a metabolomics method, MRM-MS with internal isotope-labeled standards is considered highly robust and reproducible [77]. Given the enormous physiochemical diversity of molecules in a biological matrix, multiple analytical methods -- each strategically targeting distinct classes/groups of metabolites – can be used in combination to investigate the full range of metabolites.

Application of metabolomics in the study of chronic stress

Metabolomics is well suited to elucidate the systemic changes associated with chronic stress. Because the systems underlying the stress response need to respond rapidly to threatening stimuli, and because metabolites can generate dramatic responses rapidly, the initial events associated with the acute stress response are primarily metabolite-based. At

the same time, the metabolome reflects not only the environment, but also the influence of genetic predispositions and protein or transcript levels, which change over a medium to long term. The ability to reflect these integrated influences makes metabolomics appropriate for studying a condition like stress response, which is highly multi-factorial and develops over a long time course.

The broad approach taken by metabolomics is also suitable for overcoming the research challenges associated with studies of chronic stress. In those cases where dysregulation of the HPA axis is a key aspect of the health implications of chronic stress, a broader metabolomics approach may help to improve our understanding of the system-wide effects of this shift. It could also help us find markers of HPA dysregulation that are easier to measure than changes in glucocorticoids, which require careful sampling. For example, cortisol can be challenging to measure reproducibly because it has a strong diurnal rhythm and is highly sensitive to diet [78]. In fact, for cortisol measurements to have any meaning, they must be taken at a consistent time of day and may require multiple daily measurements to determine an individual's cortisol secretion pattern [79]. Anxiety associated with the collection procedure can also influence single-point cortisol measurements: venepuncture produces an acute cortisol response in ≥30% of patients [80]. In fact, anticipation of a stressful task is sufficient to generate an acute stress response [81]. The large-scale changes in cortisol associated with diet, time of day, anxiety, and other confounding factors may obscure stress-associated variations [82], and may be partly to blame for the plethora of conflicting information about trends in cortisol secretion in stress disorders.

Alternative sampling approaches have been proposed to try to ameliorate and simplify studies involving quantitation of corticosteroids. Measurement of cortisol in saliva samples has been proposed as a less invasive alternative, but the accuracy of these measurements can be compromised by potential blood contamination due to oral injury or dental issues [83]. The measurement of corticosteroids from hair is considered a more robust approach for assessing cortisol secretion patterns. Measuring the cortisol 'banked' in hair effectively provides a measure of an individual's cortisol levels over a known period of time: it is therefore ideal for assessing variations associated with individual

traits, predispositions and variations associated with long-term influences. Hair cortisol measurements are not sensitive to high moment-to-moment variability in cortisol secretion, and studies have shown that are not influenced by time of day or acute stress response [84]. This method has therefore been successful in identifying changes that were obscured by an alternative approach such as saliva sampling [41]. Normalization strategies can be applied to compensate for 'wash-out' effects, but such effects are negligible in the 6 cm of hair closest to the head [85]. When performed by standard immunoassay or LC-MS, the results of cortisol quantitation are reproducible and both methods give generally comparable results [86, 87]. However, in spite of the availability of robust techniques, the evidence of an association between stressors/perceived stress and cortisol trends is inconsistent – BMI better predicts hair cortisol than psychosocial factors [88, 89]. Markers other than these corticosteroids, such as those potentially identified through a metabolomics approach, might have a stronger association with chronic stress.

Moreover, the broad approach offered by metabolomics provides an important opportunity for the study of chronic stress, where much of the existing literature has focused on the activity of the HPA axis to the exclusion of other targets, and where there is a limited body of research about other systems that are involved in the long-term response to chronic stress. In fact, the specific type of information generated by metabolomics directly corresponds to the purpose of my research, which is improving tools for chronic stress research. The identification of metabolites associated with the chronic stress offers promise for translation because some of these markers may provide useful supplementary information for assessing and monitoring chronic stress in research and clinical settings. Moreover, these markers may be useful for predicting those cases where chronic stress will generate significant health impacts. By better characterising the affected systems, these studies may also suggest avenues for prevention and/or treatment of these health effects, even in cases where the stressor cannot be removed or avoided. Mitigating the health impacts of chronic stress is an important emphasis since, in many instances, the patients' stressors cannot realistically be reduced or avoided. For instance, it is often difficult to remedy the stress associated with certain employment (e.g., shift

work, medical field, military), serious family situations (e.g., caregiving demands, illness or death of a loved one, divorce), or socioeconomic difficulties (e.g., financial hardship, low opportunity). Monitoring tools to quantitatively assess chronic stress might be useful for determining when intervention is necessary, for evaluating the effectiveness of prospective interventions, and to establish when the risk has been resolved (e.g., to determine when a burnout patient is ready to return to work without immediate risk of relapse).

Published models and markers of chronic stress

Models employing psychosocial stressors

In spite of the aforementioned challenges, a variety of models of chronic stress have been established and tested. In both humans and animals, efforts have usually been made to select stressors that do not impose the need for large-scale physical adaptation, which would create confounding biochemical markers. For instance, although radiation, toxicity, extreme heat or cold, exercise, injury, food/water deprivation, and other dietary manipulations all induce stress, significant exposure to such severe conditions would produce significant bodily changes specifically associated with surviving physical damage and attempting to restore homeostasis. Instead, most models focus on the use of psychosocial stressors, which include exposure to mild, non-harmful versions of physically stressful conditions (e.g., limited exposure to heat/cold, exercise, pain, etc.) or stressors that apply no direct molecular or energetic stress (e.g., social conflict). Although psychosocial stressors do not directly threaten physical harm and may not even be associated with a perceivable threat, they are equally effective at inducing an acute stress response and stressed behaviour. This is true even when a human participant knows that they are participating in a trivial exercise (e.g., Trier Social Stress Test, simulated interaction wherein bad news must be delivered) [81, 90]. It is clear that feedback from the higher brain structures does help to reduce the severity of response to stressors [91, 92]: hippocampal connections to the hypothalamus directly suppress the HPA axis and inhibit the release of glucocorticoids. However, the sensory system's direct input into the midbrain ensures that the stress response can be activated rapidly and

directly without participation from the 'higher' parts of the brain [30]. The body's irrepressible responsiveness to stimuli associated with danger or social demands should come as no surprise, given that anticipating threats and performing social adaptation are extremely valuable from an evolutionary standpoint.

The use of psychosocial stressors is one of the most useful avenues for studying chronic stress. In humans, psychosocial stressors can include threat of pain, threat of loss, social disturbances or demands (performance, conflict, isolation), sleep cycle disruptions, ambiguity/cognitive dissonance, and physical discomfort, but this list can be extended to include almost any external or internal stimuli depending on an individual's cognitive response [93]. In addition to self-report measures, a number of other quantifiable metrics have been used to assess the impact of these stressors on behaviour and physiology, including heart rate, cortisol, skin conductivity [94]. In rodent models, psychosocial stressors in mice include threatening stimuli (noise, open spaces), social challenges (conflict, negotiating dominance, isolation), day/night reversal, and physical discomfort (restraint, heat, cold) [95]. Exposure to these stimuli produce behaviour and physiology in rodents that is analogous to the chronic stress response observed in humans: rats and mice in these experimental models may exhibit an increased defense response to threat, altered sexual behaviour, learning impairments, mitochondrial dysfunction, susceptibility to "addiction" (i.e., nicotine or alcohol dependency), changes in dietary preferences (e.g., an increased preference for "comfort foods" or a decreased sucrose preference/anhedonia), abdominal weight gain, and immune suppression [96-104]. For both humans and rodents, the interval and severity of exposure to stressors is highly variable, but the presence of these physical symptoms is generally considered a positive indicator that chronic stress has been successfully applied.

Animal models of chronic stress

Previous studies in animals have used a variety of models for chronic stress with varying levels of validation, such as repeated social defeat in mice and long-haul transport in sheep [105, 106]. However, the best-validated experimental model of stress is the Chronic Unpredictable Mild Stressors (CUMS) model, in which mice or rats are

subjected to a mild stress-inducing stimulus each day for 3-5 weeks [95]. To avoid habituation to the stressor, several different stressors are used and are applied in randomized order. As an example, one study subjected Sprague-Dawley rats to forced swimming, mild heat exposure (1 hour at 40 °C), mild cold exposure (1 hour at -10 °C), water deprivation (24h), food deprivation, tail squeeze, mild electric shock, short-term restraint (2 hours), and reversal of day-night cycle. One stressor was applied each day for 27 days. According to the authors, these "daily physical and mental irritations were found to closely mimic the stress of human society" [107]. The CUMS model has been in use since the 1980s. Its validity is well-supported by the behavioural and biochemical changes observed in rodents subjected to CUMS: rats show changes in appetite, a progressive reduction in sucrose preference (anhedonia), reduced exploration in the open-field test (corresponding to depression/anxiety), and reduced cortisol levels [107]. Furthermore, the model appears to reproduce some of the health problems associated with chronic stress, *e.g.* cardiovascular vulnerabilities [108].

Biochemical evidence from the CUMS model supports the hypothesis that chronic stress is physiologically distinct from acute stress, and that the impacts of chronic stress are not tied (exclusively) to over-activation of the HPA axis. GC-MS was used to analyze the profile of 43 metabolites in urine from chronically-stress rats and non-stressed controls [107]. Univariate statistics was used to examine the fold change of each metabolite versus the control for rats at various time-points following exposure to chronic stressors. This analysis determined that the metabolite profile observed in the chronic stress condition differs significantly from both non-stressed controls *and* acutely stressed animals (Figure 3). As expected, some metabolites that are altered in acute stress (day 1) show a similar or amplified change in concentration under conditions of chronic stress (day 9, day 27). However, in other cases, the metabolite alterations observed in acute stress actually resolve in chronic stress. Cortisol, which is increased in acutely stressed animals, is no longer elevated in chronic stress. In addition, some metabolites (*e.g.* hippurate, pimelate) that are found in increased or decreased abundance during acute stress even reverse their trend in chronic stress. Other metabolites did not show any alteration until the stress becomes chronic (9 or 27 days).

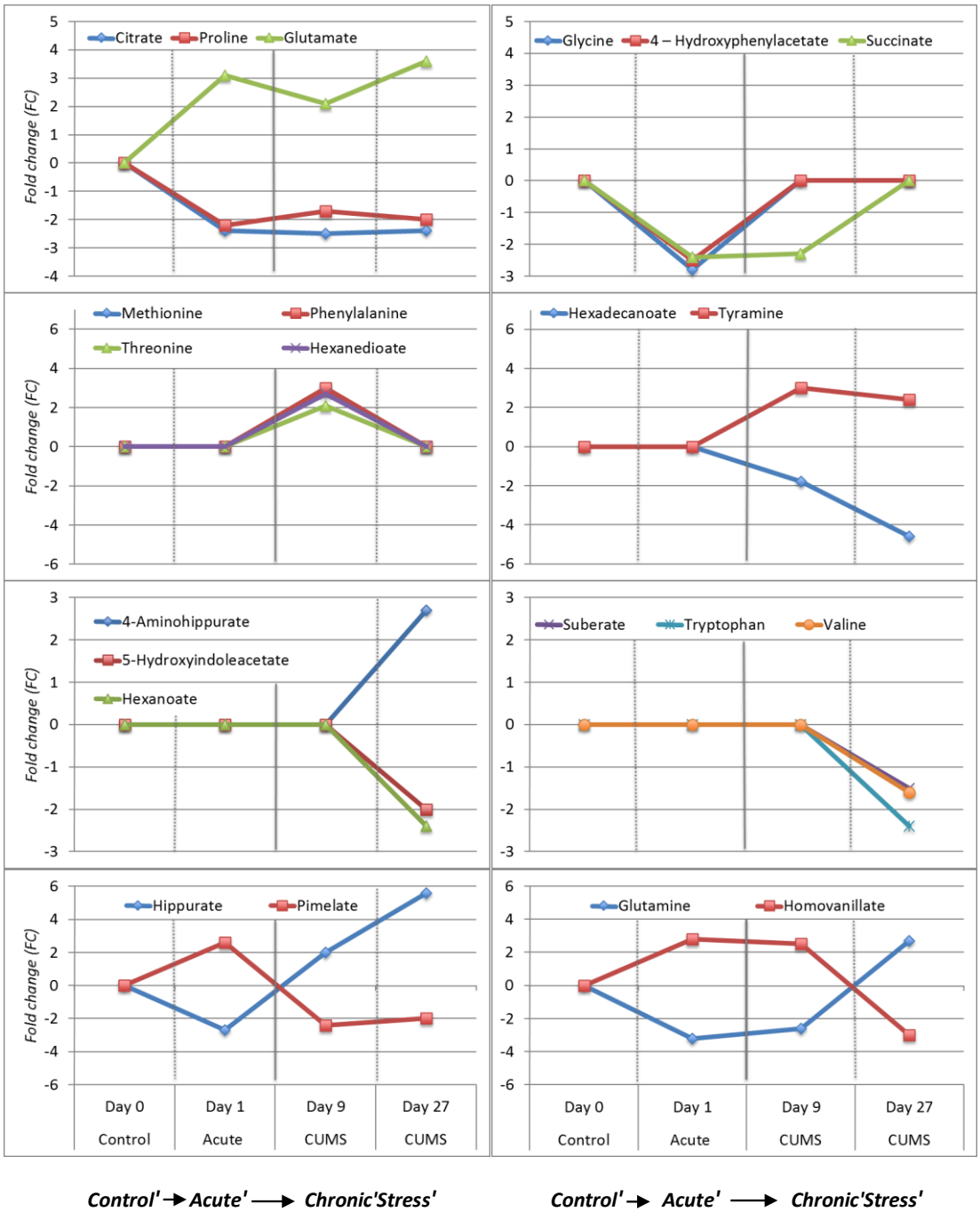

Figure 3. Metabolite profiles observed in acute versus chronic stress, as reported in Wang et al.

The unique metabolite profile generated in the urine of CUMS-model mice supports the hypothesis that the effects of chronic stress are due to some type of allostatic change, which represents a system-wide physiological adaptation to stressful environments, as opposed to habituation to stressors. This finding also aligns with the observation that many of the health impacts of chronic stress are sustained even when the immediate signs and symptoms of the acute stress response are resolved.

Human models of chronic stress

Some models of chronic stress in human patients have also been published. These include occupational 'burnout,' irregular or excessive work hours, low quality work environment (*e.g.* high noise, chemical exposure), or caregiving for an ill or disabled family member [109, 110], but many of the models in use are not clearly validated. Some studies have also used mood or personality traits to separate participants into high- and low-anxiety or high- and low-stress groups [111, 112]. It is a reasonable premise that high-anxiety trait individuals experience more stress, on average, than low-anxiety trait individuals. These studies pose a useful model in that they do not depend on analyzing stressors, which may be hard to quantify, may not induce the same level of stress in all individuals or may produce a stress response of unknown duration. Furthermore, by focusing on high stress responders, instead of high stress situations, these models may also unwittingly incorporate biological and epigenetic influences into group assignments – this may seem like a confounding variable, but in fact, this is a useful group for study because it can be predicted that they will have an enduring experience of raised stress levels.

Published markers of chronic stress

Up to this point, research on the metabolic changes associated with stress in human and animal models has focused largely on hormones and glucocorticoids. Hypothesis-driven research has provided some clues about possible gene expression or protein abundance differences in chronic stress [refs]. Recent metabolomics studies in humans have attempted to identify new markers concerning the physiology of chronic stress (Table 1), but human models are challenging. The CUMS model described above presents some of the best evidence for potential markers of chronic stress (Table 2)

In the CUMS model rat study described above, supervised partial least squares discriminant analysis (PLS-DA) analysis identified a number of metabolites whose altered concentrations distinguish the chronic stress group from the acute stress group: glutamine, homovanillate, pimelate, proline, citrate, glutamate, hippurate, tyramine [107]. Of these, glutamine, hippurate, homovanillate, and pimelate show a reversed trend in chronic versus acute stress. Pathway analysis suggested that both acute and chronic stress may be associated with changes in the tricarboxylic acid cycle, glutamate/glutamine biosynthesis, tyrosine metabolism, and gut microbiota, but chronic stress is also associated with changes in protein equilibrium & liver function and the methionine pathway. Other recent studies of urine, blood, and tissue from CUMS murine models generated additional biomarker candidates: hexadecanoate, aconitate, succinate, isocitrate, glycine, glutamic acid, glucose, ribose, valine, aspartic acid, serine, phenylalanine, oxoglutaric acid, indoleacetic acid, and beta-alanine. The affected metabolites are involved in energy metabolism, the citric acid cycle, liver function, the gut microbiome, cardiovascular protection, and amino acid synthesis [113-115].

Table 1. Published metabolomics biomarkers of chronic stress in human models

Model	Species	Technology	Metabolomic Markers Identified	Biofluid / Tissue	PUB-MED ID	Health Associations
Burnout patients	Humans		Cortisol (0)*	Saliva	12782748	Lack of sustained HPA activation
Quality of work environment	Humans	Review paper	Testosterone (-), Catacholamines (+) **Proteins:** glycated hemoglobinA(1c) (+), fibrinogen (+)	Urine / Blood	19563453	Catabolism vs. anabolism
High anxiety trait (self-reported)	Humans	GC-MS, LC-MS, NMR (untargeted)	Glycine (+), methoxytyrosine (+), beta-alanine(+), proline (+), dihydroxyphenylalanine (DOPA)(+), adrenaline (+), choline (+), lycopene and beta-carotene, p-cresol sulfate (-), aconitate (-), glycine (-), glutamate (-)	Urine	19810704	tricarboxylic acid cycle, gluconeogenesis, urea cycle, digestion and protection against oxidative stress

Table 2. Published metabolomics biomarkers of chronic stress in murine models

Technology	Markers Identified using the Chronic Unpredictable Mild Stressors (CUMS) Experimental Model	Biofluid / Tissue	PUB-MED ID	Health Associations
HPLC/NMR	Trimethylamine-N-oxide (-), alanine (-), beta-hydroxybutyrate(-), valine(-), leucine/isoleucine (-), lipids (-), TMAO (-). Phosphatidylcholine (+); choline (+). **Related proteins:** LDL (-), VLDL (-), HDL (+), N-acetyl glycoproteins (+)	Plasma	22420663	Fatty acid metabolism
GC-MS	Glutamine (-), Inosine (-), 9,12-Octadecadienoic acid (-), Proline (-), Hexadecanoic acid (-), Octadecanoic acid (-) **Related Proteins:** HSP(-), COX-2 (-)	Heart tissue	22658902	Lowered cardio-protection
GC-MS	Glutamine (+); homovanillate(-)*, pimelate(-)*, proline(-), citrate(-), glutamate(+), hippurate(+)*, tyramine(+)	Urine	19292500	Energy / Glyco-metabolism, TCA, liver function, gut microbiome, amino acid synthesis
GC-MS	Hexadecanoate (-), aconitate (-), succinate (-), isocitrate (-), glycine (+), glutamic acid (+), ribose (+), valine (-), aspartic acid (-), serine (-), phenylalanine (-), oxoglutaric acid (-), indoleacetic acid (+), beta-alanine (-)	Urine	N/A*	

[2]Zhou, Yu-Zhi, et al. Metabonomic Analysis of Urine from Chronic Unpredictable Mild Stress Rats Using Gas Chromatography–Mass Spectrometry. *Chromatographia* (2012) vol. 75 (3-4) pp. 157-164

Limitations of previous studies

Although metabolomics approaches have been applied to the study of chronic stress in the CUMS model, the total number of published studies involving metabolomics for this model is small and the methods applied thus far have been limited to lower-sensitivity techniques such as GC-MS, HPLC, and NMR. These studies therefore each reported identification and quantification of fewer than 50 medium-to-high abundance metabolites in urine, tissue or blood samples [107, 115]. Even fewer systematic studies have been performed in humans. A study by Martin et al. found that the urinary metabolic profile associated with high-anxiety individuals included some trends that were similar to those seen in mice under the well-validated CUMS model [112]. However, this study used metabolomic profiling via NMR, GC-MS and LC-MS and no quantitative values were obtained for the metabolites of interest.

Hypothesis, Objectives & Approach

Published evidence has established that there are biochemical markers that differentiate between the distinct conditions of acute stress and chronic stress. However, given the limitations of the analytical techniques so far applied, it is likely that many of the metabolomic changes that occur under conditions of chronic stress have not yet been characterized. In addition, there is a need to confirm previous findings regarding metabolite alterations associated with chronic stress. This is especially important considering the wide variety of models under consideration, the complexity of this field of research, and the high degree of dissonance in the literature about some aspects of the chronic stress response (e.g., cortisol levels).

In this project, I therefore applied a combination of high-sensitivity mass spectrometry methods to dramatically increase metabolite coverage, in an attempt to characterize novel metabolite biomarkers of chronic stress and to validate previously identified markers in alternative human and murine models. In the first portion of the project, I applied a set of targeted (LC-MS/MS, FIA-MS/MS) and untargeted (QTOF-MS) metabolomics approaches to analyze serum samples from a human epigenetic model of chronic stress in order to identify potential targets for further analysis (Chapter 1). To test the resulting

hypothesis that oxidative stress is a key feature of chronic stress, I developed a new targeted LC-MS/MS assay for the accurate quantitation of aldehyde products of lipid peroxidation (Chapter 2). The validated method for quantitation of malondialdehyde (MDA) was then applied to mouse plasma samples from model of chronic social defeat stress to determine whether animals exposed to acute stress show increases in oxidative stress (Chapter 3). Mouse plasma samples from this model were also analyzed by untargeted metabolomics using Fourier-transform (FT)-MS to identify other important metabolite features (Chapter 3), particularly those that overlap with metabolites identified in the human epigenetic model. By identifying metabolites that show consistent trends across multiple models of chronic stress, and contextualizing these metabolites in relevant pathways, this project should offer new insights into the physiology of chronic stress.

Chapter 1:
Metabolomics of Chronic Stress in a Human Epigenetic Model

Chapter Summary

Background: Early life stressors can modify DNA methylation at the promoter site for glucocorticoid receptor (GR) gene, altering the activity of the hypothalamic-pituitary-adrenal (HPA) axis and creating a lifelong predisposition to high stress reactivity. This model is advantageous for the study of chronic stress because its biochemical mechanisms are well characterized, it has been extensively studied in both humans and animals, and it produces a phenotype that includes some of the adverse health outcomes commonly associated with chronic stress.

Methods: Serum samples were obtained of children in a transgenerational study of DNA methylation and early life stressors. Samples were grouped into "high methylation" and "low methylation" groups on the basis of their average DNA methylation at 24 GR-promoter-associated CpG sites. Serum samples were first analyzed using a targeted metabolomics approach based on the use of multiple reaction monitoring mass spectrometry (MRM-MS) techniques with a Biocrates IDQ p180x kit to quantify lipids, amino acids, and biogenic amines. Untargeted metabolite profiling was also performed on the samples using two separate extraction techniques, followed by reversed phase liquid chromatography (RPLC) and detection with full scan QTOF-MS to enable measurement of polar and non-polar species.

An assay for accurate quantitation of MDA in human plasma was developed using a multiple reaction monitoring-mass spectrometry (MRM-MS) approach, using chemical derivatization with 3-nitrophenylhydrazine, isotope-labeling, and liquid chromatography (LC) with electrospray (ESI)-tandem mass spectrometry. A proof-of-principle project also demonstrated that 3-nitrophenylhydrazine can be used under alternative reaction conditions to derivatize a wide panel of other aldehydes for quantitation.

Results: Untargeted and targeted metabolomics approaches both revealed differences in the abundance of phosphatidylcholine and other phospholipid species that suggest a relationship between chronic stress and lipid metabolism or degradation.

Introduction

An epigenetic model of chronic stress

In 1964, Dr. Victor Denenberg first described an epigenetic model of stress reactivity wherein early life experiences were responsible for determining lifelong stress reactivity [116]. More recently, this model received widespread attention beyond the field of stress research, after Dr. Michael Meaney's lab demonstrated that the epigenetic modification responsible for stress reactivity can be transgenerationally modulated by maternal behaviour [117]. In this model, early life events such as maternal care influence DNA methylation of the promoter for glucocorticoid receptor at a transcription factor binding site, specifically the NGFI-A binding region on exon 1F [118-120] DNA methylation in this region has been associated with maternal stress during the pre/peri-natal period, childhood trauma/abuse, and the absence of maternal care behaviours shortly after birth [118, 119] [121]. Specifically, exposure to these early life stressors increases the degree of methylation at several sites in this region. By interfering with NGFI-A binding and the recruitment of the transcription complex, this increased methylation leads to an enduring decrease in glucocorticoid receptor (GR) expression. Since it is the binding of glucocorticoids by GR that provides inhibitory feedback to the HPA during the stress response, this reduction in GR expression is associated with less effective dampening of the stress response, resulting in more frequent and more intense HPA axis activation [122, 123] The methylation at this site is generally considered to be irreversible and maintained across cell divisions, so it is believed that these early life events set an individual's lifelong reactivity to stress [124].

Over the long-term, the altered HPA responsiveness leads to many phenotypic variations that are akin to those seen in chronic stress such as metabolic syndrome, learning impairment, immune risks, cardiovascular disease and mental health disorders [125] Some human studies have also indicated that methylation in this region may be associated with poorer lifelong stress resilience and coping, as suggested by the apparently high levels of GR promoter methylation observed at autopsy among individuals who committed suicide [126]. Among rats, the persistent increase in stress reactivity also makes it more likely that the animal will fail to engage in maternal care

behaviours such as licking of pups, recapitulating the high methylation at GR promoter in their offspring [117]. It has been shown that cross-fostering pups of high-stress mothers with a care-providing surrogate prevents the increase in methylation at GR promoter. This demonstrates unequivocally it is early life experience, and not other hereditary factors, that is causally responsible for methylation at this site.

Overall, this model has several advantages for the study of chronic stress: the epigenetic model and its biochemical mechanisms are well characterized, it has been extensively studied in both humans and animals, and it produces a phenotype that includes the adverse health risks associated with chronic stress that we wish to study (Figure 3). However, the key advantage of this model is that it effectively addresses some of the research challenges in chronic stress. By comparing groups on the basis of stress reactivity, it avoids the need to try to assess stress exposure. Because all free-living human subjects are exposed to stress, it is assumed that high stress responders will be exposed to at least as many stressors as their low methylation counterparts, but will respond more frequently and more intensely. Moreover, individual stress reactivity can be predicted by a measurable biological feature. This represents a "cleaner" approach for studying chronic stress in humans in that it does not depend as heavily on behavioural tests, clinical assessment, or self-reporting of perceived stress.

For this portion of the research, we obtained and analyzed serum samples associated with a human study of children whose mothers reported exposure to inter-partner violence (IPV) before, during, and/or shortly after pregnancy. Based on previous studies in this model by Radtke et al. [127], it was hypothesized that children in this cohort whose mothers who were exposed to peri-natal stressors would have altered methylation patterns at specific CpG sites in the promoter region for the GR gene, and would be expected to show altered HPA activity. Both broadly-targeted quantitative metabolomics and untargeted metabolic profiling were applied in an attempt to determine whether these differences in HPA reactivity were associated with alterations in other metabolites that could provide clues about the long-term systemic changes associated with chronic stress.

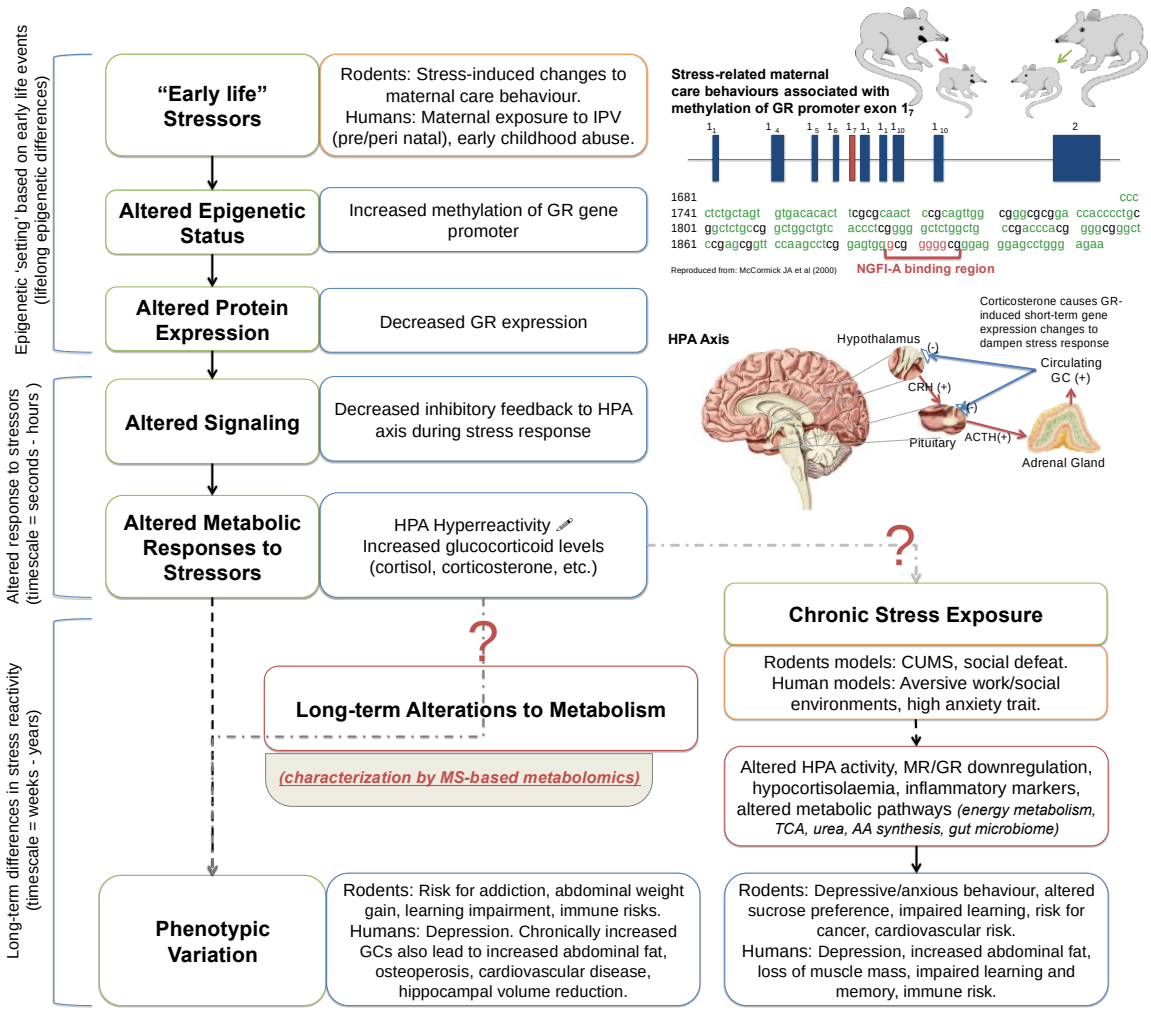

Figure 4. Overview of an epigenetic model of chronic stress

Materials & Methods

Human plasma samples & sample metadata

Samples and metadata: For the purpose of this study, a research collaboration was established between Dr. Christoph Borchers at University of Victoria, Dr. David Wishart at the University of Alberta, Clinical Biopsychologist Dr. Clemens Kirschbaum at Technical University of Dresden and Clinical Biopsychologist Dr. Thomas Elbert at the University of Konstanz. Dr. Ralf Hoffman at University of Leipzig initiated the

collaboration. Patient blood samples were collected under the supervision of Dr. Elbert at the Psychotraumatology Clinic from 44 mother-child pairs, made up of women who reported varying degrees of inter-partner violence during pregnancy and their offspring (n=44, M/F, ages 11-21).

In addition to collecting biological samples, clinicians also completed interviews with the patients, using multiple measures to quantitatively assess the degree of exposure to pre-/peri-natal stressors (trauma/abuse) and adverse childhood experiences. A host of commonly-used psychological inventories was performed to assess stress and coping, estimate overall quality of life, obtain sociodemographic information (age, sex, nationality, etc.) and to rule out any confounding psychological conditions among the patients sampled.

Blood samples were collected immediately after completion of the interviews. Following collection, blood was allowed to clot and centrifuged to generate serum, which was held in a biobank at University of Konstanz. For this study, serum samples from each participant were portioned into aliquots of 100 μL each. Dr. Borchers' laboratory and Dr. Wishart's laboratory each received a matching set of aliquots. Hair samples were also collected from both mother and child, from as close to the scalp as possible.

Associated biochemical data: Dr. Kirschbaum applied an immunoassay technique in his lab to measure cortisol, cortisone and testosterone levels in near-scalp (≤3cm) segments of the hair samples. Hair steroids were extracted using a published protocol [31] and quantified using a commercially available immunoassay with chemiluminescence detection (CLIA, IBL-Hamburg, Germany).

To measure DNA methylation, the Illumina Infinium HumanMethylation450 BeadChip Kit was used to analyse DNA extracts obtained from lymphocytes isolated from whole blood. Genome-wide analysis of DNA methylation was coordinated by Dr. Karl Radtke and Dr. Thomas Elbert and was performed at the Barts and the London Genome Centre (Queen Mary University of London, London, UK). DNA extraction was performed with the DNeasy Blood and Tissue Kit (Qiagen, Hilden, Germany), after which 1 μg of genomic DNA was bisulfite converted (EZ DNA Methylation Kit, Zymo, Irvine, CA, USA) and applied to the Human Methylation 450K array (Illumina, San Diego, CA,

USA). DNA methylation data was processed by Dr. Radtke to identify probes associated with hGR. Sample metadata -- including both psychological and biochemical measures -- was analyzed with SPSS (IBM's Statistical Package for the Social Science) software to identify correlations between variables.

Human research ethics and safety considerations: Both samples and data were originally collected under the supervision of Dr. Clemens Kirschbaum, Clinical Biopsychologist at Technical University of Dresden and Dr. Thomas Elbert of the University of Konstanz's Psychotraumatology Clinic in accordance with clinical guidelines, collection protocols and ethics requirements, under approval from their respective institutions. Samples were received at the UVic-Genome BC Proteomics Centre in a fully anonymized format with no identifying information. All non-identifying metadata and biochemical data was provided separately. Sample analysis and data handling were completed at University of Victoria under Human Research Ethics Board Approval (Ethics Protocol Number 12-527). All work involving human biofluids was completed using the recommended personal protective equipment (PPE) in a laboratory with Biosafety Level 2 (BSL2) certification.

Standards & Reagents

LC-MS grade acetonitrile, methanol (MeOH), ethanol, chloroform, isopropanol (ISP), and water (H_2O) were purchased from Sigma-Aldrich (St. Louis, MO). Pyridine (HPLC-grade), ammonium acetate (HPLC-grade), formic acid (FA), phenylisothiocyanate (PITC, 99% purity) and phosphate-buffered saline (PBS, Reagent-grade) were also obtained from Sigma-Aldrich. Strata-X polymeric reversed-phase Solid Phase Extraction (SPE) cartridges (100-mg) were purchased from Phenomenex Inc. (Torrance, CA). The BiocratesIDQ p180x kit was purchased from Biocrates Life Sciences AG (Austria).

Methods for targeted metabolomics

As part of a training exchange, I analyzed serum samples in Dr. David Wishart's BSL2 metabolomics laboratory at the University of Alberta. Targeted metabolites were quantified using a commercially available assay, the BiocratesIDQ p180x kit. The kit includes a 96-well plate with pre-fitted filter and cover, lyophilized reference plasma

(quality control samples), LC-MS calibration standards, an internal standard, and custom MS running solvent. The step-by-step operating procedures were performed according to the instructions in the kit user manual. In preparation for analysis, serum samples were thawed on ice, vortexed, and centrifuged 4ºC for 5 minutes at 16,000xg.

The provided internal standard was dissolved in 200 µL of 90% methanol. Phenyl isothiocyanate (PITC) was prepared as a 5% (v:v) solution in a reagent buffer consisting of ethanol, H_2O and pyridine (1:1:1). PITC is used for derivatization to improve the detection of low abundance and hard-to-ionize metabolites. The extraction solvent was prepared fresh by dissolving 19mg of ammonium acetate in 50 mL of methanol to generate a 5mM solution. The quality control (QC) samples (n=3) were compromised of lyophilized human plasma, each with analytes added in varying defined concentrations, and were used to verify the assay performance. Each QC sample was resuspended with the addition of 200 µL of H_2O, shaking for 15 minutes (at 600 rpm) and centrifugation (5 minutes at 16,000 x g).

Sample preparation: Wells were loaded as follows: 1 blank well (nothing pipetted), 7 external calibration samples, 3 'zero' samples (10 µL PBS), 3 QC samples, and 82 serum samples. Software was used to assign each of the serum samples to a random position on the plate to reduce any possible systematic experimental bias. Ten (10) µL of each serum sample was carefully pipetted into the centre of assigned well, avoiding contact with the filter, which is responsible for protein removal. Internal standard at a volume of 10 µL was then added to every well (excluding the blank). Samples were then fully dried in a nitrogen evaporator (~30 minutes) and resuspended in 50 µL of reagent buffer containing PITC as the derivatizing reagent. The reaction was allowed to proceed for 20 minutes at room temperature, after which the samples were dried a second time in the nitrogen evaporator. The samples were eluted by adding 300 µL of extraction buffer and shaking the covered filter plate for 30 minutes. Centrifugation of the filter plate at 500xg then enabled collection of the eluate on a lower capture plate, where it was diluted with 600 µL of Biocrates' running solvent (one ampoule, prepared in 291 mL of methanol). The kit plate with prepared samples was stored overnight at 4ºC, and held in the autosampler

at 4ºC for 2 consecutive days during MS analysis. The Biocrates manual indicates that the prepared kit is stable at this temperature for at least 5 days.

Flow Injection Analysis (FIA)-MS: During flow injection analysis (FIA)-MS/MS, 20 µL aliquots of each sample were injected with no prior separation using on an Agilent 1200-series HPLC coupled to an Applied Biosystems API QTRAP 4000 with a TurboV electrospray ionization (ESI) interface. The solvent was Biocrates' proprietary running solvent (isocratic gradient at 100%) and the flow rate was maintained at 30 µL/minute for 1.6 minutes, and then ramped from 30 µL to 200 µL/minute at 2.4 minutes, where it was maintained until 2.8 minutes. FIA/MRM-MS mass spectra were collected in both positive and negative ion mode using the settings files and acquisition lists generated by the Biocrates MetIQ software.

Liquid Chromatography (LC)-MS: Liquid chromatography (LC)-MS/MS was performed using the same HPLC and MS instrument, with an Agilent Zorbax Eclipse XDB C18 column (3.0 x 100mm x 3.5 µm) held at 50 ºC. The injection volume was 10 µL. Solvent A was H_2O with 0.2% formic acid (FA) and Solvent B was acetonitrile with 0.2% FA. A gradient from 0% B to 70% B was applied over 3.5 minutes with a steady flow rate of 500 µL/minute, after which the mobile phase was held at 70% for an additional 1.3 minutes. The column was washed with 100% A for 2 minutes and reconditioned with the initial solvent conditions for 0.5 minutes at the start of the next injection. LC/MRM-MS mass spectra were collected in both positive ion mode using the settings files and acquisition lists generated by the Biocrates MetIQ software.

Metabolite Quantitation: Internal standards were used for identification and quantitation of the targeted metabolites, with automatic calculation of metabolite concentrations using Biocrates' Met*IDQ* software. The raw spectra obtained from FIA-MS analysis were automatically batch processed in Met*IDQ*, with manual quality checking. Spectra obtained from LC-MS were first processed in Analyst and then exported to MetIQ for further processing, statistical analysis and calculation of concentration values. Concentration data for all metabolites was then exported from MetIDQ to an Excel file.

Statistical Analysis: The MetaboAnalyst webserver (www.metaboanalyst.com) was used for missing value imputation, normalization, and multivariate statistical analysis.

Methods for untargeted metabolomics

Comprehensive untargeted metabolomic profiling of both polar and non-polar metabolites was performed at University of Victoria using the workflow shown in Figure 5 to analyze a second set of 100 µL aliquots from each child serum sample (n=44).

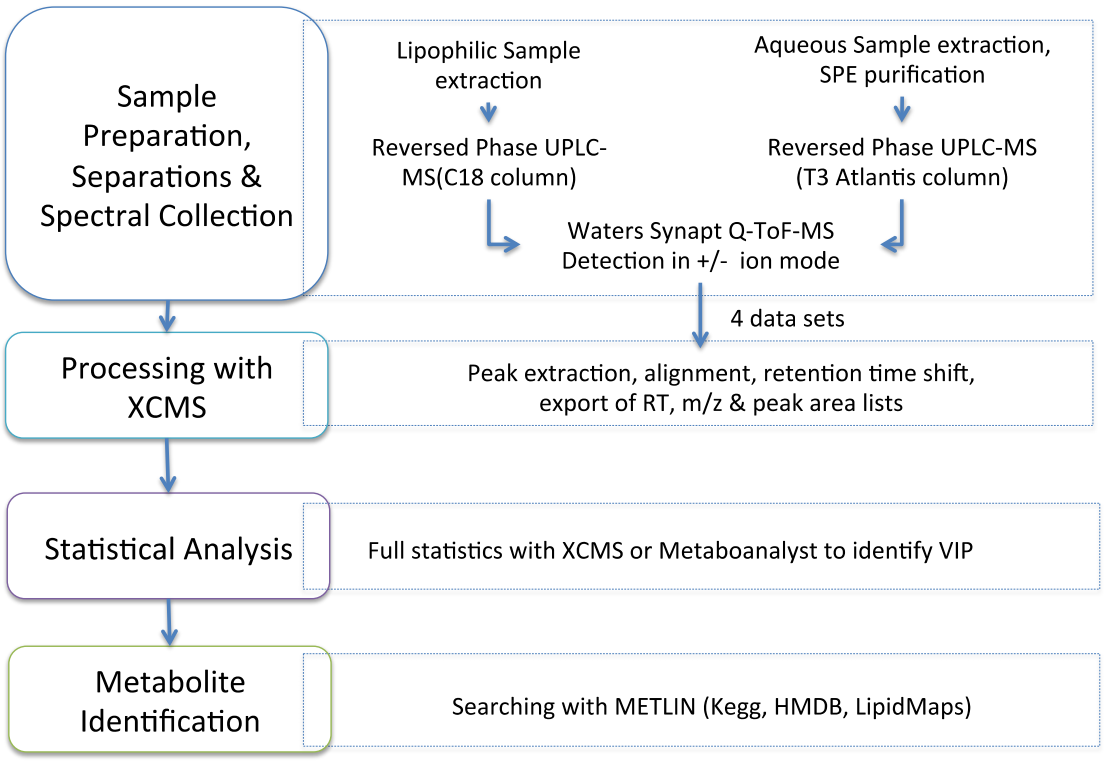

Figure 5. Workflow for untargeted metabolomics

Organic extraction of non-polar metabolites: Each 20 µL aliquot of serum was diluted by adding 80 µL of water. Non-polar metabolites were then extracted by adding 400 µL of chloroform and methanol (3:1). Samples were centrifuged for 15 minutes at 13,000 x g in an R-22 centrifuge (Beckman Coulter), after which 450 µL of the supernatant was carefully removed, without disturbing the protein pellet, and transferred to 3 mL borosilicate glass test tubes. Extracted samples were evaporated until dry (~30 minutes) in an SPD1010 centrifugal speed-vacuum concentrator (Thermo Electron Corp., San Jose, CA, USA), capped, and stored overnight at -20 ºC. Samples were resuspended in 20 µL of isopropanol for MS analysis.

Reversed phase liquid chromatography (RPLC) for non-polar compounds: Samples prepared by chloroform/methanol extraction were analyzed by online RPLC using a BEH-C18 column (2.1 mm I.D. x 50 mm, 1.7 µm particle size; Waters Corp.) on a Waters Acquity UPLC coupled to a Waters Synapt Q-TOF-HDMS. The column temperature was maintained at 50 ˚C. Water with 0.01% FA was used as solvent A. Solvent B was acetonitrile and isopropanol (1:1) with 0.01% FA. The flow rate was set at 0.15 mL/min with a linear gradient of 15% to 100% B over 20 minutes, followed by a 4-minute wash step (100% B), and 4 minutes equilibrating at the starting conditions (15% B) prior to the next injection. The autosampler was kept at 4ºC. The injection volume was 3 µL, and was performed using the partial loop injection mode with an overfill factor of 1.

Aqueous extraction of polar metabolites: A 60-µL aliquot of each sample was diluted with 40 µL of water, and extracted with the addition of 400 µL of 80% methanol. Samples were centrifuged for 15 minutes at 2732 x g in an R-22 centrifuge (Beckman Coulter), after which 450 µL of the supernatant was carefully removed, without disturbing the protein pellet. The supernatant was transferred to 1.5 mL borosilicate glass test tubes, and diluted with 550 µL of water, bringing the organic concentration in the sample to ~36% methanol. To remove non-polar metabolites, the samples were then passed through an SPE cartridge, which had been pre-wetted with 3 bed volumes of 100% methanol and equilibrated with 3 x 1 mL of 36% methanol in water. The eluate was evaporated until dry (~45 minutes) in an SPD1010 centrifugal speed-vacuum concentrator (Thermo Electron Corp., San Jose, CA, USA), capped, and stored overnight at -20 ºC. Samples were resuspended in 50 µL of 5% methanol for MS analysis.

Reverse Phase Liquid Chromatography (RPLC) for polar metabolites: Samples prepared by aqueous extraction were analyzed by online RPLC using an Atlantis T3 column (2.1 mm I.D. x 100 mm, 3 µm particle size; Waters Corp.) on a Waters Acquity UPLC coupled to a Waters Synapt Q-TOF-HDMS. The column temperature was maintained at 50 ˚C. Solvent A was water with 0.01% FA and Solvent B was acetonitrile with 0.01% FA. The flow rate was set at 0.15 mL/min with a gradient of 2% for 2 minutes, 2 to 15% B over 5 minutes, and 15 to 90% B over 5 minutes, followed by a 4-

minute wash step (100% B), and 4 minutes equilibrating at the starting conditions (2% B) prior to the next injection. The autosampler was set at 4ºC. The injection volume was 10 µL, and was performed using the partial loop injection mode with an overfill factor of 1.

Mass spectrometry: Prior to use, the MS was tuned for maximum sensitivity with a lock-mass spray solution (50 pg/µL leucine enkephalin in 50% isopropanol), and was calibrated based on the detection of cluster ions from a 2.5-mM sodium formate solution in 50% isopropanol. The instrument was operated in MS mode with the ion mobility functionality turned off. Mass spectra were collected for each extracted sample in both positive and negative ion modes. In positive ion mode, the ESI spray voltage was set at 3.0 kV. In negative ion mode, the ESI spray voltage was set at -2.9 kV. The full-mass detection range was m/z 100-1200. Other ESI-MS operation parameters were set as follows: desolvation gas (N_2) flow and temperature, 700 L/h and 350 °C; drying gas (N_2) flow and temperature, 40 L/h and 120 °C; sampling cone voltage, 35V; extraction cone voltage, 4 V; and data acquisition rate, 0.3 s per scan. The background gas (Ar) in the collision cell was held at 0.5 mL/min. The lock-mass solution was continuously injected throughout data acquisition as a reference to maintain mass accuracy over all LC-MS runs.

Untargeted data analysis: A total of 4 spectral data sets were acquired for each sample – non-polar metabolites detected in the positive ion mode, non-polar metabolites detected in the negative ion mode, polar metabolites detected in the positive ion mode, and polar metabolites detected in the negative ion mode. A local copy of XCMS, operated with R, was used for processing and analysis of raw mass spectra. For each data set, XCMS performed peak detection (matchedFilter function), and two rounds of retention time correction and peak grouping (Obiwarp, rector functions), using the parameters and commands shown in Appendix 1. XCMS compared peak intensities between groups and generated results tables, extracted ion chromatograms (XIC), and boxplots for significant features that showed a fold change of >1.5 and t-test p-value of <0.05. The features list was manually reviewed to exclude isotopic peaks, common contaminants identified in the blank injections, and features with retention times at the beginning or end of the window (<2 or >24 min for non-polar, <1.75 or >13.5 min for polar). Mass-to-charge (m/z)

values for the remaining significant features were manually searched in the METLIN database (metlin.scripps.edu). The search was restricted to the most common adducts: (M+H)+ and (M+Na)+ in the positive ion mode, and (M-H)- and (M+Cl)- in the negative ion mode. METLIN search hits were searched in the HMDB (www.hmdb.ca) to verify their presence in human biofluids and to assess their physiological relevance.

Results

Analysis of sample metadata & grouping based on epigenetic model

The mothers in this study reported varying degrees of long-term stressors, ranging from little to severe traumatic stress, through exposure to partner violence and organized violence (war). In a previous study, Radtke et al. found that the offspring of mothers who were exposed to inter-partner violence (IPV) during their pregnancies had higher methylation at NGFI-A binding sites in the GR promoter region than those with little or no exposure [127]. In the current study, Illumina technology was applied to obtain data corresponding to the average methylation percentage (non-normalized beta values) at 485,000 CpG sites. Processing by Dr. Radtke identified 41 CpG sites spanning the hGR gene according to their genomic positions. Of these, 24 sites were known to be in the promoter region and 3 sites were among those previously quantified in peripheral blood in a study of peri-natal exposure to IPV [127], specifically cg04111177 (position 142783607), cg15645634 (position 142783639) and cg15910486 (142783621) on chromosome 5. All 3 sites are in the exon 1F region. Two sites (cg…634, and cg…486) were previously found to be associated with binding of NGFI-A and specifically showed increased methlyation in response to peri-natal stressors[127]. The remaining site (cg…177) was included in the previous study because it flanks the NGFI-A binding region.

In the current data set, it was found that cg…177 was the only one of the previously identified sites that had a statistically significant correlation with peri-natal traumatic events as quantified by the Post-Traumatic Stress Diagnostic Scale (PDS) ($R = -0.32$, $p=0.049$). However, the direction of the correlation was opposite – increases in IPV scores appeared to be inversely associated with methylation at this site. The methylation

beta value at this site was 0.076 in those with IPV >1 and 0.083 in those with IPV = 0 on this measure. Given the weak significance of this correlation (p~0.05), it is possible that the current data is not significant. However, it is also worth noting that at the time of this analysis, this site was only associated with early life stressors in one case in the Radtke et al. study. This position is adjacent to, but not part of, the known NGFI-A binding site. Other probed CpG sites were assessed for their association with early life stress. Using SPSS, a Pearson 2-tailed t-test was performed to assess whether any of the 41 CpG sites associated with GR demonstrated a correlation with peri-natal stress exposure (as quantified by traumatic events scores reported by the mother on the Post-Traumatic Stress Diagnostic Scale), other early life stressors (as determined by the 'Maltreatment and Abuse Chronology of Exposure' Inventory), measures of HPA activity (hair cortisol, testosterone, cortisone), or various measures of child functioning (measured by clinical psychology tools such as the Cognitive Assessment System and the Strengths and difficulties questionnaire for detection of psychiatric disorders). Five sites were identified that were correlated with either Traumatic Events Sum score (Peri) or IPV (Peri). However, of the five sites associated with peri-natal stress exposure ($p<0.05$), four showed an *inverse* relationship between degree of violence/trauma and methylation percentage, and all 3 of the strongest correlations ($p<0.005$) were inverse (Table 3). When assessed individually, none of the 41 sites assessed demonstrated a significant correlation with cortisol, cortisone, testosterone, or any measures of child functioning ($p>0.05$).

Table 3. Methylation sites spanning the GR gene associated with early life stress

Name	Promoter associated?	Associated with	Direction of correlation	Weak / strong	p-value
…679	No	IPV peri	-	Strong, -0.475	0.001
…240	Promoter	IPV peri	-	Strong, -0.447	0.002
…893	No	Trauma peri	-	Strong, -0.461	0.004
…453	No	IPV peri	+	Weak, 0.30	0.045
…177	Promoter*	Trauma peri	-	Weak, -0.32	0.049

*from Radtke paper, adjacent to known NGFI-A binding site

Given that the expected association between methylation at GR promoter sites and interpartner violence was not reproduced in our data, further analysis was restricted to the hypothesis that high GR promoter methylation – irrespective of its etiology – would

result in corresponding decreases in GR expression and induce chronic stress. Methylation at the 24 CpG sites in the GR promoter region were therefore used to distinguish between groups. A normalized average of promoter-associated methylation percentage was calculated for each individual by converting each methylation beta value to a measurement of standard deviation from the group mean for that site, and then averaging the standard deviations across all promoter-associated sites. When calculated this way, average methylation was not found to be significantly correlated with traumatic events (peri) or IPV (peri), but did show a weak direct correlation with hair cortisol measurements (Pearson Correlation=0.31, p=0.035) and child anxiety score ($p<0.05$). In order to create discrete groups, as required for highly multivariate statistical analysis, individuals were divided into 3 groups based on their deviation from the group mean. Individuals whose average percent methylation across 24 promoter-associated sites was within +/- 0.5 standard deviations of the group mean were considered 'average,' average methylation values falling >0.5 standard deviations below the mean were labeled 'low' (n=22), and >0.5 standard deviations above the mean were labeled 'high' (n=13) as shown in Figure 6.

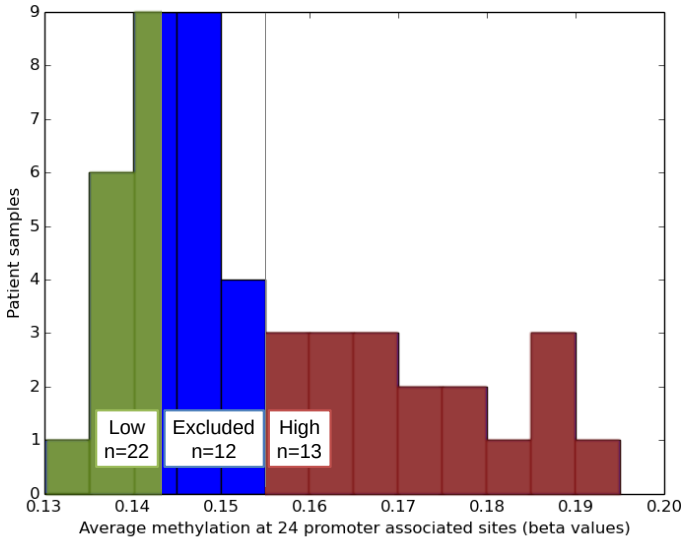

Figure 6. Summary of grouping based on methylation percentages.

Targeted metabolomics results

Samples (n=40) were analyzed using the Biocrates *AbsoluteIDQ* p180 kit for rapid quantitation of up to 180 metabolites. Accurate concentration data for a broad range of targets was used to perform an initial assessment of whether the groups showed differences and to assess sample integrity. Quantitative values were obtained for 141 metabolites. FIA-MS provided quantitative values for 112 metabolites: hexose, carnitine, 13 acylcarnitines, 82 phosphatidylcholine species including diacyl (aa), alkylacyl (ae), and lyso-PCs, and 15 sphingolipids including sphingomyelins (SM) and hydroxysphingomyelins (SM-OH). HPLC-MS quantified 29 metabolites: 21 amino acids (including Orn) and 8 biogenic amines (including creatinine, sarcosine, and seratonin). Multivariate statistics were performed using MetaboAnalyst to identify metabolites whose concentration differed between the groups. To enhance the likelihood of identifying significant differences, 'high' and 'low' methylation groups were selected for comparison, and other samples were initially excluded from statistical analysis.

Data processing: Missing values were replaced with 50% of the minimum concentration value for that metabolite. Features were normalized based on the median value for a given feature, with log transformation, and Pareto scaling (mean-centered and divided by the square root of standard deviation of each variable) (Figure 7). As a quality check, average concentration values for each metabolite were examined versus reference ranges where available.

Individual features showing differences: A volcano plot was generate to identify metabolites that differed between the groups (Figure 8). Five metabolites, all long-chain PCs, with a fold change >1.5 and t-test p-value <0.01 were identified. Several other long-chain diacyl-PCs also had a fold changes of 1.5-1.8 (PC C24:0, C32:2) or a p-value <0.01 (PC C36:4, C38:3, C38:5, C40:1, C40:5), and all were lower in the high methylation group. Carnitine (C0) was increased in the high methylation value with a fold change of 1.45 ($p<0.01$).

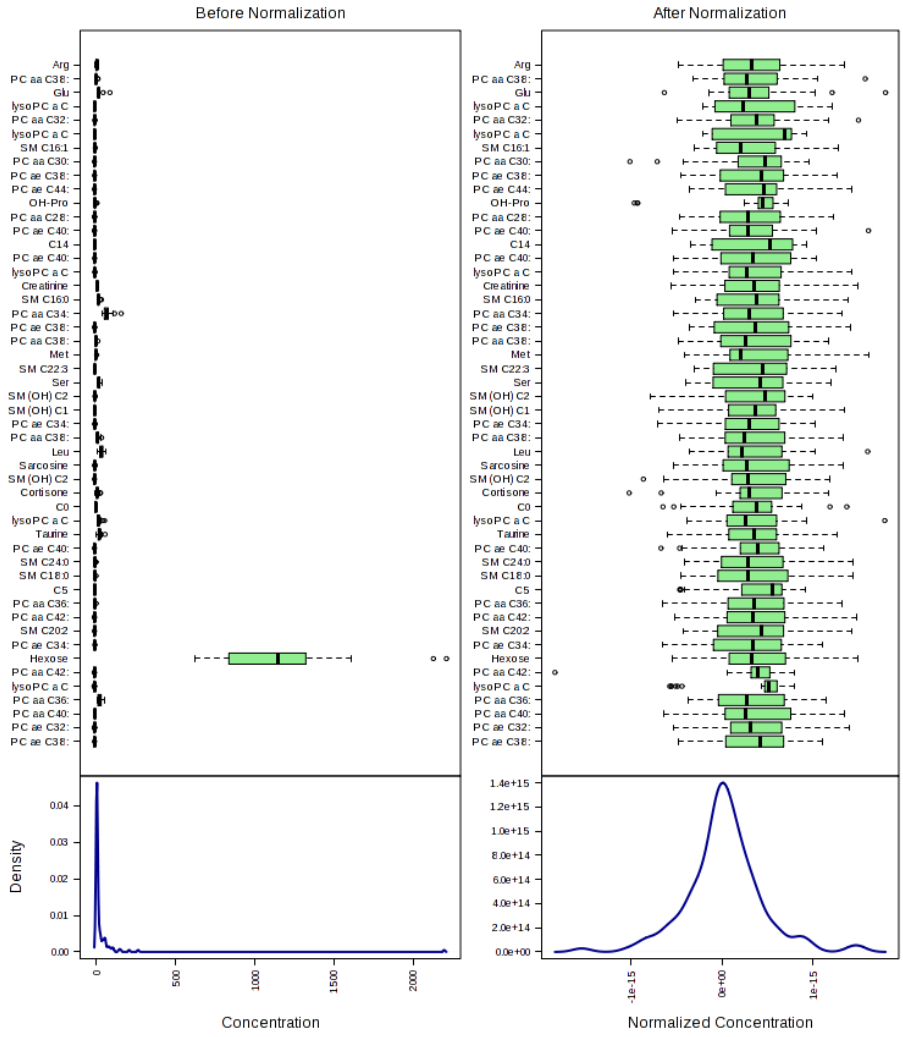

Figure 7. Data normalization with Metaboanalyst

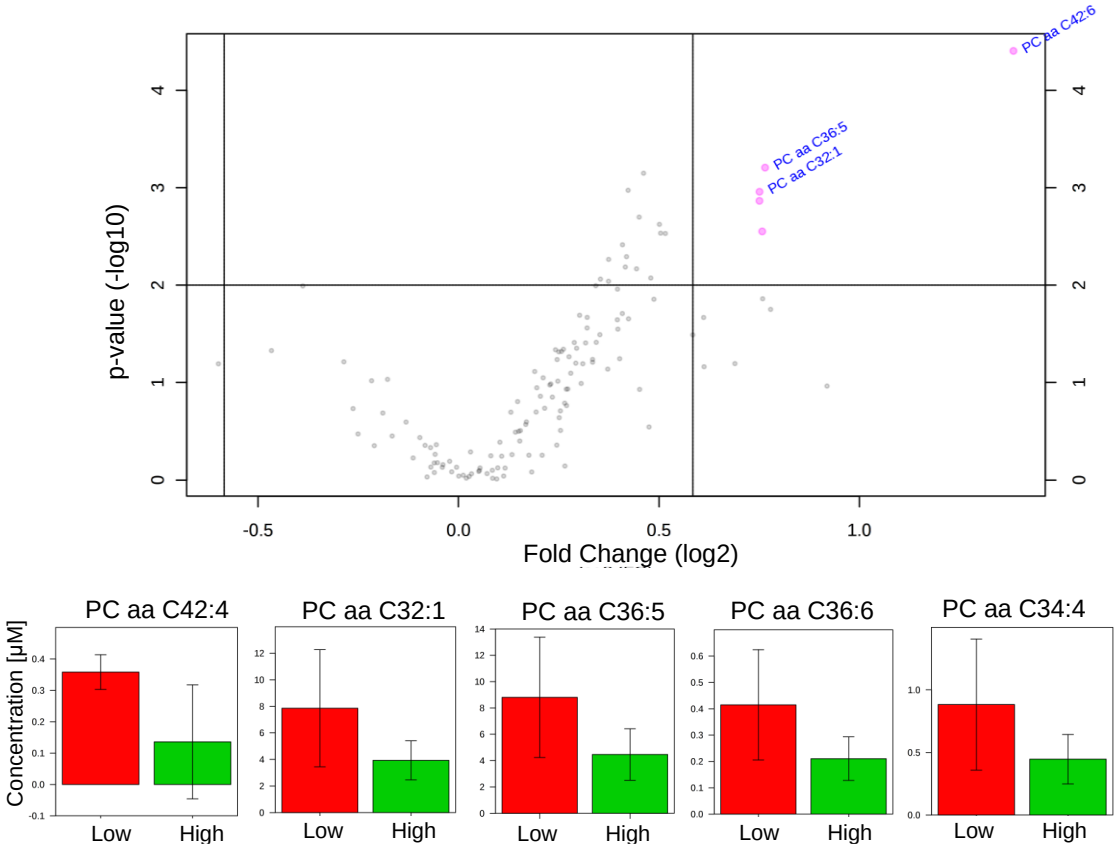

	FC in high methylation group	p-value
PC aa C42:6	-2.6106	0.0000
PC aa C36:5	-1.6991	0.0006
PC aa C32:1	-1.6829	0.0011
PC aa C36:6	-1.6827	0.0014
PC aa C34:4	-1.6907	0.0028

Figure 8. Volcano plot of features with t-test p-value <0.01 and FC >1.5 for high and low methylation groups.

Group separation: As shown in Figure 9, an unsupervised principal component analysis (PCA) was performed to look for differences between the high and low methylation groups, but did not find a high degree of natural separation. Supervised Partial least squares Discriminant Analysis (PLS-DA) yielded good separation, but the permutation statistic (p=0.18) suggested that this may be an artefact of the general variation in the dataset. Nonetheless, PCs were again selected as the most important discriminating

features in PLS-DA-based separation, and are lower in abundance in the chronic stress group. Carnitine was increased in the chronic stress group.

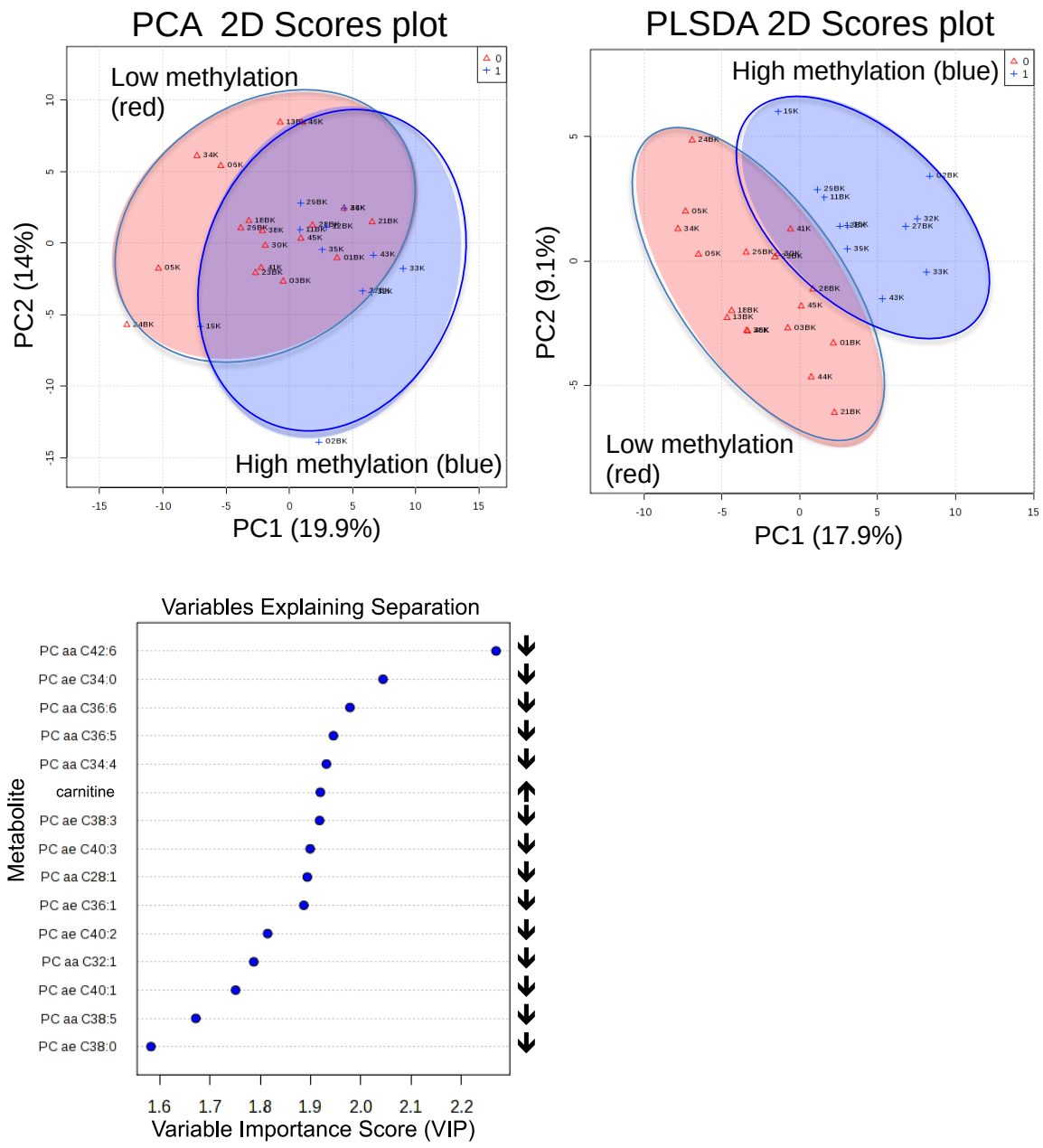

Figure 9. PCA and PLSDA plots of separation between the high (blue) and low (red) methylation groups, with 15 most important Variables in Projection (VIP).

3-group analysis: Having verified that there are features that discriminate between the high and low methylation groups, the 'average' group (n=12) was reintroduced as a third group in the analysis. The use of non-parametric ANOVA identified a similar set of important features to that identified in the two-group analysis. More importantly, it was now possible to observe trends in metabolite concentration that validate their association with methylation percentages. Using a correlation analysis, it was possible to identify a negative correlation between long-chain PCs and methylation at promoter sites, and a positive correlation between concentrations of carnitine and methylation (Figure 10).

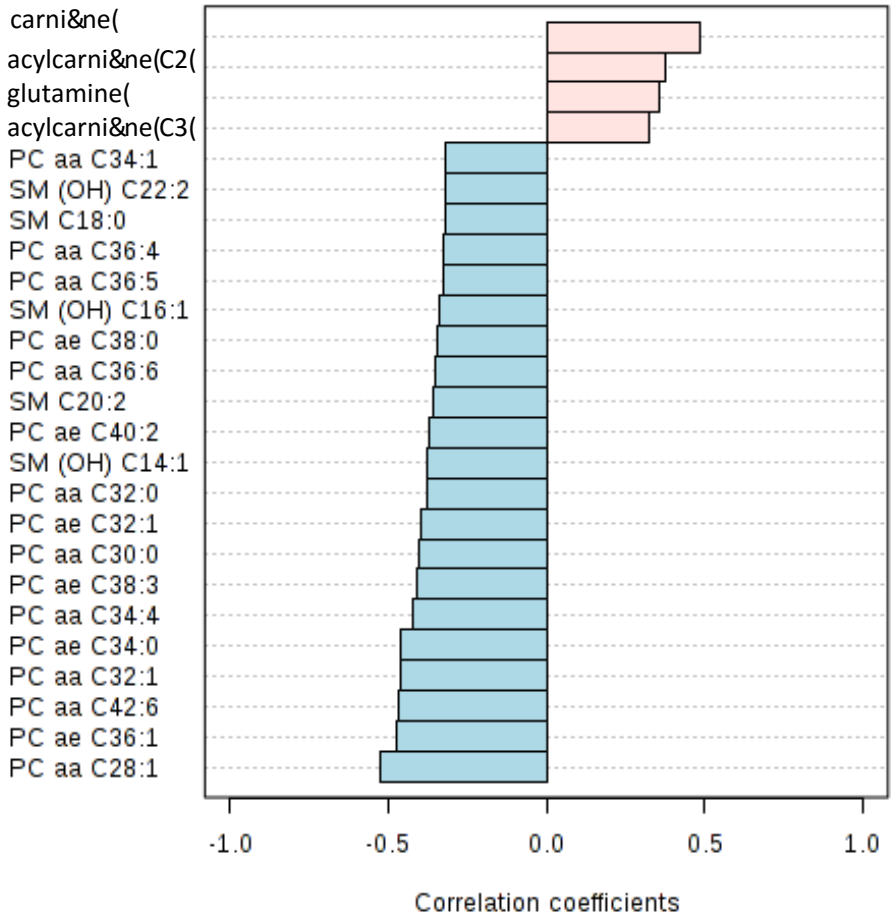

Figure 10. Pearson correlation analysis of compounds associated with a non-continuous measure of average methylation at promoter-associated sites.

Statistical analysis using non-parametric ANOVA found that there was a statistically significant (raw p-value <0.05) difference between groups for these features. Boxplots demonstrate how carnitines concentrations increased and PCs concentrations decreased from the low to medium to high methylation groups (Figure 11).

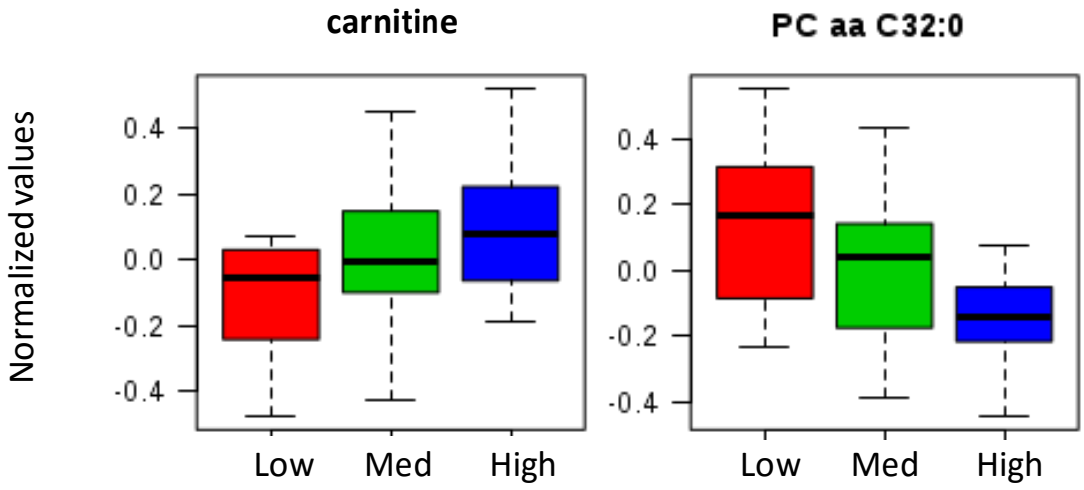

Figure 11. Comparison of metabolite concentrations between low, medium, and high methylation groups.

Separation using 3-dimensional PLS-DA also showed good separation between the low and high group, with the average group distributed between these two groups (Figure 12).

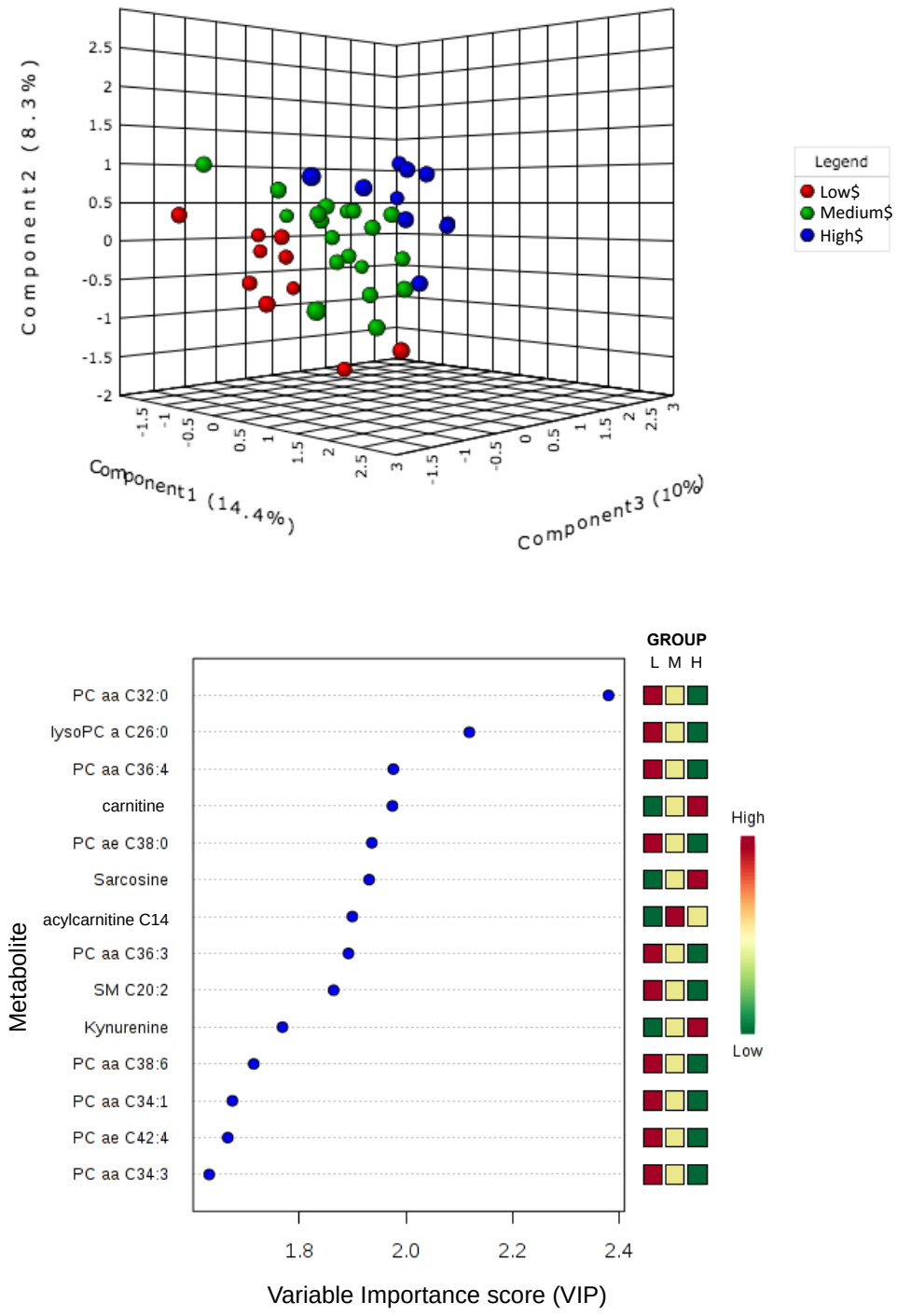

Figure 12. PLS-DA (3 components) of low, medium, and high methylation groups and important variables for separation.

Results of untargeted metabolomics analysis

To characterize previously unreported metabolite biomarkers of chronic stress, comprehensive untargeted metabolomic profiling was also performed using two separate extraction and chromatography methods to analyse lipophilic metabolites (e.g., acylcarnitines, phospholipids, fatty acids, bile acids) and water-soluble, highly-polar metabolites that can be detected without derivatization (e.g., small sugars, amino acids). Sample preparation for polar metabolites used a higher starting volume of serum and SPE to remove high-abundance lipids, in order to increase the detection of polar metabolites which are present in lower abundance. Results of targeted data analysis, specifically the observed correlation between metabolite features such as PCs and carnitines and methylation percentage, supported our assumption that high and low groups were likely to be the most distinct, so these groups were used for untargeted data analysis.

A large number of spectral features were identified via XCMS processing of the four data sets (Table 4). A subset of features was identified as "important" because their peak intensities showed a fold change of >1.5 between the groups, with a t-test p-value <0.05. Mass-to-charge ratios for important features were searched in METLIN and the HMDB in an attempt to for the purpose of identification, but only a small portion of features could be assigned to metabolites this way. The spectra in this untargeted dataset, collected on the Waters Synapt instrument, had a mass accuracy of >10 ppm, which made confident assignment difficult.

Table 4. Significant features identified by Untargeted metabolomics analysis

Dataset (extraction type & ion mode)	Groups found after processing with XCMS	Important features identified	Number of tentative identifications possible
Non-polar / Negative	1773	22	8
Non-polar / Positive	2299	23	9
Polar / Negative	574	80	7
Polar / Positive	697	43	6

Nonetheless, a number of phospholipids, which were detected in the positive ion mode after lipophilic extraction, were found to be at lower abundance in the highly methylated group. These included phosphotidylcholines (PCs), phosphotidylethanolamines (PEs), phosphatidyl-inositols (PIs) and phosphatidylserine (PS) (Table 5).

Table 5. Putative Metabolite IDs

Extraction Type	Ion Mode	m/z	Δ ppm	Adduct	Putative Assignment	Formula	Retention Time (min)	Fold Change	p-value
Lipophilic	Neg	422.229	3	[M-H]-	Phosphatidyl Ethanolamine (14:1)	C19H38NO7P	9.62	1.5495	0.0310
Lipophilic	Neg	827.469	2	[M-H]-	Phosphatidyl Inositol (34:5)	C43H73O13P	15.74	-1.5194	0.0365
Lipophilic	Neg	724.489	21	[M-H]-	Phosphatidic Acid (38:4)	C41H74O8P	17.05	-1.7579	0.0311
Lipophilic	Neg	662.489	19	[M-H]-	Phosphatidyl Ethanolamine (30:0)	C35H70NO8P	17.06	-1.6921	0.0483
Lipophilic	Neg	748.525	4	[M-H]-	Phosphatidyl Ethanolamine (38:5)	C43H76NO7P	17.21	-1.5873	0.0426
Lipophilic	Neg	772.513	19	[M-H]-	Phosphatidyl Ethanolamine (40:7)	C45H76NO7P	22.05	-1.6131	0.0289
Lipophilic	Pos	280.264	2	[M+H]+	Linoleoyl ethanolamide	C18H33NO	10.38	-1.8131	0.0411
Lipophilic	Pos	879.495	4	[M+Na]+	Phosphatidyl Inositol (36:5)	C45H77O13P	17.09	-1.7807	0.0166
Lipophilic	Pos	700.522	3	[M+Na]+	Phosphatidyl Ethanolamine (32:0)	C37H76NO7P	17.09	-1.8462	0.0476
Lipophilic	Pos	714.482	19	[M+Na]+	Phosphatidyl Serine (30:0)	C36H70NO9P	17.70	-1.5121	0.0332
Lipophilic	Pos	732.560	9	[M+H]+	Phosphatidyl Choline (32:1)	C40H78NO8P	18.25	-1.5539	0.0050
Aqueous	Neg	179.054	7	[M-H]-	Hexose	C6H12O6	4.55	-2.7098	0.0126
Aqueous	Neg	229.142	9	[M-H]-	Dodecanedioic acid	C12H22O4	11.14	-2.0144	0.0105
Aqueous	Pos	271.986	3	[M+Na]+	Dichloro-tyrosine	C9H9Cl2NO3	2.42	-1.5538	0.0238
Aqueous	Pos	195.088	10	[M+H]+	Methyl-myo-inositol	C7H14O6	5.40	-2.9030	0.0317
Aqueous	Pos	468.313	5	[M+H]+	Arachidonoyl tyrosine	C29H41NO4	11.32	-1.5987	0.0245

In particular, PC C32:0, identified in the data acquired in the positive ion mode and shown in Figure 13, has a fold value that are very similar to that observed for PC C32:1 in the targeted data.

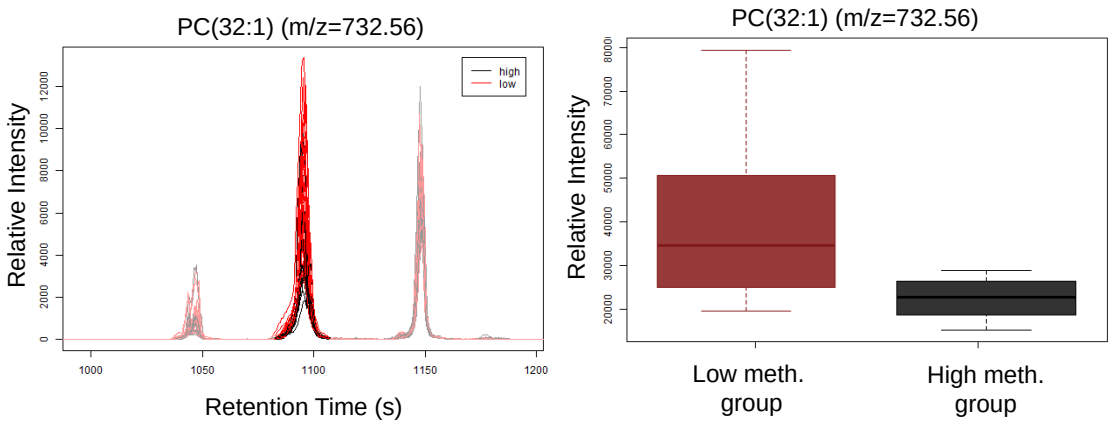

Figure 13. Boxplots and extracted ion chromatogram for PC C32:1 (FC=1.55, p = 0.0050)

Discussion

Phosphatidylcholines and other phospholipids in chronic stress

Physiological role of phosphatidylcholines: PCs are highly abundant phospholipids composed of two fatty acid chains bound to a glycerol backbone with a choline-and-phosphate headgroup. (Figure 14).

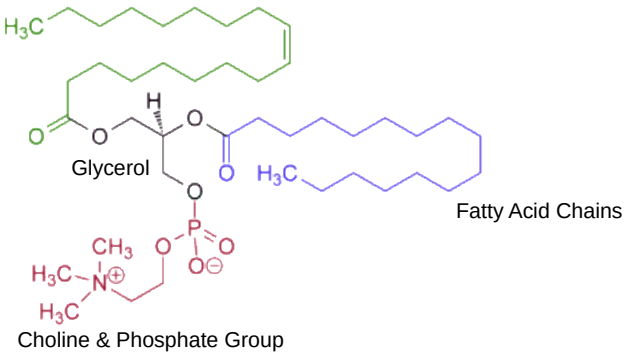

Figure 14. Generic structure of a phosphatidylcholine

PCs are synthesized through the cytidine diphosphate (CDP)-choline pathway [128][129]. In this pathway, 'salvaged' choline is phosphorylated, after which it is converted into CDP-choline and condensed with cytidine triphosphate (CTP). Diacylglycerol then replaces cytidine monophosphate (CMP), producing phosphocholine. PC synthesis therefore depends on a dietary source of choline and a population of diacylglycerols. Because of the heterogeneity of diacylglycerols, the synthesis pathway allows for the production of a variety of PC species with varying chain lengths and degrees of saturation. Of these, the diacyl (aa) species are most common in plasma. Their versatile structures – with varying lengths of fatty acids and degrees of saturation – enables them to mediate the viscosity of lipid bilayers. They are therefore the key building blocks of cell membranes, making up much of the outer leaflet of the plasma membrane. They are also found circulating in plasma at high concentrations, as they are an essential component of lipoproteins, especially high-density lipoprotein (HDL). While their principal function is structural, they are also considered to have multiple roles in cell signalling [130].

PCs concentrations are inversely correlated with the percentage of GR promoter methylation: Both targeted and untargeted metabolomics methods found lower significantly concentrations of specific long-chain PCs in the group showing high levels of GR promoter methylation, providing a high degree of confidence in their identification as important features. While the fold change is not dramatic (~1.6x), the p-values of statistical significance are strong (<0.005) in both cases. The step-wise drop in PC content between the low, medium and high group as determined by correlation and 3-group analysis (ANOVA) provide further evidence of a real relationship between the concentration of the PCs and methylation percentage at GR promoter-associated sites.

Various species of PCs are affected: In the targeted analysis portion of this study, we quantified 71 PCs with total chain-lengths (summed between the two fatty acids) from 28-42 carbons, and varying degrees of saturation. The majority of these are toward the high end of the carbon count -- as the number of carbons increase, a larger number of distinct species appear corresponding to the additional double-bonds that are now possible with longer chain-lengths. The average total abundance of all phosphatidylcholine species was 712 µM, of which 90% (647 µM) was comprised of

diacyl species and 10% (65 uM) was comprised of akylacyl species. Most of the individual PC species each only account for ≤1% of the total PC concentration (n=61, total abundance = 16%). (Figure 15).

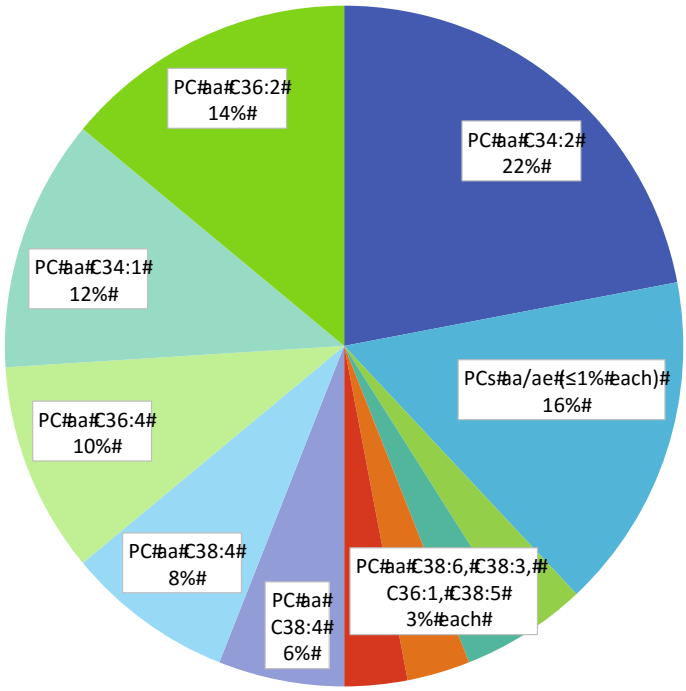

Figure 15. Proportion of total PC abundance accounted for by different groups of PC subspecies.

The type (aa/ae), chain-lengths, and degrees of saturation observed in the PCs that were identified as important features are reflect the distribution of these features in the list of all PCs quantified, irrespective of their total abundance. For instance, both diacyl (aa, n=36) and akylacyl (ae, n=35) species are equally represented in the list of metabolites quantified and also in the list of important features (from 2-group analysis, aa: n=7 and ae: n=7 with Variable Importance in Projection Score (VIP score) >1.6). Overall, PCs make up a large proportion of the targeted compounds (71 out of 141). However, they are still over-represented in the "important features list" as compared to the other classes of metabolites quantified (14 out of 15 metabolites with VIP score >1.5). A significant number of sphingomyelins (n=15), which share some membrane structure functions with PCs, were quantified but did not appear to be as strongly associated with GR promoter

methylation as PCs. Perhaps more importantly, all of the identified PCs, regardless of the species, show the same trend of lower concentration in the high methylation group, whereas carnitines and acylcarnitines quantified in the same assay are increased in the high methylation group.

Given the scope of the metabolites targeted and the analytical approach used, this work cannot provide information about the potential roles of other PC species not quantified or about the specific compositions (i.e., the individual chain length and double-bond placement) of the long-chain species. Without detailed information about the exact structures of the lipid species measured, it is difficult to know whether some of the PCs have unique roles (e.g., for signalling, enzymes, etc.) However, the findings overall indicate an important role for long-chain PCs, including very long chain polyunsaturated fatty acids. Specific long-chain PCs have been shown to destabilize HDL [131]. Long-chain PCs are also involved in the transport of fatty acids from the inter-membraneous space in the mitochondria into the mitochondrial matrix during the breakdown of lipids for the generation of metabolic energy.

Associated pathways: PCs are involved in a variety of pathways. Phosphatidylethanolamines (PEs) are converted to PCs in the methionine pathway during the process of DNA, RNA, protein, and lipid methylation [132]. However, the epigenetic model here is based on persistent methylation of only specific CpG sites in the region of GR promoter, so it is not clear what role pathway-level effects could have on maintaining this epigenetic mark.

Several of the *putative* IDs (PEs, PIs, PS) from the untargeted data can be mapped to glycerophospholipid metabolism [133], suggesting a potential relationship of chronic stress to phospholipid biosynthesis. An effect on phospholipid biosynthesis has been previously suggested in the literature, with specific reference to PCs, which were altered in the plasma of rats in a CUMs model of chronic stress [113]. However, interpretation of the results presented depends on the mechanism by which phospholipid synthesis is altered. For instance, phospholipids depend on a similar fatty acid pool for synthesis, so it would be expected that SMs would be similarly decreased if the availability of fatty acid precursors was a significant factor [134]. Furthermore, if a specific step in fatty acid

biosynthesis were affected, it might be expected to result in observable relationships between the affected lipids. For example, an effect on steaoryl-CoA desaturation might mean that the most important features were lipids of the various approximate chain lengths, but with a similar degree of saturation. Effects on enzyme-dependent elongation might result in the identification of PCs with similar levels of saturation but a disparity in the common chain lengths. Alternatively, changes in phospholipid concentration could be attributed to degradation instead of synthesis. The concomitant increases in carnitine may also suggest a relationship to fatty acid degradation, since carnitine and acylcarnitines are associated with transferring fatty acids into the mitochondria for beta-oxidation [133].

Important caveats

The interpretation of data from these samples is restricted by limitations associated with the study design. Because of the large number of features present in untargeted metabolomics data, it is necessary to create discrete groups that can be compared for statistical purposes, but such binary groupings are inherently artificial in human populations, especially when attempting to separate a complex human population on the basis of a continuous feature such as stress responsiveness or other psychological traits. With complex conditions such as chronic stress, one of the biggest challenges is producing meaningful groups that are most likely to have clinical applicability. In fact, this challenge is shared by many other research areas (e.g., cancer, metabolic syndrome) where patients given the same diagnosis may actually consist of distinct subpopulations based on molecular features which are associated with specific profiles of symptoms, disease progression, and treatment responsiveness.

Meaningful interpretation of the methylation data is challenging, especially given that previously published relationships between methylation and early life stressors were not reproduced in the present study. Neither the combined methylation values nor the methylation at any individual site correlated significantly with any measure or combined measure of pre- or peri-natal stress as was expected. This necessitated the approach of grouping samples into ‘high’ and ‘low’ average promoter-associated methylation based on deviation from the mean at 24 sites. However, the lack of reference values for methylation beta values at specific CpG sites means that these groupings depend on

deviation within a small population. Whether these values are generally high, low, or average with respect to the broader population is not known, and because patients were recruited through the Psychotraumatology clinic, they may not be representative. The values obtained (i.e., beta values) are based on a relative measure (chemiluminescence) so they cannot be readily compared across studies.

Individuals' average methylation at 24 promoter associated sites was found to have a weak but statistically significant positive correlation with hair cortisol level ($R=0.312$, $p=0.035$), which is believed to be a more reliable indicator of individuals' stress "traits" than other sampling strategies [88]. However, as discussed in the introduction, the role of the HPA in chronic stress is unclear, so the association of methylation levels with cortisol levels may not be informative about the significance of methylation at these sites. Furthermore, the statistical significance of this association was eliminated when a high-methylation, high-cortisol outlier was removed.

The annotation of which sites are promoter associated was based on information generated by Dr. Radtke. However, on closer examination, several of the sites identified as "promoter-associated" were highly methylated (beta values of 0.38-0.83), suggesting that these may be misannotated. Three of these (positions 142780254, 142781498 and 142781532) were found to be promoter-associated only in specific cell types, and thus were probably not relevant for analysis performed on peripheral blood. Some studies have questioned altogether the relevance of methylation of the NGFI-A binding site in specific human tissues [135], while others have argued that DNA methylation in peripheral cells is equally informative [124]. While the mechanism by which increased methylation modulates GR expression is well understood, the significance of DNA methylation at this site in peripheral blood is unclear, since it is GR expression in the hypothalamus and pituitary that would be responsible for negative feedback. Since the original analysis of this data, new publications from Radtke's group have identified additional CpG sites that may be associated with early life stressors using a similar Illumina-based analysis [127]. The new information might help to clarify which sites are relevant for classifying patients into groups.

Small group size is also a major limitation of this study. The exclusion of the mid-range

samples and the heterogeneity of the patient population (both sexes, ages 11-21) exacerbate this issue. It is well known that analysis of highly multivariate data with small group sizes and high variability is biased toward finding differences between groups [136]. While significant psychiatric information was available for the patients, clinical information such as BMI was not available, but would be very important for interpreting the findings about fatty acid metabolism/degradation.

Finally, the samples themselves pose some concerns: anomalously low hexose measurements were observed across many of the samples, suggesting that there may be issues with the quality or storage of the samples. The date of sample collection could not be ascertained from the collaborators, but the samples were most recently aliquoted in 2012, meaning that they may have been stored for 2-4 years, likely resulting in the degradation of some metabolites in the samples.

Next steps

Confident identification of metabolites of interest from the untargeted data is challenging, given the low mass accuracy of the dataset. While it might be possible to make additional identifications from the raw data or put additional effort into pathway mapping, it did not make sense to undertake these efforts given the limitations resulting from the sample set, the study design, the untargeted data quality, and the lack of additional sample volume for follow-up experiments. Instead, it was decided to follow the clues provided by this data by taking a hypothesis-driven approach, using targeted metabolomics methods to explore potential mechanisms of phospholipid depletion in additional models of chronic stress.

Chapter 2:
Development of Methods to Analyze Aldehyde Markers of Oxidative Stress as a Potential Feature of Chronic Stress

Chapter Summary

Background: Based on a mounting body of evidence for the relationship between oxidative stress and chronic stress, biomarkers of oxidative stress were selected as targets for further study, with a particular emphasis on aldehydes as markers of lipid peroxidation. To overcome limitations in existing methods for the quantitation of aldehydes, I developed and validated a new method to quantify malondialdehyde (MDA).

Methods: An assay for accurate quantitation of MDA in human plasma was developed using a multiple reaction monitoring-mass spectrometry (MRM-MS) approach, using chemical derivatization with 3-nitrophenylhydrazine, isotope-labeling, and liquid chromatography (LC) with electrospray (ESI)-tandem mass spectrometry. A proof-of-principle project also demonstrated that 3-nitrophenylhydrazine can be used under alternative reaction conditions to derivatize a wide panel of other aldehydes for quantitation.

Results: The assay for MDA was found to be linear ($R^2 = 0.9999$) over a 10,000-fold concentration range with a lower limit of quantitation of 30 fmol (on-column). Intra- and inter-run coefficients of variation (CVs) were <10%. The derivative was stable for >36 hours at 5ºC. Standards spiked into human plasma had recoveries of 92-98%. Comparison with a commonly used LC-UV method for quantifying MDA showed strong agreement between the two methods. A pilot project to quantify MDA in human plasma samples (n=26) from patients in a study of major depressive disorder with winter-type seasonal pattern (MDD-s) confirmed previously known associations between plasma MDA concentrations and measures of obesity ($p<0.02$).

Conclusions: The LC/MRM-MS method provides high sensitivity and high reproducibility for quantifying MDA in human plasma. The simple sample preparation and rapid analysis time (5 times faster than LC-UV methods) provides high throughput suitable for large-scale clinical applications.

Introduction

Oxidative stress as a potential feature of chronic stress

In the first part of this project, we identified phospholipid depletion as a potential feature of chronic stress. Based on the known association between lipid degradation and oxidative stress, and a mounting body of evidence for a relationship between oxidative stress and chronic stress, we elected to pursue the hypothesis that oxidative stress and the associated lipid peroxidation may be responsible for the decreased abundance of serum phospholipids observed in chronic stress. If oxidative stress is found to be a feature of chronic stress, this would offer significant insight into how chronic psychosocial stress produces long-term health risks.

Background on Oxidative stress: Oxidative stress occurs when the body's scavenging systems are unable to detoxify reactive oxygen species (ROS) as quickly as they are produced. It is a known feature of many health conditions, including a predisposition to or manifestation of cardiovascular disease, diabetes, cancer, and acute tissue injury [137-147]. The ROS produced in oxidative stress cause cellular damage through non-specific reactions with lipids, proteins, and DNA, producing a variety of markers. Low molecular weight aldehydes, such as maldondialdehyde (MDA), result from the peroxidation of lipids and, as reactive compounds themselves, form part of a positive feedback cycle that causes further cellular damage.

Links between oxidative stress & chronic stress: A number of studies have already drawn a direct connection between psychosocial stress and oxidative stress, including a large number of studies of acute and chronic psychological stress in rodents and people [111, 148, 149]. In rodents, several types of acute psychosocial stress induce oxidative stress including restraint stress, noise stress, and communication box stress [150-152] In humans, oxidative stress is associated with a variety of psychiatric disorders, particularly those with anxious features [143, 153]. Biomarkers of oxidative damage to DNA have also been found in various models of human stress, including acute stress (e.g., students on exam days) and chronic stress (e.g., work burn-out or caregiving stress) [154, 155].

Various mechanisms have been proposed to explain the link, including both cortisol-

dependent and cortisol-independent mechanisms. For instance, one study found that anticipatory cortisol response correlated with elevated F2-isoprostanes (a marker of lipid peroxidation) and 8-oxoG (a marker of DNA oxidative damage) but only in individuals who had been subjected to chronic stress [155]. Oxidative stress can also be directly induced by corticosterone treatment [156]. However, it has also been suggested that protein expression changes in psychosocial stress may be responsible for the increase in oxidative stress [157].

Oxidative stress is clearly associated with phospholipid degradation, including degradation of PCs and PEs [158], which could potentially help explain the observation that increased GR promoter methylation is associated with decreased phospholipid levels.

Methods for quantifying oxidative stress

The instability of the ROS produced in oxidative stress has traditionally made these direct markers difficult to study [159]. Direct measurement of ROS is challenging due to their reactivity, so most existing tests for oxidative stress measure products of oxidative damage (Figure 16).

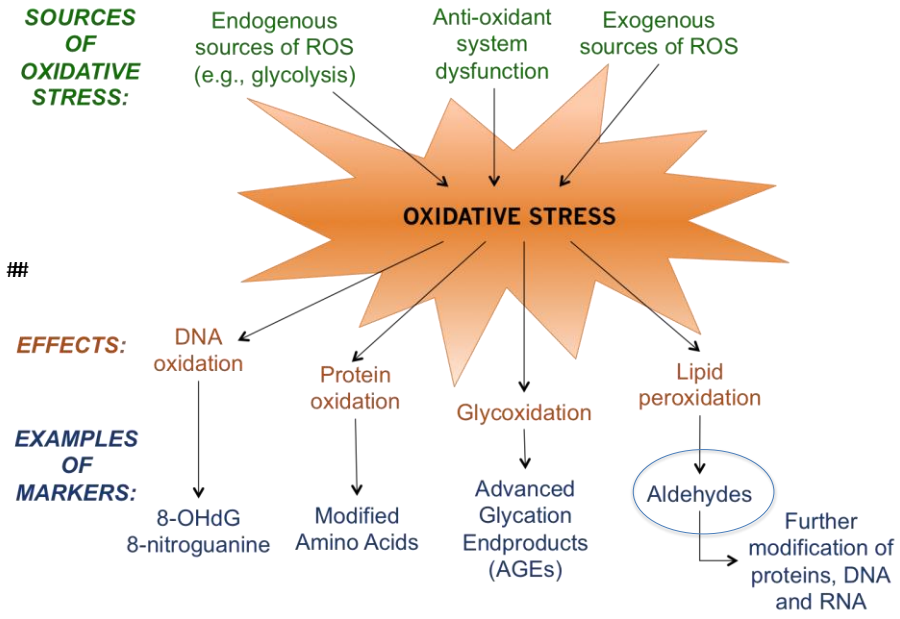

Figure 16. Markers of oxidative stress.

Aldehydes are small lipid peroxidation products, with structures characterized by the presence of one or more carbonyl groups. Aldehydes are relatively stable and can easily diffuse across and outside of the cell, making them an attractive target for measurement [144, 158].

They are also part of a positive feedback cycle in oxidative stress: as reactive species themselves, they exert carbonyl stress and go on to further modify additional proteins, DNA, and RNA. Given that our purpose is to investigate, in particular, effects associated with lipid peroxidation in oxidative stress, aldehydes offer opportune targets.

Challenges with existing methods for quantitation: Extensive research has been published on aldehyde biomarkers, which can be found at high concentrations in peripheral biofluids such as blood. However, while these markers are well-established and widely used, there are caveats associated with their use, particularly with respect to the accuracy, robustness, sensitivity, and specificity of their measurement. Much of the existing research has focused on a handful of targets, including malondialdehyde (MDA), which is a marker of the oxidation of polyunsaturated fatty acids.

MDA's wide usage as a marker of oxidative stress is reflected in the large number of methods that have been published describing its quantitation. However, despite significant development efforts, there continue to be challenges associated with its measurement by available methods. For example, MDA is still commonly measured with the thiobarbituric acid (TBARS) assay, i.e., liquid chromatography (LC) with ultraviolet (UV) detection [160, 161], but this assay has very low analytical specificity and has been shown to overestimate MDA concentrations and potentially obscure inter-individual variations in MDA levels [162]. Alternatively, MDA is sometimes measured by derivatization with 2,4-dinitrophenylhydrazine (DNPH) followed by LC-UV at a detection wavelength of 310 nm [163]. While this method is considered very reliable and highly specific, it requires >100 µL of plasma and has limited analytical sensitivity, typically achieving lower limits of quantitation (LLOQs) of >0.25 µM [163, 164] . Its throughput is also limited because the assay's specificity depends on an extended gradient elution to separate the DNPH-MDA derivative from interfering compounds, which requires analysis times of 15-35 minutes per sample [163-165] A method has

been published using TBA derivatization with visible light detection and a significantly shorter gradient (8 minutes per sample) [166], but this method requires additional extraction steps to remove interfering compounds, which prolongs and complicates sample preparation. Moreover, the visible light detection method has a limited linear range (0.28-6.6 µM) that does not allow for accurate measurement of plasma MDA concentrations of >6.6 µM, which are commonly reported within the physiological range [162, 165]. Methods for measuring MDA using gas chromatography (GC)-MS do offer increased specificity and modest increases in sensitivity, but their linear range remains limited (0.156-5.0 µM), run times exceed 20 minutes, and extensive sample preparation is often required [167].

As discussed in the Introduction, LC-MS/MS-based metabolomic methods offer a number of advantages that make them compatible with complex samples, low-abundance metabolites, and high multiplexing, while offering a very high level of sensitivity and specificity. The objective of this portion of the project was therefore to develop new MRM-MS methods to improve on the quantitation of MDA and other aldehyde biomarkers of lipid peroxidation. The assays were intended to expand the range of targets, provide higher throughput, and offer enhanced sensitivity and specificity over currently used methods. These enhanced tools for studying oxidative stress will allow us to collect high quality evidence to test the hypothesis that oxidative stress is a central feature of chronic stress.

Materials & Methods

Standards & Reagents

Target selection: PubMed and the HMDB (www.hmdb.ca) were searched to identify aldehydes that were endogenous in humans and had previously been reported as potential biomarkers of lipid peroxidation. The search identified 24 candidate aldehydes, of which 15 were selected for screening and development on the basis that it was possible to obtain high-purity commercial standards for these compounds in a format compatible with MS analysis.

Chemical reagents: Aldehyde standards were purchased from commercial vendors. Propanal, butanal, 2-methylbutanal, pentanal, hexanal, heptanal, octanal, and decanal were obtained from Santa Cruz Biotechnology, Inc (Dallas, TX). Glyoxal, acetaldehyde, acrolein, malondialdehyde, methylglyoxal, and crotonaldehyde were purchased from Sigma-Aldrich (St. Louis, MO). 4-hydroxynonenal was purchased from Enzo Life Sciences (Farmingdale, NY). Analytical reagent-grade 3-nitrophenylhyrdrazine (3NPH.HCl), 2-nitrophenylhyrdrazine (2NPH.HCl), 4-nitrophenylhyrdrazine (4NPH.HCl), 2,4-dinitrophenylhydrazine (DNPH), 4-Phenylsemicarbazide hydrochloride (4-PSC), 3-Amino-9-ethylcarbazole (3-AEC), Girard's reagent T (GRT), Girard's reagent P (GRP), dansylhydrazine, N-(3-Dimethylaminopropyl)-N′-ethylcarbodiimide hydrochloride (EDC), and sodium cyanoborohydride ($NaBH_3CN$) were purchased from Sigma-Aldrich (St. Louis, MO). HPLC-grade pyridine, trichloroacetic acid (TCA), trifluoroacetic acid (TFA), sodium hydroxide (NaOH), and LC-MS grade acetonitrile(ACN), water, formic acid (FA), and acetic acid were also purchased from Sigma-Aldrich. For experiments involving aldehyde standards, stock solutions were prepared at a concentration of 10mM. Volatile aldehydes were handled in a fume hood.

Derivatizing reagents: EDC was prepared at a concentration of 150 mM in 50% acetonitrile with 6% pyridine. 2NPH, 4NPH, 3NPH and 2,4-DNPH were prepared at a concentration of 100mM in 50% acetonitrile. 4-PSC was prepared at a concentration of 25mM in methanol. $NaBH_3CN$ was prepared at a concentration of 50 mM in dH_2O. GRT was prepared at a concentration of 100mM in 50% acetonitrile. Dansylhydrazine and GRP were prepared at 100mM in 75% acetomitrile.

Calibration standards for 3NPH-MDA quantitation: For derivatization of MDA, 3NPH was prepared at a concentration of 100 mM in 75% acetonitrile containing 0.2% TFA. In these experiments, standard calibration solutions of MDA were prepared from a 10 mM stock solution using a dilution series to obtain concentrations of 2000, 400, 80, 16, 3.2, 0.64, 0.12, and 0.024 µM of MDA in H_2O.

Internal standard for 3NPH-MDA quantitation: $^{13}C_6$-3NPH.HCl was custom-synthesized by IsoSciences Inc. (King of Prussia, PA, USA). According to the accompanying certificate of analysis, the compound was structurally confirmed by 1H-

NMR spectroscopy on a Varian Mercury 300 MHz spectrometer (Palo Alto, California, USA) and by MS/MS on a Waters TQD triple-quadruple mass spectrometer (Billerica, MA, USA). The compound's chemical purity was determined by LC-UV to be 98.2%. The incorporation of six ^{13}C atoms into the benzyl ring of 3NPH was confirmed by ^{13}C-NMR spectroscopy and the isotopic purity was determined to be 99.0% by flow-injection analysis MS. The $^{13}C_6$-3NPH-MDA internal standard was prepared at a concentration of 5 µM by adding 200 µL of 1.25 mM MDA in 75% acetonitrile-0.2%TFA to a 3-mL borosilicate test tube containing 1 mg of $^{13}C_6$-3NPH.HCl. The mixture was reacted at 50ºC for 30 min, and then transferred to a volumetric flask and diluted with 20% aqueous acetonitrile to 100 mL. This solution was used as the internal standard (IS) for subsequent experiments. It did not show any observable degradation over >4 months when stored at -20ºC.

Human plasma samples

The human plasma samples (n=2) used for screening derivatizing reagents were purchased from BioreclamationIVT (Westbury, NY, USA). The human plasma sample used for 3NPH-MDA assay development was obtained by pooling 10 x 1 mL volumes of human plasma, also from BioreclamationIVT. Patient plasma samples used in the study of Major Depressive Disorder with seasonal-type pattern (MDD-s) and associated clinical data were provided by Dr. Walter Swardfager and Dr. Anthony Levitt, our collaborators at Sunnybrook Research Institute. The consenting of patients and collection and handling of clinical samples and data was performed at Sunnybrook Health Science Centre using protocols approved by their Research Ethics Board (Project #300-2014, Approval dated July 31, 2014). Analysis of the anonymized clinical samples was completed at University of Victoria under Human Research Ethics Board Approval (Ethics Protocol Number 16-014). All work involving human biofluids was completed in a laboratory at the UVic-Genome BC Proteomics Centre, under Biosafety Level 2 certification administered by Occupational Health and Safety and the University of Victoria.

Testing of Chemical Derivatization Reagents

For the initial screening of prospective derivatizing reagents, each of 9 reagents (3AEC, 2,4-DNPH, 2NPH, 3NPH, 4NPH, 4-PSC, GRT, GRP, and dansyl hydrazine) were tested

with standards of 4 selected aldehydes (MDA, glyoxal, acetylaldehyde, and crotonaldehyde) for the reagent's ability to yield complete reactions, a small number of products, and stable ionizable and detectable products. Aldehydes were individually prepared at a concentration of 5 µM in 50%-75% acetonitrile or methanol, depending on the intended reaction conditions. The reaction conditions tested were selected to mirror those published for use of the derivatization reagents for other targets, including the use of catalysts (e.g., pyridine) and condensing reagents (EDC). The concentrations of organic solvent in each reaction were adjusted through multiple iterations to ensure that the solubility of the derivatives was maintained. The reaction conditions used prior to MS screening of derivatives are shown in Table 6.

Table 6. Reaction conditions used in screening derivatizing reagents

Reagent	Reaction mixture	Reaction conditions
2NPH	50 µL aldehyde standard (1 mM, 50% ACN) 25 µL 2NPH (100 mM, 50% ACN) 25 µL EDC (150mM with 6%pyridine, 50% ACN)	Solvent: 50% ACN Time: 45 min Temp: 22ºC Quench with 400 µL H2O
4NPH	50 µL aldehyde standard (1 mM, 50% ACN) 25 µL 4NPH (100 mM, 50% ACN) 25 µL EDC (150mM with 6%pyridine, 50% ACN)	Solvent: 50% ACN Time: 45 min Temp: 22ºC Quench with 400 µL H2O
2,4-DNPH	50 µL aldehyde standard (1 mM, 50% ACN) 25 µL DNPH (100 mM, 50% ACN) 25 µL EDC (150mM with 6%pyridine, 50% ACN)	Solvent: 50% ACN Time: 45 min Temp: 22ºC Quench with 400 µL H2O
4-PSC	50 µL aldehyde standard (1 mM, 75% MeOH) 150 µL PSC (25mM, MeOH) 50 µL NaCNBH3 (50mM, H2O) 25 µL acetic acid	Solvent: 75% MeOH Time: 90 min Temps tried: 30,40,50ºC Quench on ice 1 min, then add 725 µL H2O
GRT	50 µL aldehyde standard (1 mM, 50% ACN) 100 µL GRT (100 mM, 50% ACN) 50 µL EDC (150mM with 6%pyridine, 50% ACN)	Solvent: 50% ACN Time: 45 min Temps tried: 30, 40 ºC Quench on ice 1 min, then add 800 µL H2O
GRP	50 µL aldehyde standard (1 mM, 75% ACN) 100 µL GRP (50 mM, 75% ACN) 50 µL EDC (150mM with 6%pyridine, 75% ACN)	Solvent: 75% ACN Time: 45 min Temp: 30 ºC Quench on ice 1 min, then add 800 µL H2O
Dansyl-hydrazine	50 µL aldehyde standard (1 mM, 75% ACN) 100 µL DH (50 mM, 75% ACN) 50 µL EDC (150mM with 6%pyridine, 75% ACN)	Solvent: 75% ACN Time: 45 min Temp: 30 ºC Quench on ice 1 min, then add 800 µL H2O

3NPH (basic) – initial screening	50 µL aldehyde standard (1 mM, 75% ACN) 100 µL 3NPH (50 mM, 75% ACN 50 µL EDC (150mM with 6%pyridine, 75% ACN)	Solvent: 75% ACN Time: 45 min Temp: 30 ºC Quench on ice 1 min, then add 800 µL H2O
3NPH (basic) - further screenng	100 µL aldehyde standard (0.5 mM, 75% ACN) or human plasma extract (75% ACN) 50 µL 3NPH (100 mM, 75% ACN 50 µL EDC (150mM with 6%pyridine, 75% ACN)	Solvent: 75% ACN Time: 45 min Temp: 30 ºC Quench on ice 1 min, then add 800 µL H2O

The use of 3NPH under basic conditions was further tested by performing the derivatizing reaction on a wider panel of aldehyde standards and on extracts from human plasma samples taken from two different patients. For this experiment, a mixture of 15-aldehyde standards was prepared in 75% ACN, containing glyoxal, acetylaldehyde, MDA, methylglyoxal, 4-HNE, crotonaldehyde, 4-ONE, 2-methylbutanal, propanal, butanal, pentanal, hexanal, heptanal, octanal, and decanal, each at 0.5 mM. Plasma extracts were prepared for derivatization by adding 300 µL of ACN to 100 µL of human plasma, mixing, centrifuging at 4 ºC for 15 minutes at 2762 x g, and collecting the supernatant.

Mass spectrometry for screening of derivatization products

The products of each derivatization reaction were assessed by injecting 10 µL of the reaction mixture into an Acquity UPLC system (Waters Corp., Milford, MA) coupled to a Synapt HDMS quadropole time-of-flight (QTOF) MS (Waters).

To screen derivatives from reactions with 2NPH, 3NPH, 4NPH, DNPH, PSC, and GRT, reversed phase liquid chromatography (RPLC) was performed on a Waters BEH C_{18} (2.1 x 100nm x 1.7) column, using water with 0.01% FA (solvent A) and ACN with 0.01% FA (solvent B) as the mobile phase to elute the derivatives from the column. The column flow rate, column temperature, and autosampler temperature were set at 0.35 mL/min, 40ºC, and 4ºC. The time and slope of the elution gradient was modified for each derivatizing reagent tested, depending on the percentage of organic solvent in the derivative sample following the reaction and the predicted chemical properties of the derivative (e.g., polarity, size). Typically, solvent B was increased from 5% to 85% over a total period of 10 to 15 minutes. Gradient elution was followed by a column wash step

of at least 2 minutes with 100% Solvent B, and an equilibration period of 3 minutes at the initial solvent composition before injection of the next sample.

To screen derivatives from reactions with GRP and DH, hydrophilic interaction liquid chromatography (HILIC) was performed on a Waters Atlantis amide column (2.1 mm I.D. x 100 mm, 1.7 µm particle size), using 90% ACN with 2mM NH_4Ac (solvent A) and water with 2mM NH_4Ac (solvent B) as the mobile phase. The column flow rate, column temperature, and autosampler temperature were set at 0.3 mL/min, 40ºC, and 4ºC, respectively. A linear elution gradient was used: Solvent B was increased from 5% to 90% over 11 minutes, followed by a 4 minute column wash step with 100% Solvent B, and an equilibration period of 3 minutes at the initial solvent composition before injection of the next sample.

Depending on the predicted derivatives for a given experiment, the instrument was operated in either negative or positive ion mode with a wide scan range (m/z 100-1200) intended to encompass both singly- and doubly-derivatized aldehyde products of the reaction. Prior to use, the instrument was tuned using a lockmass spray containing leucine encephalin, and calibrated with sodium formate. The lockmass spray was continuously injected at a flow rate of 10 µL/minute and was used to maintain mass accuracy throughout data acquisition. Individual ESI-MS parameters were adjusted prior to each experiment during tuning to compensate for variations in instrument performance (e.g., fluctuations in sensitivity). An example of typical operation parameters for ESI-MS is: spray voltage, -2.8 kV in negative ion mode or 3.0 kV in positive ion mode; desolvation gas (N2) flow and temperature, 750L/h and 350ºC; drying gas (N2) flow and temperature, 50L/h and 125ºC; sampling cone voltage, 35V; extraction cone voltage, 4V; data acquisition rate, 0.25s; collision cell background gas (Ar), 0.5 mL/min. UPLC-MS spectra were processed using the MassLynx software suite (Waters).

Optimization of Chemical Derivatization of MDA with 3NPH

In order to develop a derivatization strategy that was compatible with quantitation of MDA, we tested the use of 3NPH under acidic conditions. 3NPH was prepared at a concentration of 50mM in 75% ACN with 0.2% TFA. A standard solution of 5 µM of MDA in water was used to optimize reaction conditions. 100 µL aliquots of 5 µM MDA

standard solution were mixed with 100 µL of 50 mM 3NPH in 3-mL borosilicate test tubes. The mixtures were individually reacted at different temperatures (0, 10, 20, 30, 40, 50, 60, 70, and 80ºC) and for different time periods (0, 10, 20, 30, 40, 60, and 70 min). After reaction, the mixtures were cooled on ice for 1 min before being diluted with 600 µL of water. LC-MS analysis was performed by injecting 10 µL aliquots of each sample.

Mass spectrometry (LC/MRM-MS)

Transition Optimization: Multiple reaction monitoring (MRM) transitions were optimized via direct infusion of the derivatives in 0.01% FA on an AB 4000 QTRAP mass spectrometer. For all of the derivatives, the Q1/Q3 pairs were evaluated in the MRM scan mode to optimize the collision energies for each analyte, and the two most sensitive pairs per analyte were selected as the transitions to be monitored. For 3NPH derivatives of various aldehydes produced under weakly basic conditions, the instrument was operated in negative ion mode. For 3NPH-MDA, the same instrument was operated in positive ion mode.

In negative ion mode, full-mass Q1 scans were performed over the mass range from m/z 50 to 500 in profile mode, using a 0.5-second scan time. In the enhanced product ion scans, the collision-induced dissociation (CID) fragment ions were produced by ramping the collision energy for the precursor ion from -110 V to -5 V in the collision cell, and the resulting fragment ions were detected using the Q3 mass analyzer to obtain the Q1/Q3 pairs. The nebulizer, curtain, collision, and auxiliary gas (N2) flows, as well as the temperature of the auxiliary gas, were optimized for the UPLC/MRM-MS runs during continuous injection of a solution of the derivative. The optimized ESI-MS parameters determined in this manner were: ESI capillary voltage, -4200V; nebulizer gas (N_2), 25 (arbitrary units); curtain gas (N_2), 20 (arbitrary units); collision gas (N_2), 15 (arbitrary units); entrance potential, 10 V; collision cell exit potential, 20 V. The drying gas (N_2) flow and temperature were 35 (arbitrary units) and 500ºC, respectively.

In positive ion mode, full-mass Q1 scans were performed over the mass range from m/z 50 to 400, using a 0.5-second scan time. In the enhanced product ion scans, the collision-induced dissociation (CID) fragment ions were produced by ramping the collision energy for the precursor ion from 110 V to 5 V in the collision cell, and the resulting fragment

ions were detected using the Q3 mass analyzer to obtain the Q1/Q3 pairs. The nebulizer, curtain, collision, and auxiliary gas (N_2) flows, as well as the temperature of the auxiliary gas, were optimized for the UPLC/MRM-MS runs during continuous injection of a solution of 3NPH-MDA. The optimized ESI-MS parameters determined in this manner were: ESI capillary voltage, 4000V; nebulizer gas (N_2), 40 (arbitrary units); curtain gas (N_2), 35 (arbitrary units); collision gas (N_2), 15 (arbitrary units); entrance potential, 10 V; collision cell exit potential, 20 V. The drying gas (N_2) flow and temperature were 35 (arbitrary units) and 500ºC, respectively. Q1 and Q3 were set to unit resolution during the UPLC/MRM-MS runs. The same parameters were used to obtain transitions for the isotope-labeled $^{13}C_6$-3NPH-MDA derivative.

Data acquisition for quantitation of 3NPH-MDA: The highest-sensitivity MRM transition with acceptable background was used for quantitation. The second most sensitive transition was selected as the "qualifier" and was used to verify the identity of the compound based on co-elution with the quantifier. UPLC/MRM-MS analysis was performed on an Ultimate 3000 RSLC system (Thermo Scientific-Dionex Inc., Sunnyvale, CA) coupled to a 4000 QTRAP triple-quadrupole mass spectrometer (SCIEX, Concord, ON, Canada), equipped with an ESI source and operated in positive-ion mode. Chromatographic separation was performed on an Agilent ZORBAX Eclipse Plus C18 (4.6 x 50 mm, 1.8 µm) UPLC column. The mobile phase was 35% ACN containing 0.1% FA for isocratic elution. The column flow rate was 0.35 mL/min, the column temperature was 40 ºC, and the autosampler temperature was 5ºC. LC/MRM-MS data was acquired in "scheduled MRM" mode using Analyst 1.5 software and processed using MultiQuant 2.0 software (SCIEX, Concord, ON, Canada). The retention time window for scheduled MRM was 1 min.

Preparation of human plasma samples for MDA quantitation

Aliquots of 50 µL thawed spun-down human plasma were transferred to 3-mL glass test tubes. When measuring "free" (unbound) MDA, proteins were precipitated by adding 150 µL of 75% ACN, followed by centrifugation in a Beckman X-22R centrifuge for 15 minutes at 2782 x g, after which the clear supernatant was collected.

When measuring "total" MDA in plasma, hydrolysis was performed on plasma samples prior to derivatization to liberate the bound MDA that has modified proteins, lipids, and DNA/RNA. In this case, 25 µL of 6 M NaOH was added to each 50 µL aliquot of spun-down plasma and diluted with 50 µL of water, after which the tubes were sealed, shaken at 60ºC for 30 minutes and then cooled on ice. The solution was acidified and proteins were precipitated by adding 250 µL of 20% TCA and centrifuging for 15 minutes at 2782 x g, after which the clear supernatant was collected. Modifications of the protocol using precipitation with 10% TCA or derivatization in plastic Eppendorf tubes (instead of glass) were also assessed for their effect on the measured concentration of the analyte.

For derivatization, 50 µL aliquots of the supernatant from extracted plasma or calibration standard or water (blank) were added to 100 µL of 3NPH in 3-mL borosilicate glass tubes, which were then capped and sealed with parafilm. The reaction proceeded for 30 minutes at 50 ºC, after which the tubes were cooled on ice. The reaction was quenched by adding 100 µL of 30% ACN. A 50 µL aliquot of the resulting reaction mixture was mixed with 50 µL of the internal standard (IS) solution in LCMS certified sample vials, and 10 µL of this solution was injected for LC-MS/MS analysis.

3NPH-MDA Assay Performance Testing

To determine analytical sensitivity in the absence of matrix, a standard solution of 200 µM MDA was diluted (1:4) with H_2O. The resulting standard solution was derivatized with 3NPH, and LC/MRM-MS was performed as described above. The lowest concentration for which two injections gave peak area coefficients of variation (CVs) of <5% while yielding ≥4 or ≥20 times the background S/N ratio were considered as the lower limit of detection (LLOD) and lower limit of quantitation (LLOQ), respectively. A least squares regression was used to estimate the concentration range of linearity, with a minimum correlation coefficient (R^2) of 0.999. The sensitivity in matrix was determined by spiking 50 µL aliquots containing decreasing concentrations of $^{13}C_6$-3NPH-MDA (4.1, 0.82, 0.16, 0.033, 0.0065, and 0.0013 µM) into 50 µL aliquots of hydrolyzed, derivatized plasma.

Linearity in the presence of matrix was determined by adding 50 µL aliquots of MDA in varying concentrations (400, 80, 16, 3.2, 0.64, and 0.12 µM) to 50 µL aliquots of human

plasma prior to hydrolysis and derivatization. The precision of quantitation was measured in terms of the intra- and inter-run CVs by preparing and analyzing 6 analytical replicates of a pooled human plasma sample and 4 standard calibration curves.

The accuracy of quantitation was evaluated by determining the recoveries of known amounts of an MDA standard, spiked into pooled plasma at amounts corresponding to ~100%, 200%, and 500% of the endogenous concentration. Recoveries were calculated as [(the observed concentration-the endogenous concentration)/(the spiked concentration)] x100%.

Quantitation of MDA with 2,4-DNPH Derivatization - LC-UV

A calibration standard curve was prepared by diluting a 10 mM MDA solution with H2O to produce standards with concentrations of 123, 41.2, 13.7, 4.57 and 1.52 µM. Derivatization was performed by adding 75 µL of 10mM 2,4-DNPH in 75% ACN-0.2% TFA to 175 µL of calibration standard or clear supernatant from hydrolyzed, extracted plasma. The reaction was allowed to proceed for 60 minutes at 50ºC, after which the reaction mixture was cooled on ice and centrifuged for 5 minutes at 2782 x g before being transferred into sample vials. For sample analysis, LC was performed on the Dionex Ultimate 3000 series UHPLC system, using a Waters Acquity BEH C18 column (2.1 x 100mm, 1.7 µm), with H_2O:FA (100:0.1, v/v; solvent A) and ACN:FA (100:0.1, v/v; solvent B) as the mobile phases. The column flow rate was set at 0.35 mL/min, column temperature at 40ºC, and autosampler at 5ºC. Elution was performed with a 7-minute gradient: 20% B to 100% B in 7 min; 100% B for 1 min. The column was equilibrated for 4 min between sample injections for a total analysis time of 12 minutes per sample. UV detection was performed using a Dionex variable wavelength UV detector set at 310 nm. External calibration based on the standard solutions was used to perform quantitation.

Results

Assay Development

Selection of Reagent: Nine derivatizing reagents were tested with a subset of the selected aldehydes (MDA, glyoxal, acetylaldehyde, and crotonaldehyde) for their ability

to yield complete reactions that resulted in a small number of stable, ionizable, and detectable products. Each reagent was assessed on the basis of how many of the aldehydes were detected, the signal intensity, the number of peaks, and the peak shape. Most of the reagents tested displayed poor characteristics in at least one of these parameters. AEC produced double peaks with differing m/z ratios for some aldehydes suggesting multiple products. DNPH and PSC resulted in the production of derivatives that gave weak signal intensities. GRT and 4-NPH were associated with poor peak shape; in the case of GRT, this was likely due to the need to use HILIC for retention of the polar derivatives. Of the remaining reagents tested, GRP, 2-NPH, and DH produced detectable derivatives for only 1 or 2 aldehydes out of the 4 of the aldehydes tested. When used under weakly basic conditions and catalyzed with EDC and pyridine, 3NPH was able to produce detectable derivatives for 3 out of 4 aldehydes, with a single observable reaction product for each.

3NPH was selected for further development based on its MS compatibility (i.e., it does not produce detectable interferences in full-scan MS) , the quality of the derivatives produced (i.e., high signal intensity, one or two clean peaks per compound), and the simplicity of performing the reaction. A further advantage of 3-NPH is that is can be isotopically-labeled ($^{13}C_6$). By labeling the derivatizing reagent, it is possible to readily produce stable isotope-labeled internal standards for each compound that has a commercially-available unlabeled standard, which will facilitate future quantitation. Further screening against a larger panel found that standards for 10 out of the 15 aldehyde targets could be detected in buffer following a derivatization reaction with 3-NPH (Figure 17-A). The condensation reaction followed a nucleophilic addition-elimination mechanism (Figure 17-B). QTOF-MS screening of two reference samples of human plasma found that it was possible to directly detect 3NPH derivatives for methylglyoxal, butanal, methylbutanal, octanal, and decanal in without any prior optimization of the sample preparation, reaction conditions, LC parameters, or MS settings (Figure 17-C).

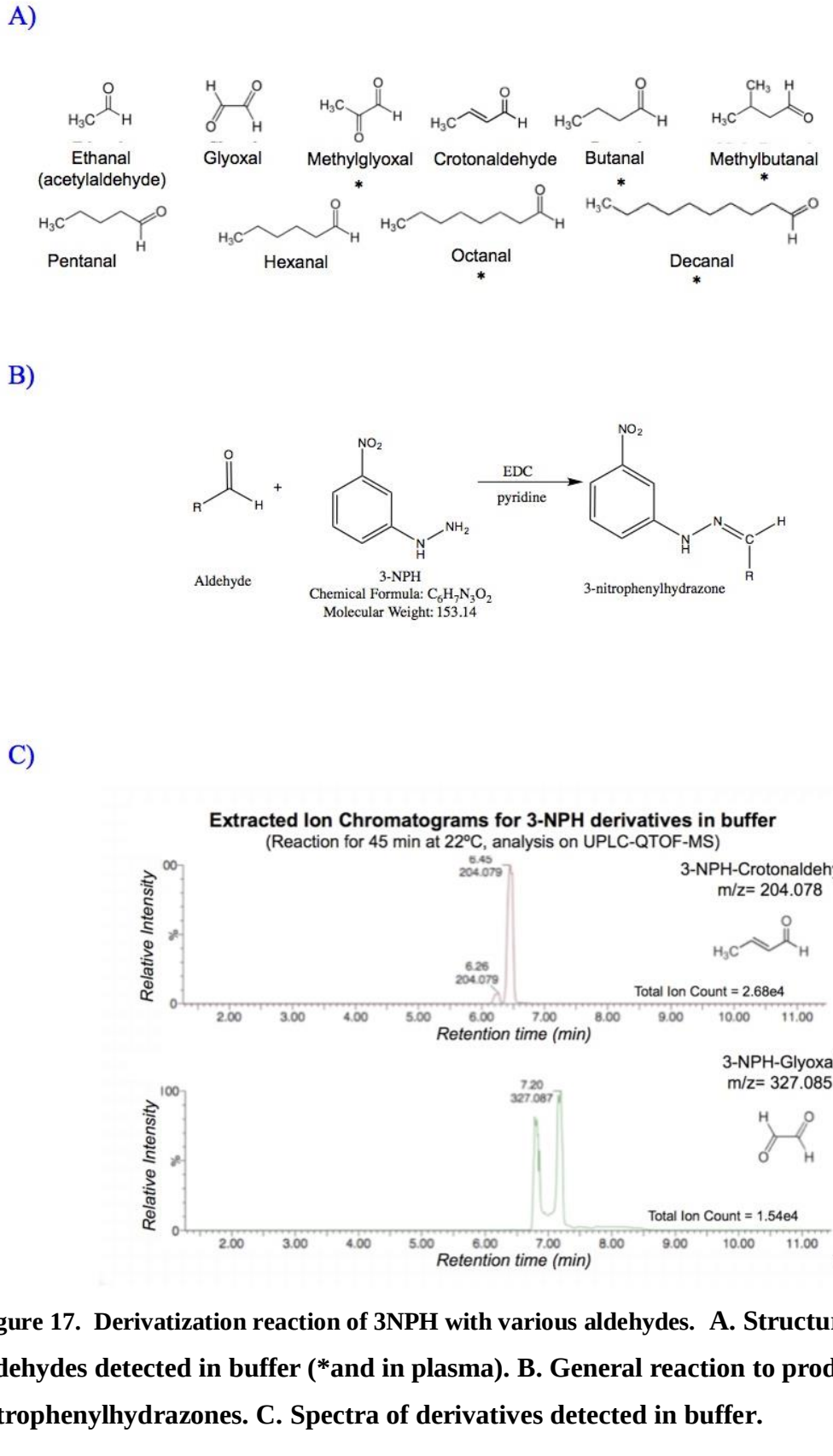

Figure 17. Derivatization reaction of 3NPH with various aldehydes. A. Structures of the aldehydes detected in buffer (*and in plasma). B. General reaction to produce nitrophenylhydrazones. C. Spectra of derivatives detected in buffer.

MDA was not initially detected with 3NPH derivatization, mostly likely because at this pH, MDA exists in an equilibrium between the keto and enol forms; this could result in multiple products, as the portion of MDA in enol form may undergo singular derivatization while the portion of MDA in keto form may be derivatized at one or both carbonyl groups. 2,4-dinitrophenylhydrazine (DNPH) has frequently been used to derivatize MDA in biological samples for measurement by LC-UV, but this approach is not compatible with MS due to the high background signal that DNPH produces. *p*-NPH has been previously used under weakly acidic conditions to derivatize MDA for UV detection [168]. However, 3NPH was preferable for developing a panel to quantify a variety of aldehydes with a limited number of reagents. In order to modify the equilibrium to favour a single product, the 3NPH reaction was performed under strongly acidic conditions using 0.1% trifluoroacetic acid (TFA). We found that derivatization of MDA with 3NPH under acidic conditions followed a nucleophilic addition-elimination to yield a stable, cyclic derivative, with no observable side products, which was detectable in both buffer and plasma in positive ion mode.

Optimization of Multiple Reaction Monitoring Parameters for Derivatives. Transitions were determined for all 11 aldehyde derivatives, along with the relevant MS/MS parameters (e.g., gas and electrospray settings, declustering potentials, and collision energies) using direct injection of the derivatives into a QTRAP 4000 MS/MS instrument (Table 7).

Table 7. MRM-MS transitions for aldehyde derivatives

Derivative	m/z	Declustering potential	Transitions (m/z)	Collision energy
3NPH-glyoxal	327.084	-83	137	-27.61
			189	-22.77
			107	-43.50
3NPH-acetylaldhyde	178.061	-85	150	-11.82
			122	-15.86
			92	-20.32
3NPH-methylglyoxal	341.099	-95	137	-27.16
			203	-24.28
			107	-44.36
			189	-33.21

3NPH-crotonaldehyde	204.077	-79	137	-24.09
			189	-15.25
			107	-32.26
			161	-19.45
3NPH-methylbutanal	220.108	-65	182	-10.20
			137	-23.59
			152	-24.00
3NPH-butanal	206.092	-80	137	-22.67
			188	-15.94
			107	-29.47
3NPH-hexanal	234.124	-80	137	-24.51
			182	-38.86
			216	-19.58
			107	-33.61
3NPH-octanal	262.155	-82	137	-28.13
			244	-20.62
			119	-34.21
3NPH-decanal	290.186	-94	137	-31.70
			107	-39.65
			119	-36.76
			155	-25.88
3NPH-pentanal	220.108	-86	137	-27.58
			119	-28.07
			107	-28.02
3NPH-MDA	189.977	+73	144	27.56
			117	37.92
			90	46.12

**Transitions are presented in order of sensitivity*

Optimization of chemical derivatization for 3NPH-MDA: The first step was to optimize and finalize the MDA assay. In order to develop a quantitative assay, it is crucial for the reaction conditions to be optimized to ensure that a high and consistent percentage of the target compound present in the sample is derivatized and prepared for detection. The derivatization reaction for 3NPH-MDA was optimized as a function of different times and temperatures (Figure 18). Figure 18A shows the condensation reaction, which follows a nucelophilic addition-elimination reaction mechanism to release two molecules of H2O while forming a cyclic derivative. As shown in Figure 18B, no significant increase in product (as measured by LC/MRM-MS peak areas) was observed for reactions performed at temperatures >40ºC. Figure 18C shows that no significant increase in product is observed beyond 15 minutes for reactions held at 50ºC. To ensure complete derivatization of MDA by 3NPH, we selected 50ºC as the reaction temperature and 30 minutes as the reaction time for subsequent experiments. As shown in Figure 18D, the 3NPH-MDA derivative was found to be highly stable for at least 36 h when held

at 5ºC in the autosampler and repeatedly re-injected at 3-6 hour intervals. The stability of 3NPH-MDA derivatives offers an advantage over DNPH derivatization as DNPH-MDA derivatives are light-sensitive, causing signals to degrade by up to 20% during the first hour of light exposure [163].

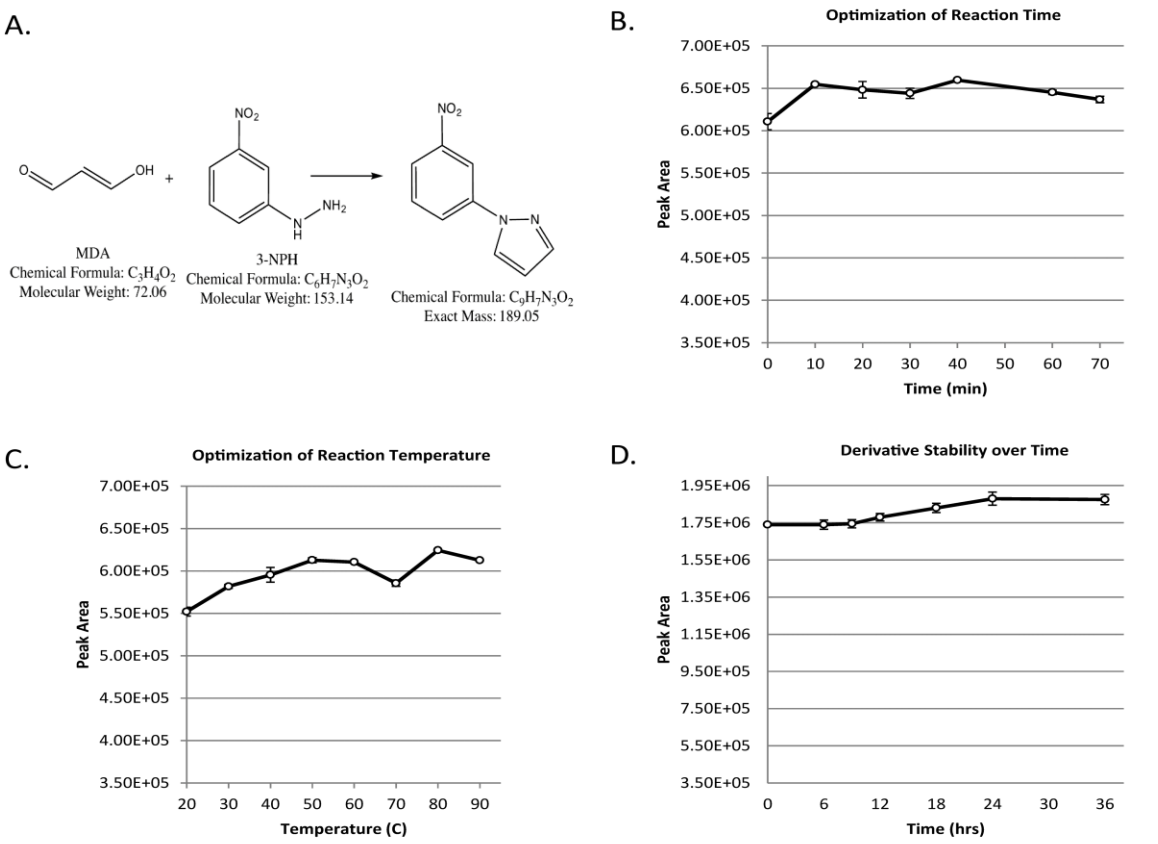

Figure 18. Effect of reaction conditions on the 3-nitrophenylhydrazine derivatization of MDA. (A) Derivatization reaction and derivative structure of 3NPH-MDA. (B) Peak area of 3NPH-MDA derivative as a function of reaction temperature. (C) Peak area of 3NPH-MDA derivative as a function of reaction time. (D) In-solution chemical stability of 3NPH-MDA derivatives at 5ºC, with error bars based on the measured peak areas from duplicate injections.

Hydrolysis and sample precipitation methods: Since aldehydes are highly reactive species, they react with lipids and proteins in a biological sample; this type of damage is a feed-forward consequence of oxidative stress. As a result, much of the aldehyde content in a biofluid sample is protein- or lipid-bound. Hydrolysis can be performed to

liberate bound MDA so that it can be measured along with circulating MDA. However, the amount of hydrolysis must be balanced so that all the aldehyde groups are cleaved, without cleaving the proteins; excessive hydrolysis of the proteins produces small peptides that add complexity to the sample and are hard to precipitate. Several protocols for hydrolysis and protein precipitation were attempted. A protocol using sodium hydroxide for hydrolysis followed by 20% tricholoracetic acid (TCA) to precipitate the proteins was found to produce the highest signal for the MDA derivative (Figure 19). The importance of using glass tubes for the reaction was demonstrated, as a comparison with plastic vials revealed a substantial loss of signal. Comparison of samples extracted with and without prior hydrolysis found that prior to hydrolysis, ~99.5% of MDA in the sample was bound.

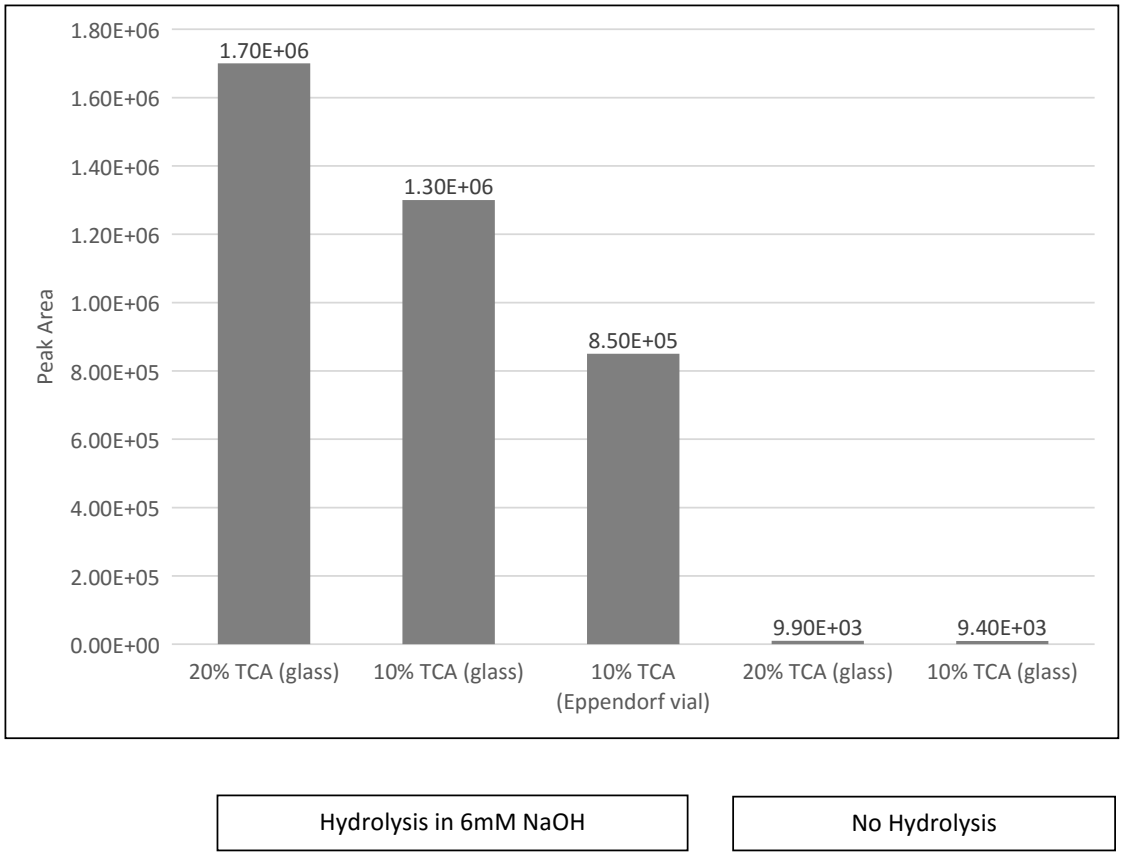

Figure 19. Comparison of sample preparation protocols and signal intensities for free vs. total MDA in human plasma. Average of two injections, based on monitoring of the 190/117 transition.

UPLC/MRM-MS with a $^{13}C_6$-labeled Internal Standard (Final Method): Optimized MRM transitions were used for quantitative monitoring of the 3NPH-MDA derivative. In optimization, the transition (m/z=190/144) that produced the highest signal also showed significant noise that substantially reduced its linear range for quantitation, so the transition with the second-highest signal was selected as the "quantifier" (m/z=190/117; declustering potential = 73V; collision energy = 38V). Another high-sensitivity transition with acceptable background signal (m/z= 190/90; declustering potential = 74V; collision energy = 46V) was selected as the "qualifier". Matching transitions for the $^{13}C_6$-3NPH-MDA derivative used as an internal standard (m/z=196/123, m/z=196/96) indicate a fragmentation pathway that maintains all 6 labelled carbons on the monitored fragments (Figure 20).

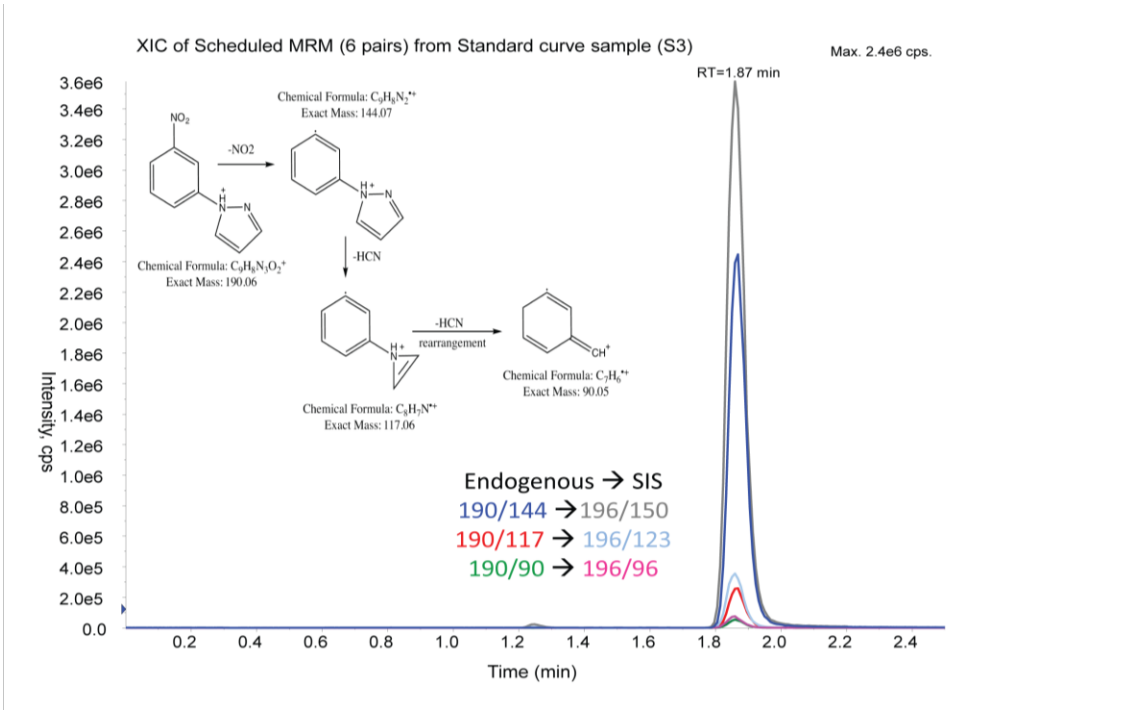

Figure 20. LC/MRM-MS chromatogram acquired from a pooled human plasma sample after hydrolysis and derivatization. The inset shows the fragmentation pattern in the MS/MS mode.

In testing of the assay on extracted human plasma, it was found that the 3NPH-MDA in these samples could be detected by MRM-MS/MS, and that, after LC separation, there were no interferences affecting the selected transitions. Accurate concentrations were calculated based on the calibration curve and the peak area ratios obtained from spiking

the sample with the $^{13}C_6$-labeled IS prior to LC/MRM-MS measurement. The isotope-labeled $^{13}C_6$-3NPH-MDA, which was spiked into $^{12}C_6$-3NPH-derivatized samples (standards, plasma extracts, blanks), compensated for the matrix effects inherent in ESI-MS [169]. The use of a ^{13}C isotope avoids any potential retention time variations that might result from a deuterium-labelled analogue. Using an isocratic flow of 35% ACN:65% water (each containing 0.1% FA) on a C18 column, no interferences were observed for the selected transitions, and it was possible to achieve baseline separation of the 3NPH-MDA in human plasma with an elution time of <2.5 minutes, as confirmed by the co-elution of the isotope-labeled IS (Figure 20). Since the derivative's identity is verified by the use of two MRM transitions and an internal standard spiked into every samples, the assay provides an extremely high degree of specificity for MDA.

Assay performance

Sensitivity The assay had an on-column LLOD of <10 fmol and an on-column LLOQ of <30 fmol in buffer, corresponding to concentrations of 0.007 µM and 0.02 µM in the initial 50-µL aliquot of the standard MDA solution used in the derivatization. Using $^{13}C_6$-3NPH-MDA spike-in, the LLOQ in plasma was found to be <5 fmol on-column. This is significantly more sensitive than the commonly used HPLC-based methods for MDA, which have LLODs ranging from 0.1 µM to 0.3 µM and LLOQs of 0.17 to .84 µM [162-164, 166].

Linearity: As shown in Figure 21, the linearity of 3NPH-MDA was found to be the same in plasma as in buffer, with equal slopes (i.e., a difference of <2%), indicating that ion suppression effects were minimal and that the quantitative determination of MDA in plasma was not affected by the sample matrix when the IS is used.

Dynamic range: In all cases, a linear regression line with a regression coefficient (R^2) of >0.9999 was obtained, showing an excellent quantitative relationship between the MS responses and analyte concentrations over a concentration range of 4 orders of magnitude (Figure 21).

Precision & reproducibility: The precision of quantitation was measured as the intra- and inter-run CVs for the concentration of 3NPH-MDA in reference plasma samples. As shown in Table 8, intra- and inter-run CVs were 2.6% (n = 6) and 6.7% (n = 4), respectively, for total MDA including the hydrolysis step.

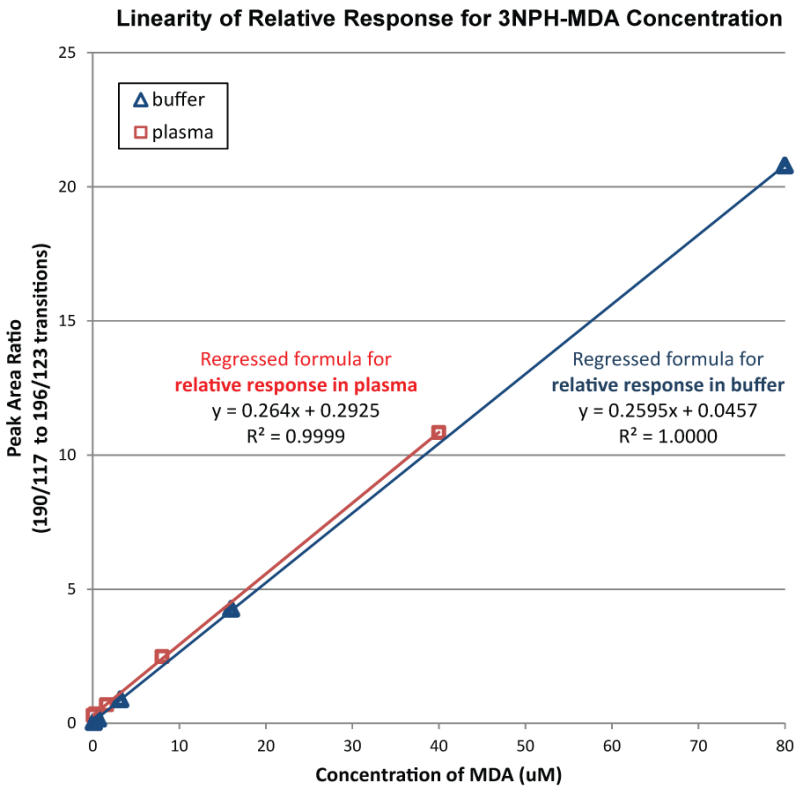

Figure 21. Linearity of 3NPH-MDA in plasma and buffer.

Table 8. Intra- and inter-run CVs for Quantitation of 3NPH-MDA.

Six (6) full-process replicates were prepared from the same pooled human plasma reference sample. Four standard curves were produced from freshly prepared MDA standard using a 1:4 dilution series. Concentrations were calculated for each plasma sample using each of the 4 standard curves to assess inter-run reproducibility.

	Concentration calculated from Std Curve #1 (µM)	Concentration calculated from Std Curve #2 (µM)	Concentration calculated from Std Curve #3 (µM)	Concentration calculated from Std Curve #4 (µM)	Average inter-run Concentration (µM)	C.V.
Replicate #1	16.56	15.51	13.71	15.51	15.32	
Replicate #2	15.46	14.48	12.81	14.48	14.31	
Replicate #3	16.35	15.32	13.54	15.32	15.13	
Replicate #4	16.73	15.67	13.85	15.67	15.48	
Replicate #5	15.95	14.93	13.21	14.93	14.75	
Replicate #6	16.05	15.04	13.30	15.04	14.86	
Average intra-run concentration	**16.18**	**15.16**	**13.40**	**15.16**	**14.98**	**6.7%**
C.V.	**2.60%**	**2.62%**	**2.59%**	**2.61%**	**2.60%**	

Recovery: To determine the accuracy of quantitation, a spike-in/recovery experiment was conducted. The endogenous concentration of MDA was measured in three aliquots of the pooled human plasma reference sample, as well as in aliquots of the same reference sample that were spiked with unlabeled MDA standard solution at 100% (n=3), 250% (n=3) and 500% (n=3) of the endogenous level prior to hydrolysis. The amount of MDA measured in each sample was compared to the known spiked-in amount plus the measured endogenous amount. Recoveries were found to be 98.0%, 92.2%, and 94.4% of the expected amount at the 100%, 250%, and 500% spike-in levels respectively. This represents a high degree of quantitative accuracy, which was achieved through the use of the isotope-labeled IS. Moreover, since the spiking was performed as the first step of sample preparation, the high rates of recovery showed that the hydrolysis and derivatization protocols did not result in significant loss of volatile MDA from the samples over the course of sample preparation, even when many samples are prepared in parallel.

Quantitation of MDA in human plasma samples

Comparison to LC-UV: In order to compare the MDA concentrations obtained using the new method with those determined using an established method, MDA was quantified in aliquots of the same pooled human plasma using both the new LC/MRM-MS method and using the older DNPH-LC-UV method. As shown in Table 9, the average concentration obtained by LC-UV detection for 3 full-process replicates was 9.85 µM (1.0% CV), and the average concentration obtained by LC/MRM-MS for 3 full-process replicates was 10.06 µM (0.5% CV). The methods are in good agreement (<2% difference in final concentrations). The excellent agreement between the two methods supports the utility of the new method for reliably quantifying MDA in human plasma.

Table 9. Comparison of two methods for quantifying MDA in human plasma.

	Method A: 2,4-DNPH LC-UV		Method B: 3NPH LC/MRM-MS	
Sample	**Average conc. (µM)**	**CV (3 injections)**	**Average conc. (µM)**	**CV (3 injections)**
Replicate #1	9.72	0.7%	10.11	0.1%
Replicate #2	9.97	1.7%	9.99	1.3%
Replicate #3	9.85	1.7%	10.09	1.0%
Average	**9.85**	**1.0%**	**10.06**	**0.5%**

Application of MDA quantitation to a clinical study of MDD-s

Background on Major Depressive Disorder with Seasonal Pattern

The assay was subsequently applied to characterize clinical samples in a study of patients with major depressive disorder with winter-type seasonal pattern (MDD-s), previously referred to as "seasonal affective disorder" (SAD). MDD-s is characterized by an extended low mood state that resembles atypical depression, usually with a pattern of onset beginning in fall or winter, and remitting in the spring or summer. Furthermore, vitamin D insufficiency has been associated with temporal depressive symptoms in some groups [170], and vitamin D supplementation continues to be investigated for its potential to improve symptoms in MDD-s [171]. It has previously been found that vitamin D levels are inversely correlated with malondialdehyde levels, which suggests that vitamin D may exert an antioxidant effect [172]. We therefore decided to investigate whether features of oxidative stress, as represented by elevated plasma MDA levels, may be observable in patients during the onset of MDD-s symptoms.

Plasma samples were obtained from 13 patients (6 male, 7 female) in accordance with study protocols approved by the Research Ethics Board of Sunnybrook Health Sciences Centre. Samples were collected at baseline (Fall) and in the same patients following onset of MDD-s symptoms (Winter). Patients were assessed at each time-point for depressive symptoms using the Beck Depression Index (BDI, 2nd edition) and the Structural Clinical Interview for Depression (SCID). Patients' weight, waist size, Body Mass Index (BMI), and use of vitamin D supplements were recorded at each time-point.

Patients who met the criteria for a depressive episode at the fall time-point (n=2), or who did not develop a depressive episode at the winter time-point (n=2) based on their SCID scores, were excluded from further analysis.

Using the MRM-MS method for quantifying MDA, it was found that total plasma MDA concentrations in this group ranged from 13.25 to 15.29 µM (mean=14.31±0.71) at baseline and from 12.85 to 17.33 µM (mean=15.47±0.87) at the symptomatic time-point. Plasma aliquots that did not undergo hydrolysis were also analyzed to measure free unbound MDA. Based on this data, >99% of total MDA was bound in each of the samples analyzed. Among the patients who showed the typical pattern of depression with onset in the winter months (n=9), the concentration of total plasma MDA at the fall time-point was found to be strongly positively correlated with age (R^2=0.84, p<0.001), BMI (R^2=0.67, p<0.02), weight (R^2=0.74, p<0.01), and waist size (R^2=0.77, p=0<0.005). At this time-point, patients with low-normal BMIs (BMI<25, n=5) had a plasma MDA concentration of 13.74±0.63 µM while patients with higher than normal BMIs (BMI≥25, n=4) had an average plasma MDA concentration of 14.75±0.37 µM (Figure 22). This difference was significant using an unpaired student's t-test with unequal variance (p<0.05).

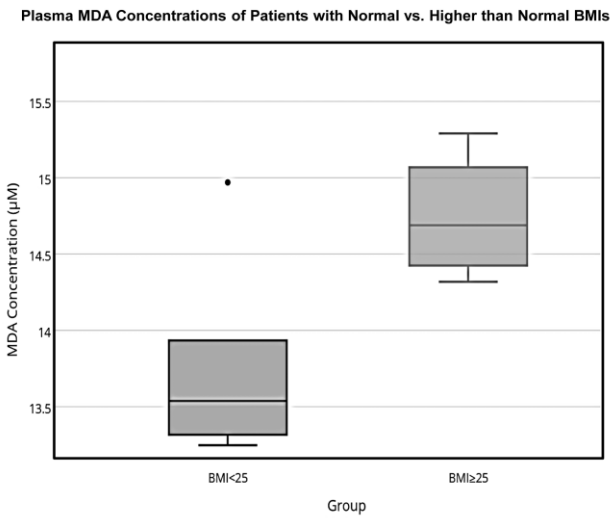

Figure 22. Comparison of total plasma MDA concentrations for patients with low-normal BMI (<25) verus high BMI (≥25) at the fall and winter timepoints.

Among MDD-s patients, an association between the number of previous episodes of seasonal depression and baseline plasma MDA concentrations was observed (R^2=0.62, $p<0.05$).

Discussion

Proof-of-concept for 3NPH as a derivatizing reagent for aldehydes:

In this stage of the project, novel analytical methods using MRM-MS to quantify aldehyde biomarkers of lipid peroxidation from biofluid samples were developed. It was shown that derivatization with 3-NPH, when used under weakly basic reaction conditions, is broadly applicable to a large panel of 10 aldehyde markers of oxidative stress, at least 5 of which could be directly detected by LC-MS in human plasma without any optimization. The use of 3NPH, as compared to other derivatizing reagents, enhances chromatographic performance, stability, and detectability of aldehydes. It was also demonstrated that 3NPH can be used under strongly acidic conditions to derivatize malondialdehyde (MDA).

MRM-MS assay for 3NPH-MDA: Since MDA is a well-established biomarker of oxidative stress, the MDA assay was first optimized and finalized, so that it could be used for cross-validation with the new aldehyde panel. In order to overcome limitations in the existing methods for quantitation of MDA, a new method using chemical derivatization with 3NPH, separation by UPLC, and detection with MRM-MS was developed. The derivatization approach requires only simple sample preparation and does not necessitate sample clean-up prior to analysis. Isotopically-labeled $^{13}C_6$-3NPH was used to generate an internal standard ($^{13}C_6$-3NPH-MDA) to ensure precise and accurate quantitation. The method was validated in terms of derivative stability, assay performance, reproducibility, and recovery. The new MRM-MS-based method is similar to previously published methods in that it offers very high precision (CVs of <7% vs. 4-11% in published methods) and good recoveries (92-98% vs. 89-101%), but it also improves on existing protocols in several ways. Firstly, it is significantly more sensitive for quantifying MDA in human plasma (LLOD of 0.007µM vs. 0.1 µM), 2) and has a greater linear range (10^4 vs 10^1) that encompasses clinical concentrations, which have previously been reported to range from 0.1-13.8 µM [173]. Secondly, it offers dramatically shorter analysis times

(2.5 min vs. 15-35 minutes) [162, 163, 165, 166, 174, 175]. Given the simple sample preparation and the rapid analysis time, the method has the high throughput required for large-scale clinical applications.

Quantitation of MDA in human samples: As a demonstration of the method's utility, the MRM-MS method for MDA quantitation was then applied to 26 human plasma samples from patients with major depressive disorder with seasonal pattern (MDD-s) participating in a longitudinal study. The observed relationships between total MDA plasma concentrations and obesity, and between MDA concentration and age, confirm previously published findings [176, 177]. Individuals in the MDD-s group also showed a non-significant increase in weight between the two time-points (gaining an average of 0.39kg, $p>0.05$ using student's paired t-test) and a significant increase in waist size (mean increase of 3.35 cm, $p<0.05$ using student's paired t-test). The increase in waist size without corresponding weight gain may be due to a loss of muscle mass and gain of fat. Neither a group comparison nor within-patient comparisons found any statistically significant differences in MDA concentrations at the baseline vs. symptomatic time-points ($p>0.05$). However, at the symptomatic time-point, the concentration of MDA no longer showed a significant correlation with age or obesity measures, which may suggest that other non-correlated factors are having a greater effect on total MDA concentrations during the symptomatic phase.

Previous studies have found that patients with bipolar disorder (BD) receiving psychotropic agents had lower MDA levels than healthy controls [178], and specifically that patients with BD that had concurrent metabolic syndrome (unhealthy obesity) did not show the expected increases in MDA that were seen in their non-BD counterparts. Together with the current results, this may indicate that MDD-s patients also display this disturbed signature of oxidative stress during symptomatic phases. However, the current study does not provide specific evidence that changes in total plasma MDA concentration is a significant feature of MDD-s. Although MDA concentrations appear not be suitable to monitor phases of illness, the observed correlations with MDA concentrations (i.e. those with measures of obesity, age, and the number of previous episodes) suggest that

MDA may be associated with some features of MDD-s. The precise independent relationships between these often highly correlated characteristics will need to be disentangled in larger studies. Further investigations in large cohorts might employ additional longitudinal time-points and include complementary quantitation of vitamin D to follow up on prior work investigating the role of antioxidants and oxidative stress in MDD-s [170-172].

Within this cohort, the expected correlations between plasma MDA and obesity, as well as plasma MDA and age were observed. Moreover, the overall values for total MDA reported for the patients in this study (mean=14.32 μM) were similar to previously reported values of 13.79 μM in pooled plasma [162] and 13.8 μM (mean value) in 20 healthy volunteers [165]. The wide range of values reported in the literature [166, 173] may be partially attributable to differences in hydrolysis procedures, resulting in different proportions of MDA being effectively liberated from proteins and lipids. Alkaline hydrolysis, as was used here, has been shown to yield up to twice as much total MDA other methods [179]. Dilution of plasma samples has also been suggested to promote the effective release of MDA that is bound to other biomolecules in the matrix [165]. Overall, the good agreement between the LC/MRM-MS method and the LC-UV method for quantifying MDA in the reference samples suggests that the concentrations for MDA in human plasma obtained in the current study can be accepted with high confidence for the particular hydrolysis protocols employed.

Next steps: MDA is a product of peroxidation of long-chain polyunsaturated fatty acids. This is the type of lipid that was identified in Chapter 1 as having reduced abundance in the serum of individuals in an epigenetic model of chronic stress, so one would expect MDA to be a sensitive measure of whether oxidative stress is responsible for phospholipid oxidation during chronic stress. The newly validated method was therefore applied to the quantitation of MDA to determine whether lipid peroxidation is a feature of chronic social defeat stress in a mouse model. Accompanying lipidomics analysis was performed to identify whether chronic stress in this model was also associated with decreased concentrations of phosopholipids, as had been observed for the human epigenetic model.

Chapter 3:
Assessment of Mouse Plasma MDA and Lipid Profiles in a Model of Chronic Social Defeat Stress

Chapter Summary

Background: Exposure to chronic social defeat stress produces physiological and behavioural changes in mice similar to those observed in other models of chronic stress. However, not all mice are susceptible to these adverse effects: some mice are "resilient" and do not show the typical anxious and depressive-like behavioural changes associated with chronic social defeat stress.

Methods: Plasma samples were obtained from mice after 10 days of exposure to chronic social defeat stress. The mice belonged to 3 groups: controls (no stress exposure), susceptible (stress exposure resulting in behavioural changes), and resilient (stress exposure resulting in no behavioural deficits). Malondialdehyde (MDA), a lipid peroxidation marker of oxidative stress, was measured in the plasma samples using a newly developed method for multiple-reaction-monitoring monitoring mass spectrometry (MRM-MS). Untargeted profiling of lipids was also performed using reversed phase liquid chromatography (RPLC) with detection by FT-MS and FT-MS/MS.

Results: Total MDA was measured at concentrations between 60 to 90 µM in mouse plasma. No significant differences in MDA concentration were observed between the groups. Untargeted profiling of lipophilic components extracted from the samples revealed a unique metabolomic phenotype associated with animals exposed to chronic social defeat stress, characterized by changes in fatty acid composition, as well as metabolites associated with amino acid metabolism and cell death. The characteristic pattern of changes in metabolite concentrations was observed in both stress-exposed groups, irrespective of whether or not they showed behavioural symptoms of stress -- in fact, the metabolomic phenotype was exaggerated in the "resilient" mice, suggesting a possible protective effect of changes in energy metabolism under conditions of chronic stress.

Introduction

Mouse model of chronic social defeat stress

In the previous chapter, I reported development of a new targeted LC/MRM-MS approach to quantify malondialdehyde (MDA) as a marker of lipid peroxidation in oxidative stress. With the new method fully developed and validated, I returned to the original question of whether oxidative stress could be responsible or partially responsible for the lowered levels of long-chain phospholipids observed in human serum in an epigenetic model of chronic stress. Given the relationship between obesity and oxidative stress, and the many other potential variables (e.g., age, diet) that contribute to MDA levels, it was particularly important to identify an animal model that would help to limit the confounding variables. Dr. Michael Meaney, the professor at McGill University who pioneered the use of the epigenetic model described in Chapter 1, is now studying stress susceptibility and resiliency in mice using a model of chronic social defeat.

In the social defeat stress model employed by Dr. Meaney, normal inbred C57BL/6 mice are positioned as intruders in a cage with large aggressive resident CD-1 mice, to whom they are forced to submit. After 10 days of repeated exposure, the defeated animals typically begin to show depressive-like symptoms, characterized by the avoidance of social contact, decreased exploratory behaviour in the open-field test, reduced sexual behaviour, increased immobility in forced swim test, and a loss of sucrose preference [180-184]. They also demonstrate decreased exploration in the elevated plus maze, which is considered an indicator of increased anxiety [185].

Furthermore, animals exposed to chronic social stress show prolonged and increased HPA activation [186], reflected by increased secretion of ACTH, cortisol, and corticosterone [181]. They also show reduced expression of genes for glucocorticoid and mineralocorticoid receptors in specific regions of the hippocampus [187]. Physical symptoms mirror human stress responses: mice and rats subjected to chronic social stress show increased heart rate and blood pressure, disturbed circadian rhythms, impaired immunological function, and reduced resistance to disease [181, 188, 189].

However, not all defeated animals develop these symptoms; even though all animals in a given study are exposed to the same type, degree, and frequency of aggression, and all are equally required to submit, some mice and rats in each study do not develop depressive-like symptoms in spite of repeated exposure. Since its first use in the early 1990s, this well-validated model has consistently produced both "susceptible" and "resilient" phenotypes [190]. Resilient animals do not develop the characteristic depressive or anxious symptoms, and do not develop some physical symptoms (e.g., Metabolic syndrome) that are observed in susceptible animals [191]. Given that the resilient animals share the same genetic background, rearing conditions, and stressful experiences as the susceptible animals, there has been considerable research interest in determining what factors (e.g., genetic variants, gene expression changes, differences in brain anatomy) may be responsible for the divergent responses [191].

Hypothesis, Objectives & Approach: For this portion of the project, I obtained mouse plasma samples from a 10-day study by Dr. Meaney's group using the chronic social defeat stress model. The samples provided corresponded to three groups: a control group that was not exposed to aggressor animals, a susceptible group that displayed behavioural changes in response to repeated social defeat, and a resilient group that did not display any behavioural changes in spite of repeated domination by aggressor animals. We applied the new method to measure the concentration of MDA, a marker of lipid peroxidation, in plasma from mice in the chronic defeat stress model to test whether oxidative stress may be a feature of chronic stress. Complementary lipid profiling experiments were performed using high resolution Fourier transform (FT)-MS and MS/MS to confirm whether mice in this study demonstrated a pattern of differences in plasma phosopholipid concentrations similar to that observed in the epigenetic study. The data generated provided an additional opportunity to compare the metabolomic profiles of the susceptible and resilient phenotypes, which may yield new insights into the mechanisms of social stress resilience in mice.

Materials & Methods

Standards & Reagents: LC-MS grade acetonitrile (ACN), methanol (MeOH), ethanol, chloroform, isopropanol (ISP), and water (H_2O) were purchased from Sigma-Aldrich (St. Louis, MO). Malondialdehyde (MDA), analytical reagent-grade 3-nitrophenylhyrdrazine (3NPH.HCl), pyridine, formic acid (FA), trichloroacetic acid (TCA), trifluoroacetic acid (TFA), and sodium hydroxide (NaOH) were also obtained from Sigma-Aldrich.

Mouse plasma samples: Dr. Meaney provided plasma samples from C57BL/6 mice (n=23) in a model of chronic social defeat stress. Chronic social defeat was imposed according to a standard protocol [192] as described in the 2015 Biological Psychiatry paper by Anacker et al. [193] using CD1 and C57BL/6 mice obtained from Charles River Laboratories (Sherbrooke, Quebec, Canada). The experimental procedures were performed as approved by the McGill University Animal Care Committee. Briefly, a 3-day screening procedure was used to quantify the degree of aggressive behaviour exhibited by single-housed CD1 mice toward a novel C57BL/6 mouse placed in their home cage. CD1 mice that attacked quickly and frequently were selected as aggressors for further experiments. During the social defeat stress procedure, 8-week old naïve pair-housed C57BL/6 mice were placed in the home cage of a novel-CD1 aggressor, where they were physically defeated for 5 minutes each day for 10 days. The defeated mice were then housed in the same cage with the aggressor, separated by a perforated plexiglass divider, for 24 hours. Control C57BL/6 mice (n=8) were housed in similar cages, separated by a plexiglass dividers, and paired with a new non-aggressor control C57BL/6 mouse each day. At the end of the 10-day paradigm, social interaction behaviour was measured by allowing C57BL/6 mice to explore an open field area with a central mesh enclosure for 2.5 minutes, first in the absence of and then in the presence of a CD1 mouse. Mice that demonstrated social avoidance (i.e., spent significantly less time in the interaction zone near the mesh cage when it was occupied) were considered susceptible (n=8), whereas mice that engaged in normal social behaviour (i.e., spent more time in the interaction zone when the cage was occupied) were considered resilient (n=7). All mice were sacrificed and perfused 24 hours after the social interaction test, at which

point blood samples were collected into anticoagulant-coated tubes and centrifuged to generate plasma.

Targeted quantitation of MDA

Quantitation and comparison of total malondialdehyde by MRM-MS: The final MRM-MS method for analyzing total plasma MDA, described in Chapter 2, was adapted for use with smaller volumes of mouse plasma. Thawed mouse plasma samples were spun down in a benchtop centrifuge and 40 µL aliquots were transferred to 3-mL glass test tubes and diluted with 40 µL of water. Hydrolysis was performed on each sample by adding 25 µL of 6 M sodium hydroxide, after which the tubes were sealed with parafilm, shaken at 60ºC for 30 minutes, and then cooled on ice. The solution was acidified and proteins were precipitated by adding 200 µL of 20% TCA and centrifuging for 15 minutes at 2782 x g. The clear supernatant was then collected and 50 µL aliquots were transferred to 3-mL borosilicate glass tubes.

A 7-point calibration curve was prepared by diluting a stock solution of 10mM MDA, prepared from a commercial standard (Thermo Scientific) in water, to concentrations of 400, 80, 16, 3.2, 0.64, 0.12, and 0.0025 µM. Two blanks (water only) were also prepared in parallel.

For derivatization, 100 µL of 3NPH in 75% ACN with 0.2% TFA was added to 50 µL of blank, calibration standard, or plasma extract. Tubes were immediately capped and sealed with parafilm. The reaction proceeded for 30 minutes at 50 ºC, after which tubes were cooled on ice. The reaction was quenched by adding 100 µL of 30% ACN. A 50-µL aliquot of the resulting reaction mixture was mixed with 50 µL of the 13C6-3NPH-MDA internal standard solution in an LCMS certified sample. 10 µL of this solution was injected for LC-MS/MS analysis.

The optimized LC/MRM-MS parameters determined in Chapter 2 were used for quantitation on an Ultimate 3000 RSLC system (Thermo Scientific-Dionex Inc., Sunnyvale, CA) coupled to a 4000 QTRAP triple-quadrupole mass spectrometer (SCIEX, Concord, ON, Canada), equipped with an ESI source and operated in positive-ion mode. Chromatographic separation was performed on an Agilent ZORBAX Eclipse Plus C18

(4.6 x 50 mm, 1.8 µm) UPLC column using 35% ACN with 0.1% FA for isocratic elution. The column flow rate was 0.35 mL/min, the column temperature was 40 ºC, and the autosampler temperature was 5ºC. LC/MRM-MS data was acquired in "scheduled MRM" mode (1 minute window) using Analyst 1.5 software and processed using MultiQuant 2.0 software (SCIEX, Concord, ON, Canada).

Untargeted lipid profiling using UPLC-FT-MS

Organic extraction of lipophilic metabolites: Thawed mouse plasma samples were spun down and 20 µL aliquots were transferred to 0.65-mL Eppendorf vials and diluted with 20 µL of water. Extraction was performed by adding 80 µL of methanol to each vial and sonicating for 1 minute to dissociate lipids from proteins in the sample. Proteins were precipitated with the addition of 80 µL of ACN, after which the samples were sonicated and held on ice for 15 minutes, prior to centrifugation at 2782 x g in an R-22 centrifuge (Beckman Coulter). 150 µL of the clear supernatant was then carefully removed, without disturbing the protein pellet, and transferred to LC-MS certified autosampler compatible glass vials. Samples were dried in an SPD1010 centrifugal speed-vacuum concentrator (Thermo Electron Corp., San Jose, CA, USA) for 30 minutes at 45ºC, and then another 30 minutes at room temperature. Dried samples were stored overnight at -20 ºC, and then resuspended in 60 µL of 75% methanol for MS analysis.

Reversed phase UPLC: Online RPLC-FTMS was performed using a BEH-C8 column (2.1 mm I.D. x 50 mm, 1.7 µm particle size; Waters Corp.) on a Waters Acquity UPLC coupled to a Thermo LTQ-Orbitrap Velos Pro MS. The column temperature was maintained at 50 ˚C. Water with 0.01% FA was used as Solvent A. Solvent B was acetonitrile and isopropanol (2:1) containing 0.01% FA. The flow rate was set at 0.35 mL/min with a multistep gradient from 8% to 40% B over 6 minutes, then from 40% B to 100% B over 14 minutes, followed by a 2-minute wash step (100% B), and 4 minutes equilibrating at the starting conditions (8% B) prior to the next injection. The autosampler temperature was held at 4ºC. The injection volume was 5 µL, and injections were performed using the partial loop injection mode with an overfill factor of 2.

UPLC-FTMS: Ultrahigh resolution MS data were collected in positive and negative ion mode on a Thermo LTQ-Orbitrap Velos Pro MS with a heated electrospray ionization (ESI) source. For lipid profiling, the MS was operated in the FT-MS full scan mode with the following parameters: resolving power of 60,000 full-width at half-maximum (FWHM) at m/z 400, automatic gain control (AGC) target of $5x10^5$, and maximum injection time 100 ms.

The ESI-MS parameters were: ESI capillary voltage, 3500V / -2500 in positive and negative ion mode respectively; nebulizer gas (N_2), 42 (arbitrary units); curtain gas (N_2), 12 (arbitrary units); and m/z detection range was 100-1600. Centroid data was collected in positive and negative ion modes. A ubiquitous formic acid background ion (m/z = 112.98563) was used for lockmass calibration to continuously maintain mass accuracy across runs. Masses were measured within a mass error of ±3 ppm, as verified.

UPLC-MS/MS: MS/MS data were acquired from a pooled sample of mouse plasma, prepared using the same extraction technique. Spectra were collected in both positive and negative ion mode using high-energy collision dissociation (HCD) fragmentation with Orbitrap detection to acquire MS/MS spectra for high abundance ions, and collision-induced dissociation (CID) fragmentation with ion trap detection, to acquire MS/MS spectra for ions with low signal intensity.

For UPLC-MS/MS with HCD fragmentation, the MS instrument was operated in the data-dependent mode with the ions corresponding to the top 10 most intense signals detected by Orbitrap being selected and isolated by the quadrupole for subsequent HCD in the collision cell, prior to secondary detection in the Orbitrap. A normalized collision energy of 25% was employed with a stepped collision energy of 5%. The resolving power was set at 15,000 full-width at half-maximum (FWHM) with an AGC target of 50,000, and a m/z range of 80 to 1500.

For UPLC-MS/MS with CID fragmentation, the MS instrument was operated in the data-dependent mode with selection priority given to the least intense ions. Ions were first detected in the Orbitrap, and selected ions were isolated by quadrupole for subsequent HCD in the collision cell, and detection by ion trap. A normalized collision energy of

30% was employed with a stepped collision energy of 5%. The resolving power was set at 15,000 full-width at half-maximum (FWHM) with an AGC target of was 20,000, and a scan range from m/z 80 to 1500. UPLC-MS/MS data were acquired and processed using Thermo's XCaliber software.

Data analysis: Full scan UPLC-FTMS Raw spectra were acquired with Xcalibur in Thermo's .raw data format, and converted to mzXML using the msConvert function in Proteowizard [194]. mzXML files were then uploaded to XCMSOnline version 2.0.1 (xcmsonline.scripps.edu) for processing and analysis. Positive ion mode data and negative ion mode data were processed separately. Full details of the XCMS methods and settings applied are shown in Appendix I. Feature detection was performed using the centWave function. To reduce noise in the data, features were filtered based on peak width, peak intensity (both absolute and signal-to-noise cutoffs), and the appearance of peaks in a minimum number of consecutive scans. The thresholds were determined based on visual inspection of the raw spectra in Xcalibur. Retention time correction was performed using 'obiwarp'. Peaks were then grouped, and integrated. A visual inspection of all overlaid total ion chromatograms (TIC) following retention correction was used for quality control to confirm correct alignment of spectra and to identify outliers whose TICs deviated dramatically (>100% increase or decrease in intensity) from the vast majority of samples in multiple areas of the chromatogram. Outliers were removed and the analysis process was repeated until quality criteria were met. Peak intensities were compared using an ANOVA parametric test to perform multigroup comparison. The p-value cutoff for highly significant features was 0.01. The list of significant features was carefully reviewed: isotopic peaks, peaks matching known contaminants or attributable to peptides/small proteins, and peaks displaying poor peak shape or poor integration of peak area were manually removed prior to further analysis.

Putative IDs were generated by searching the m/z values of significant features against common adducts in the METLIN database. The credibility of these putative identifications was first evaluated based on whether the metabolite was expected to be present in mouse plasma at detectable levels, would likely be extracted and be stable in the solvent conditions, and be eluted at a retention time appropriate to its chemistry. For

features with potentially credible putative identifications, MS/MS data was inspected in Xcalibur to try to obtain additional evidence to support or reject the identification. The m/z values of observed fragments associated with the precursor ion were compared to published MS/MS spectra or to fragment ions that are commonly observed for compounds in that class.

Results

MDA analysis

Total MDA was quantified in 20 mouse plasma samples. Total plasma concentrations of MDA ranged from 60.1 – 92.6 µM, with a mean of 75.1 µM +/- 7.4 µM. The control (n=7), susceptible (n=6), and resilient groups (n=7) did not show any significant differences in terms of the observed concentrations of total plasma MDA (see Figure 23).

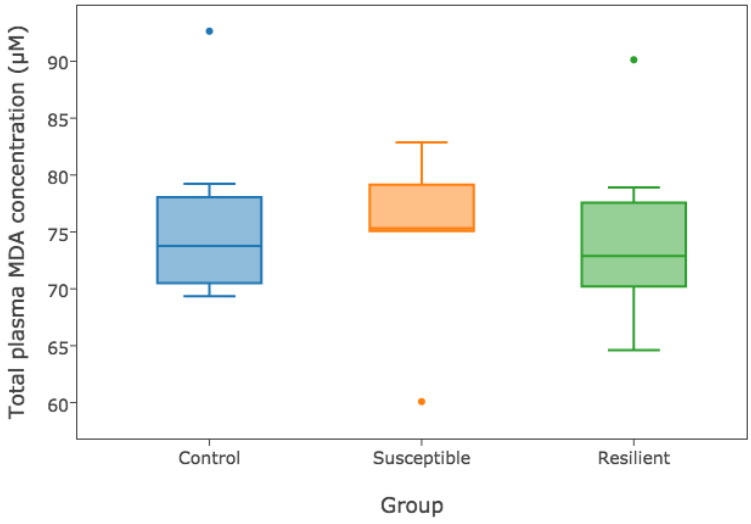

Figure 23. Total plasma MDA concentration in mice subjected to chronic social defeat stress.

Lipid Profiling

In addition to the targeted analysis of MDA in these mouse plasma samples, I also performed untargeted analysis of the lipid component of these samples to determine if there were any changes in phospholipid abundances that were similar to those observed in the epigenetic model. For each of the 23 samples, spectra were acquired in both positive and negative ion mode using a Thermo Obitrap Velos mass spectrometer. The use of a 20-minute UPLC gradient and an Orbitrap mass spectrometer with extremely high mass resolution supports the detection of significant features from the spectra and will facilitate subsequent metabolite identification. Complementary MS/MS data was also collected at the time of sample analysis to provide further evidence to support or reject putative metabolite assignments.

The initial rounds of processing with XCMS identified outlier samples whose total ion chromatograms deviated dramatically from the other overlaid spectra. These samples (n=5) were removed from further data analysis to ensure appropriate retention time correction and peak grouping (Figure 24).

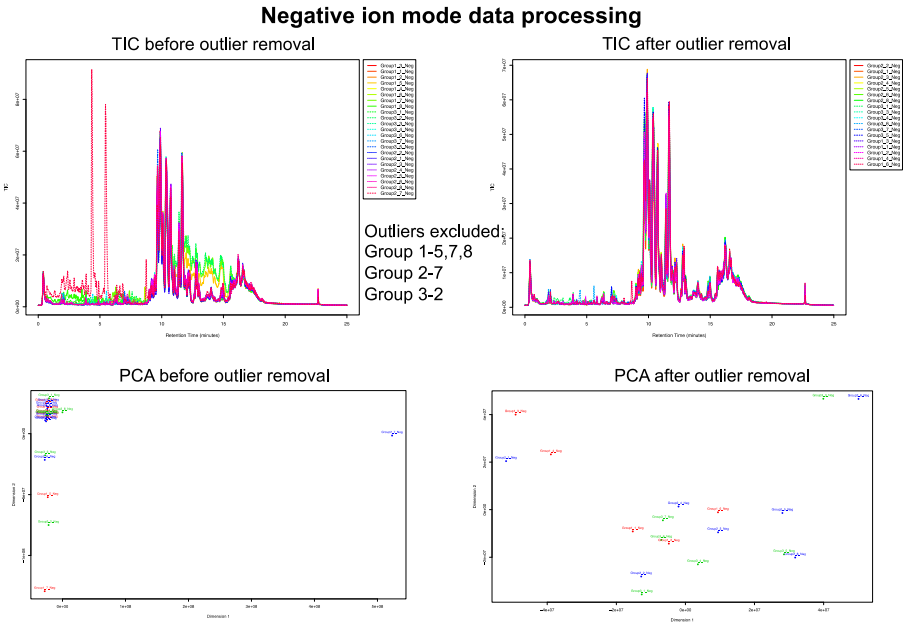

Figure 24. Example of stacked total ion chromatograms and corresponding PCA plots before (left) and after (right) outlier removal.

A large number of spectral features were identified via XCMS processing of the four data sets -- more than 3000 in the negative ion mode data and more than 5500 in the positive ion mode data (Table 10). A subset of features was identified as "important" because they discriminated between at least two groups using a parametric ANOVA test. For each important feature, the extracted ion chromatogram and mass spectra were individual reviewed as a quality check; poorly integrated peaks, isotopic peaks, and peaks resulting from peptides or small proteins were manually removed from the list. A significant amount of peptide contamination was observed in the positive ion mode data, perhaps due to insufficient precipitation of protein by the ACN-Methanol extraction. About 50% of the 'important features' in negative ion mode data and 75% of the 'important features' in the positive ion mode data were discarded at this step. Mass-to-charge ratios for remaining features were searched in METLIN and LipidMAPS for the purpose of identification, and more than half of the features could be identified this way. The accurate mass data obtained from the Orbitrap facilitated precursor compound identification and MS/MS data was used to confirm identifications, either through matching with existing spectra libraries (e.g., METLIN) or through the identification of common fragments. For example, the identification of a phosphatidylcholine was supported if the typical m/z 184.07 fragment mass was observed (Figure 25) [195].

The acquisition of separate MS/MS spectra for high intensity ions and low intensity ions increased the amount of data available for confirming identifications: 6 MS/MS fragmentation patterns could be viewed only in the CID-fragmentation spectra of low abundance ions. Overall, 71 important features remained after QC, 46 of which could be assigned putative IDs. MS/MS spectra provided additional evidence in support of 27 identifications, provided no additional information in 14 cases, and provided evidence to reject the identification in 5 cases.

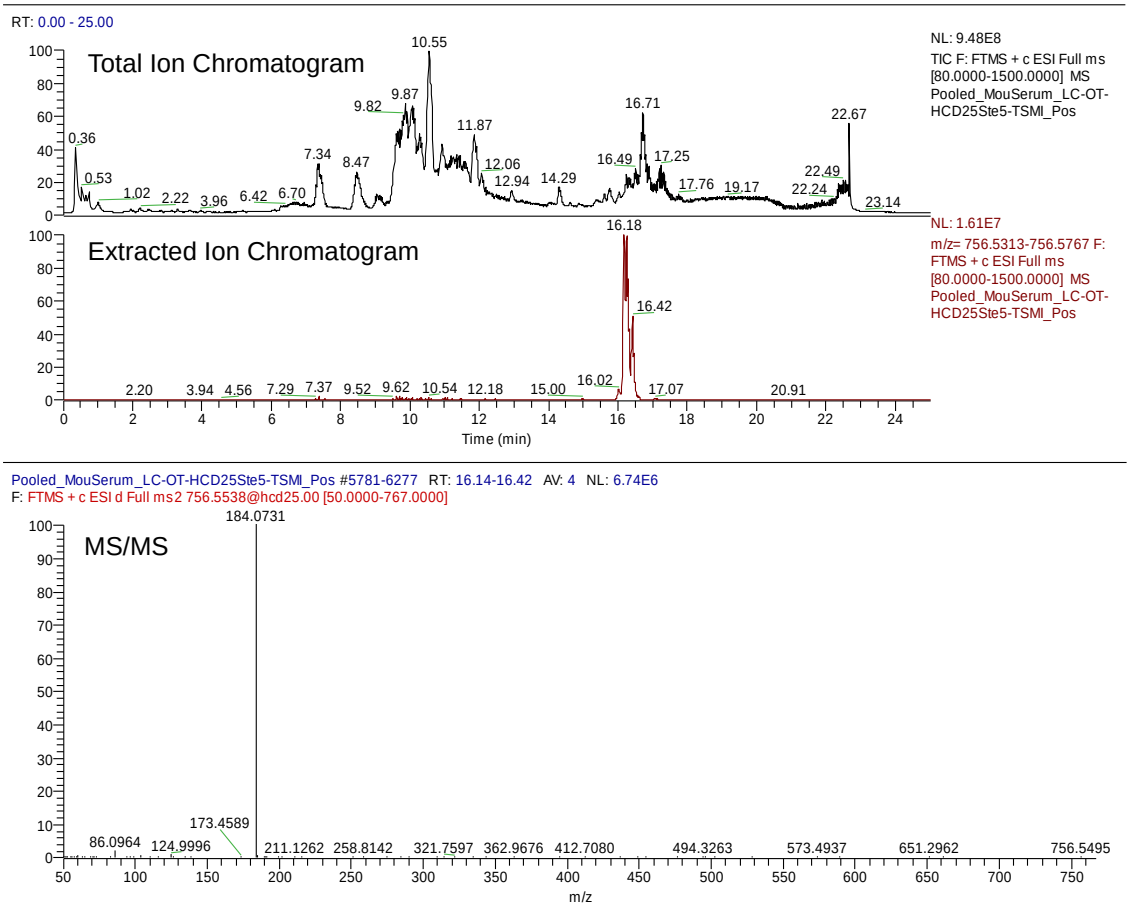

Figure 25. MS/MS spectra of putative phosphatidylcholine (m/z= 756.553) with fragments commonly observed for PCs (m/z=86.09, 184.07)

A list of the identified metabolites is shown in Table 11. The majority of compounds identified were fatty acids, amino acids, and phospholipids. Several trends are immediately observable in the data when comparing the control group to the two stressed groups (susceptible and resilient). First, all of the amino acids characterized (phenylalanine, tryptophan, and tyrosine) were reduced in concentration in the stress-susceptible group as compared to the control, and the same is true of the products of their catabolism (indoleacrylic acid, 2-hydroxycinnamic acid). Second, of the 8 fatty acids and hydroxy-fatty acids confidently identified by MS/MS, 7 were increased in the stressed mice over the controls. The exception was hydroxy-oxo-cholestenoic acid, a product of cholesterol metabolism, which was significantly decreased in the susceptible group. Most of the identified phosopholipids, including diacyl-phosphatidylcholines (PCs),

phosphatidylethanolamines (PEs) and phosphatidic acids (PAs), were decreased in the stressed group, while lower abundance alkylacyl PCs were increased. Acylcarnitines (hexanoylcarnitine, palmitoyl carnitine) were also increased in the stress group. Phosphatidyl serines, tenatively identified ceramides and stearoylserine were also increased. The same trend was observed for both the stress-susceptible and stress-resilient groups, but with a more exaggerated phenotype in the resilient group.

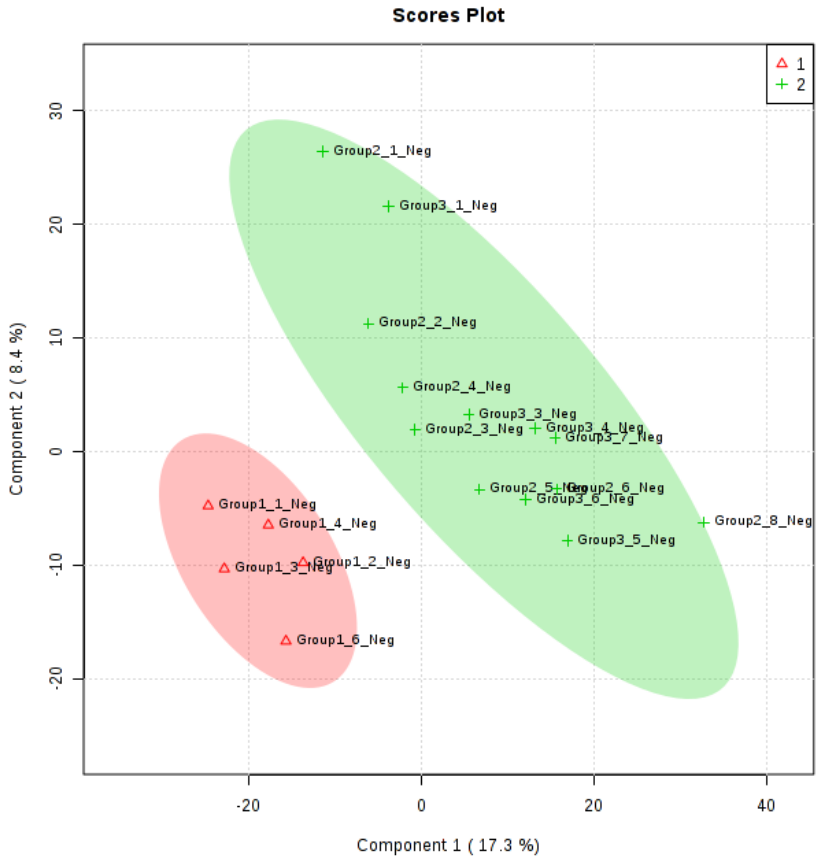

Figure 26. PLS-DA of MS peak intensities for control versus stressed mice

Analysis of the normalized peak-intensity data for control versus stressed animals with PLS-DA, performed in MetaboAnalyst, produced a pronounced separation between the groups (Figure 26). In negative ion mode, the 5 most important discriminating features were the relative abundances of small fatty acids. In positive ion mode, the 5 most important discriminating features were oleoylserine, stearoylserine, acylcarnitines, and alkyl,acyl-PCs.

Table 10. Summary of features identified in UPLC-FTMS and UPLC-MS/MS lipid profiling of mouse plasma

Dataset	**Samples excluded**	**# of groups identified** (XCMS online)	**Important features identified** (ANOVA parametric test, p-value ≤ 0.01)	**Significant features remaining after QC**	**Features with putative IDs**	**MS/MS data** (supported / no evidence / rejected)
Negative ion mode	1-5, 1-7, 1-8, 2-7, 3-2	3248	64	31	20	9 / 10 / 1
Positive ion mode	1-5, 1-7, 1-8, 2-7, 3-1, 3-2	5502	174	40	26	18 / 4 / 4

Table 11. List of metabolite IDs obtained from lipidomic profiling of mouse plasma

Putative ID	**Metabolite class**	**Ion mode**	**m/z**	**Retent. time**	**Adduct**	**m/z ppm**	**Supported by MS/MS?**	**Avg peak intensity -controls**	**Avg peak intensity -susceptible**	**Avg peak intensity -resilient**	p-value
Hydroxy dodecanoic acid	Medium-chain hydroxy fatty acid	Negative	215.165	7.78	[M-H]-	1	yes: matching spectra	1.08E+05	1.48E+05	2.05E+05	0.0092
Tetradecanoid acid (myristic) acid	Long-chain fatty acids	Negative	227.201	11.42	[M-H]-	2	yes: matching fragments	1.14E+05	1.71E+05	1.62E+05	0.0058
Oxo tetradecenoic acid	Long-chain keto fatty acids	Negative	239.165	7.93	[M-H]-	1	yes: matching fragments	2.40E+05	4.03E+05	5.23E+05	0.0142
Hydroxytetradecanoic acid	Long-chain hydroxy fatty acids	Negative	243.196	7.42	[M-H]-	2	*not acquired*	5.91E+04	1.08E+05	1.80E+05	0.0040
Dihydrohydroxy naphthalenylthiooxopropanoic acid	Short-chain keto fatty acids	Negative	263.038	0.75	[M-H]-	1	*ambiguous*	1.02E+05	8.58E+04	7.51E+04	0.0127
Hydroxy hexadecenoic acid	Long-chain hydroxy fatty acids	Negative	269.212	8.16	[M-H]-	0	yes: matching fragments	9.77E+04	2.39E+05	4.65E+05	0.0107
(9/13)-HODE	Lineolic acids	Negative	295.227	8.84	[M-H]-	2	yes: matching fragments	4.54E+05	9.67E+05	1.47E+06	0.0059

Hydroxy octadecanoic acid	Long-chain hydroxy fatty acids	Negative	299.259	13.22	[M-H]-	0	yes: matching fragments	1.61E+05	2.22E+05	2.39E+05	0.0014
Dihydroxy octadecenoic acid	Long-chain hydroxy fatty acids	Negative	313.237	8.05	[M-H]-	4	yes: matching fragments	1.01E+06	1.23E+06	1.78E+06	0.0068
docosenoic acid	Long-chain fatty acids	Negative	337.310	13.00	[M-H]-	3	*not acquired*	1.61E+05	1.30E+05	1.19E+05	0.0135
Hydroxyoxo cholestenoic acid	Bile acids	Negative	429.300	9.33	[M-H]-	1	yes: matching fragments	6.32E+05	4.81E+05	5.18E+05	0.0038
LysoPE (22:4)	Phospho ethanolamines (unsaturated)	Negative	528.308	9.92	[M-H]-	2	yes: matching fragments	1.29E+07	1.75E+07	1.34E+07	0.0057
LysoPE (24:1)	Phospho ethanolamines (unsaturated)	Negative	562.386	13.00	[M-H]-	3	*not acquired*	1.04E+06	8.70E+05	7.46E+05	0.0092
PS (21:1)	Phosphatidyl cholines (unsaturated)	Negative	566.345	11.31	[M-H]-	2	*ambiguous*	2.23E+05	2.05E+05	1.37E+05	0.0086
PE-Nme (36:2) or PC (34:2)	Phosphatidyl cholines (unsaturated)	Negative	756.553	16.92	[M-H]-	2	*not acquired*	6.01E+05	5.13E+05	4.88E+05	0.0011
GlcCer(36:1)	Ceramides	Negative	762.564	16.87	[M+Cl]-	2	*not acquired*	8.12E+04	9.94E+04	1.09E+05	0.0073
GlcCer(36:0)	Ceramides	Negative	764.579	17.36	[M+Cl]-	2	*not acquired*	1.72E+05	2.29E+05	2.64E+05	0.0107
Thioetheramide-PC	Phosphatidyl cholines	Negative	769.548	15.47	[M+Cl]-	3	*not acquired*	1.73E+05	1.20E+05	1.30E+05	0.0065
PS (38:1)	Phosphatidyl serines (unsaturated)	Negative	816.573	9.69	[M-H]-	3	*not acquired*	9.53E+04	8.93E+04	1.57E+05	0.0023
PS(40:2)	Phosphatidyl serines (unsaturated)	Negative	842.589	17.00	[M-H]-	3	*not acquired*	2.84E+05	2.25E+05	1.98E+05	0.0006
niacinamide	Nicotinamides	Positive	123.055	0.52	[M+H]+	0	yes: matching spectra	7.58E+05	9.29E+05	9.89E+05	0.0165
2-Hydroxycinna	Hydroxy cinnamic acids	Positive	165.054	0.51	[M+H]+	0	yes: matching	5.13E+05	4.03E+05	3.52E+05	0.0026

mic acid							spectra				
Phenylalanine	Amino acids	Positive	166.086	0.64	[M+H]+	1	yes: matching spectra	3.67E+07	3.13E+07	2.82E+07	0.0112
Tyrosine	Amino acids	Positive	182.081	0.51	[M+H]+	0	yes: matching spectra	2.55E+06	2.03E+06	1.74E+06	0.0030
Indoleacrylic acid	Indoles	Positive	188.070	0.73	[M+H]+	0	yes: matching spectra	3.41E+07	2.69E+07	2.31E+07	0.0082
Tryptophan	Amino acids	Positive	205.097	0.73	[M+H]+	1	yes: matching spectra	3.78E+07	2.94E+07	2.51E+07	0.0088
Tryptophan	Amino acids	Positive	227.079	0.73	[M+Na]+	0	yes: matching spectra	4.90E+06	4.01E+06	3.43E+06	0.0079
L-Hexanoylcarnitine	Acylcarnitines	Positive	260.185	1.92	[M+H]+	0	yes: matching spectra	2.99E+05	4.50E+05	4.99E+05	0.0324
Dihydroxy octadecenoic acid	Long-chain hydroxy fatty acid	Positive	337.234	8.10	[M+Na]+	1	*not acquired*	9.56E+05	1.43E+06	2.39E+06	0.0033
Tetrahydro pentoxyline	Alkaloids	Positive	367.149	0.72	[M+H]+	0	*not acquired*	1.36E+06	9.96E+05	7.38E+05	0.0117
Oleoyl-Serine	Amino acids	Positive	370.295	8.30	[M+H]+	0	*ambiguous*	7.86E+05	1.08E+06	1.22E+06	0.0082
Stearoyl serine	Amino acids	Positive	372.310	9.00	[M+H]+	0	yes: matching spectra	1.10E+06	1.45E+06	1.74E+06	0.0109
Hexadecenoyl carnitine	Acylcarnitines	Positive	398.326	9.45	[M+H]+	0	*ambiguous*	4.39E+05	7.33E+05	1.02E+06	0.0003
Palmitoylcarnitine	Acylcarnitines	Positive	400.341	10.36	[M+H]+	0	yes: matching spectra	3.57E+06	4.45E+06	4.86E+06	0.0143
PA (18:0)	Phosphatidic acids (saturated)	Positive	459.248	10.11	[M+Na]+	0	*not acquired*	2.59E+06	2.38E+06	2.29E+06	0.0072
PS(O-18:0)	Phosphatidyl serines (saturated)	Positive	512.334	7.06	[M+H]+	0	yes: matching fragments	1.92E+06	2.92E+06	8.25E+06	0.0139
PS (O-20:0)	Phosphatidyl	Positive	540.365	8.38	[M+H]+	0	yes:	4.64E+05	6.73E+05	2.00E+06	0.0132

	serines (saturated)						matching fragments				
PC / LysoPC (20:2)	Phosphatidyl cholines (unsaturated)	Positive	548.370	11.07	[M+H]+	0	yes: matching fragments	2.93E+07	2.96E+07	2.41E+07	0.0078
PC / LysoPC (22:1)	Phosphatidyl cholines (unsaturated)	Positive	578.417	13.04	[M+H]+	0	yes: matching fragments	5.90E+06	5.48E+06	4.22E+06	0.0043
PC(O-32:1)	Phosphatidyl cholines (unsaturated)	Positive	718.574	16.89	[M+H]+	0	yes: matching fragments	1.14E+06	1.42E+06	1.52E+06	0.0052
PC(O-32:0)	Phosphatidyl cholines (unsaturated)	Positive	720.590	17.39	[M+H]+	0	*ambiguous*	2.85E+06	3.74E+06	4.12E+06	0.0092
PC (34:3)	Phosphatidyl cholines (unsaturated)	Positive	756.554	16.11	[M+H]+	0	yes: matching fragments	1.82E+08	1.41E+08	1.31E+08	0.0036
PE (38:3)	Phosphatidyl cholines (unsaturated)	Positive	770.569	16.46	[M+H]+	0	*ambiguous*	1.16E+07	1.00E+07	8.31E+06	0.0025
PC (34:2)	Phosphatidyl cholines (unsaturated)	Positive	780.550	16.67	[M+Na]+	1	yes: matching fragments	3.10E+07	3.02E+07	3.26E+07	0.0099
PC (36:3)	Phosphatidyl cholines (unsaturated)	Positive	784.584	16.75	[M+H]+	0	yes: matching fragments	3.98E+08	3.75E+08	3.42E+08	0.0265
PE (42:7)	Phosphatidyl cholines (unsaturated)	Positive	818.567	16.19	[M+H]+	1	*ambiguous*	1.45E+06	1.33E+06	8.74E+05	0.0080
(not identified)		Negative	826.556	16.53			no: initial ID not supported	1.43E+07	1.49E+07	1.36E+07	0.0034
(not identified)		Negative	271.069	0.76			*ambiguous*	1.28E+05	1.13E+05	1.02E+05	0.0126
(not identified)		Negative	277.059	0.60			no: initial ID not supported	6.27E+04	7.85E+04	1.03E+05	0.0053
(not identified)		Negative	427.321	12.85			no: initial ID not supported	1.31E+05	8.87E+04	8.81E+04	0.0068
(not identified)		Negative	473.326	6.25			no: initial ID	4.25E+05	3.58E+05	2.69E+05	0.0139

							not supported				
(not identified)		Negative	487.112	0.74			no: initial ID not supported	1.31E+05	9.51E+04	8.13E+04	0.0091
(not identified)		Negative	563.144	9.87			*ambiguous*	1.87E+05	1.79E+05	2.07E+05	0.0147
(not identified)		Negative	622.407	13.00			*ambiguous*	1.38E+06	1.16E+06	9.88E+05	0.0066
(not identified)		Negative	660.259	9.70			*ambiguous*	1.26E+05	1.28E+05	9.72E+04	0.0082
(not identified)		Negative	904.603	17.03			*not acquired*	1.14E+05	9.84E+04	8.00E+04	0.0044
(not identified)		Negative	1413.092	10.37			*ambiguous*	9.76E+04	1.04E+05	8.32E+04	0.0048
(not identified)		Positive	120.080	0.64			*ambiguous*	2.04E+07	1.76E+07	1.58E+07	0.0112
(not identified)		Positive	142.065	0.73			*ambiguous*	4.81E+05	3.59E+05	3.18E+05	0.0087
(not identified)		Positive	170.060	0.73			*ambiguous*	1.84E+06	1.41E+06	1.18E+06	0.0102
(not identified)		Positive	198.308	10.38			*ambiguous*	4.21E+05	4.54E+05	3.78E+05	0.0041
(not identified)		Positive	243.052	0.73			*ambiguous*	6.33E+05	4.80E+05	4.10E+05	0.0136
(not identified)		Positive	275.644	7.07			*not acquired*	6.83E+04	1.14E+05	3.23E+05	0.0108
(not identified)		Positive	304.154	11.05			*not acquired*	3.48E+05	3.07E+05	2.69E+05	0.0043
(not identified)		Positive	325.211	12.20			no: initial ID not supported	3.12E+06	3.31E+06	3.50E+06	0.0143
(not identified)		Positive	396.310	8.69			*not acquired*	3.80E+05	4.45E+05	5.68E+05	0.0258
(not identified)		Positive	431.315	9.37	[M+H]+	0	*ambiguous*	5.51E+05	4.28E+05	4.48E+05	0.0062
(not identified)		Positive	562.347	8.40			*ambiguous*	1.78E+05	2.28E+05	7.31E+05	0.0116
(not identified)		Positive	803.036	15.75			*ambiguous*	5.38E+05	4.19E+05	3.67E+05	0.0062
(not identified)		Positive	1031.704	10.77			*ambiguous*	1.92E+06	1.82E+06	1.46E+06	0.0060
(not identified)		Positive	1043.607	9.98			*ambiguous*	7.42E+05	7.42E+05	6.34E+05	0.0122

Discussion

Findings of MDA quantitation experiments: The MDA analysis did not generate any evidence in support of a relationship between oxidative stress and lipid peroxidation in chronic stress. It is however worth noting that the very high MDA levels observed in mouse plasma (~60-90 μM) reinforce the importance of using an assay with a broad linear range such as the MRM-MS quantitation method. As previously discussed, many currently used assays (e.g., GC-MS analysis) have a linear range whose upper limit is not sufficient to study total MDA in humans and these would certainly be insufficient to work with mouse plasma [196].

Findings of lipid profiling experiments: The results from untargeted lipid profiling provide new evidence concerning the pathophysiology of chronic stress. Decreases in the concentration of many phospholipids were observed in the plasma of chronically stressed mice, similar to those seen in the serum of human patients with high DNA methylation at the promoter for the glucocorticoid receptor gene (Chapter 1). However, the high resolution high mass accuracy Orbitrap data obtained also enabled the identification of a number of other metabolites that, combined, provide much more context for interpreting this observation.

A large number of the metabolites identified as important features map to glycerophospholipid metabolism, indicating significant disturbances in energy metabolism beyond the changes in phospholipid concentrations. The increase in free fatty acids and acylcarnitines, which are responsible for transporting fatty acids into the mitochondria, may suggest a shift in metabolism between beta-oxidation and glycolysis. On the other hand, the increased pool of free fatty acids could also be attributed to a defect in phospholipid synthesis, and this is potentially supported by the appearance of increased concentrations of atypical alkyl,acyl-PCs, which generally make up a very small portion of the phospholipid content in plasma. Since ether lipids are produced through a completely different synthesis pathway, it is possible that increased synthesis

of alkyl,acyl-phospholipids is being driven by the increased pool of fatty acids due to reduced synthesis of or increased catabolism of diacyl-phospholipids.

In addition, several of the observed markers suggest cell distress. The appearance of increased phosphatidylserines and phosphatidylinositol, which are usually restricted to face the cytosol, may indicate that plasma cells are undergoing apoptosis. Both acyl-amides (e.g., stearoyl serine) and ceramides have been proposed as potential lipid signalling molecules, and ceramides have been specifically associated with regulating programmed cell death, perhaps having a link to the presence of phosphatidylserines in plasma. Interestingly, increased ceramides and cholesterol are also associated with membrane oxidative stress [197].

Both tyrosine and tryptophan depletion have been previously observed in rats following high adrenal activation [198]. Decreased tryptophan has also been associated with depression [199] and increased immune activation [200]. The finding of increased abundance of niacinamide among the stressed groups might suggest differences in absorption efficiency, since its primary source in animals is dietary, and previous studies have suggested that chronic social defeat stress induces changes in food consumption and may increase intestinal inflammation [201, 202].

Context and caveats: Some outlying spectra had to be excluded from the data, due to massive differences in their total ion chromatograms, likely as a result of handling errors at the time of sample collection. Since the samples were collected at the time of perfusion, some samples may have been exposed to contamination from either animal tissue or other materials used in the procedure. Errors in the fractioning of blood into plasma could also be responsible, and this is not unlikely as the colour and viscosity of samples was highly variable after thawing. Still, even with the smaller group sizes resulting from outlier removal, a clear metabolomic phenotype was observed.

The biochemical data presented covers a much wider range of metabolites than previously published studies linking chronic stress to changes in energy metabolism and amino acid metabolism (e.g., in the CUMS model), especially with respect to the inclusion of high molecular weight phospholipids. However, the metabolite

identifications in this dataset, though considered to be reliable, cannot be confirmed. The MS/MS data available in METLIN and used for comparison is primarily QTOF-MS data, so they cannot strictly be used as references for data collected on a different type of instrument. To confirm these identifications, standards would need to be purchased and reference spectra collected on the Orbitrap. In addition, isomers cannot be distinguished in this dataset, but this distinction may ultimately be important for correctly determining the affected pathways and the health implications. Overall, additional work needs to be done to determine the significance of the observed phenotype. Many of the important metabolites are the product of multiple pathways (e.g., there are several potential pathways for PC synthesis). Ultimately, follow-on targeted metabolomics experiments need to be performed to confirm the findings, identify the associated pathways, and provide quantitative metabolite concentrations that can be compared to reference values. Nonetheless, this study provides important clues about the metabolic signatures of chronic stress that will help to direct future research.

Implications about the pathophysiology of chronic stress: Both stress-susceptible and stress-resilient mice share a clear metabolomic profile that differentiates them from the control animals. However, what is perhaps most striking about the data is that for the majority of these features, the metabolomic phenotype that appears in the susceptible group is even more pronounced in the resilient group – fatty acids are further increased and phospholipids are further decreased in the resilient group as compared to the susceptible group. Although the resilient mice display fewer symptoms of stress and depression, their metabolism is significantly more disturbed than their stress-susceptible counterparts. This unexpected finding has significant implications for understanding stress physiology: it may suggest that this potentially harmful molecular phenotype of phospholipid dysregulation is actually exerting protective effects against some of the adverse impacts of chronic stress. If true, this might lead to a significant reframing of the role of lipid metabolism in chronic stress.

Conclusions & Outlook

Major outcomes

Findings: The purpose of this project was to generate new insights into the biochemical processes and pathways associated with chronic stress. Metabolomic analysis was conducted in two very different models of chronic stress: a human epigenetic model and a mouse social defeat stress model. As expected, the application of modern MS-based technologies offered a sensitive analytical technique for performing robust highly-multiplexed quantitation of a large number of analytes and for relative profiling of metabolites across several different classes, while obtaining a high degree of coverage. Results from both models support the premise that chronic stress is a unique condition with distinct physiology, and specific biochemical markers. Analysis of the data from both models reveals a distinct metabolomic profile associated with chronic stress: significant dysregulation of energy metabolism characterized by the depletion of phospholipid concentrations.

Discussion: The convergence of the findings from multiple models provides strong evidence for a specific, significant, and reproducible relationship of energy metabolism to chronic stress. The appearance of this profile in a human epigenetic model suggests that the changes observed in lipid profiles are not exclusively a by-product of well-known confounders (e.g., dietary alterations or socioeconomic factors associated with chronic stress), since it is also appears in a mouse model where such variables are controlled. Furthermore, the direct association of this profile with the degree of glucocorticoid promoter methylation supports the importance of this epigenetic factor in modulating stress response, irrespective of the factors contributing to methylation. This is important to note since previous studies have focused on recruiting patients exposed to early life stressors resulting in increased DNA methylation; however, these patients are not necessarily representative of the general population. The findings presented in Chapter 1 suggest that for the purpose of chronic stress research, it may be possible to sample a

wider portion of the population and produce meaningful groupings based on variations in the DNA methylation alone, without the need to measure external factors influencing methylation. With respect to the mouse model, the appearance of a matching profile of lipid dysregulation in chronic social defeat stress may lend additional support for the clinical applicability of this model intended for translation to human health.

Finally, this convergence may also be considered support for the utility of the metabolomics methods applied, particularly the use of untargeted metabolomic profiling, which has known challenges in its application to heterogenous human populations and has occasionally been criticized in relation to its analytical limitations (e.g., difficulties with confident identification, non-quantitative data) [203, 204] [205]. With respect to untargeted metabolomics, the results generated in this project certainly demonstrate the importance of recent technological advancements in MS: the quality and quantity of evidence that can be obtained from Orbitrap MS instruments is much higher than older technologies because very high mass resolution and mass accuracy facilitate confident identifications. In addition, these systems (e.g., the Thermo Orbitrap Velos or Fusion) offer a high level of versatility for metabolomics workflows, e.g., the ability to implement multiple workflows for acquisition of MS/MS data with different fragmentation approaches.

In addition to applying existing methods, a new LC/MRM-MS method for the quantitation of malondialdehyde (MDA) was successfully developed and validated. The method displays high accuracy and reproducibility, and offers significant advantages over previous methods in terms of its sensitivity, linear range, and throughput. Although the analysis completed in this project did not demonstrate a relationship between lipid peroxidation and chronic stress in plasma from mice, the simple experimental workflow, favourable performance characteristics, and high throughput of this assay will no doubt make it useful to other researchers, particularly those interested in conducting large-scale studies. Oxidative stress is associated with a wide variety of diseases, so it has wide applicability; for instance, application of the method to clinical samples in this project reproduced the relationship between oxidative stress and obesity. In addition to developing the method for MDA, we also performed proof-of-concept experiments

demonstrating the use of a complementary derivatization strategy using the same reagent (3-nitrophenylhydrazine) that would be suitable to develop quantitative assays for a larger panel of aldehydes. Overall, the project has provided new insights into the metabolomic profile associated with chronic stress, evidence about the utility of specific models and methods in chronic stress research, and new tools for metabolomics analysis.

Metabolomics-derived insights into chronic stress

The metabolomic profile of chronic stress: By identifying metabolites that showed consistent trends across multiple models of chronic stress, we were able to obtain some new insights into the physiology of chronic stress and to provide further evidence for some previously published markers. Both models demonstrated decreases in the concentrations of many phospholipid species, and increases in carnitines. In addition, high quality untargeted metabolomic data from mouse study suggested an increased plasma concentration of fatty acids and hydroxy-fatty acids, an increased concentration of ether phospholipids, increased concentration of lipid signalling molecules such as acyl-amides and ceramides, and decreased concentrations of certain amino acids (phenylalanine, tryptophan, and tyrosine).

Overall, the findings support the idea that chronic stress is characterized by a massive dysregulation of energy metabolism. The association between chronic stress and energy metabolism appears in a plethora of literature; however the exact metabolites identified and trends observed vary from paper to paper [206, 207]. Several published papers describe alterations in the lipid profile that are opposite to our findings: studies of chronic stress and major depressive disorder have found an increase in phosphatidylcholine and phospholipid levels, with a decrease in fatty acid concentrations [113, 208, 209]. However, many of the previous studies profiled metabolites from tissue or urine, where the changes in metabolism may be quite distinct. Evidence from the mouse model suggests a relationship of chronic stress to other pathways, including amino acid metabolism and possibly cell death, both of which agree with previous findings [210, 211]. While the studies of MDA concentration did not generate evidence regarding

a potential role for oxidative stress, the observed increases in ceramides may reopen this question. Additional evidence for or against the role of oxidative stress could perhaps be generated by measuring alternative targets. Overall, more work needs to be done to confirm the findings by repeating the lipid profiling experiments in additional plasma samples from the same model and in samples from additional models of chronic stress.

Direct extensions

There are a number of opportunities that could be pursued to expand on the work so far completed. In particular, more work needs to be done to determine how phospholipid levels become dysregulated. Follow-on studies should seek to assess citric acid cycle activity, as the citric acid cycle is fed by products of amino acid metabolism as well as fatty acid oxidation. Outputs from this cycle also feed forward into fatty acid biosynthesis and elongation, making this a potentially interesting set of targets to help elucidate the exact pathways by which fatty acid composition is altered in chronic stress. The tricarboxylic acid cycle (TCA cycle) would also be a compelling target for further studies. Metabolomics flux analysis could also be used to assess shifts in activity between glycolysis and other parts of the pathway. Certainly, given the complexity of fatty acid composition in cells and considering that previous work has shown different changes in fatty acid composition, carefully-designed targeted lipidomics studies need to be performed to determine, in greater detail, the individual changes in concentration for each subspecies present. With respect to the models employed, additional studies using chronic social defeat stress should consider using longer timepoints and including multiple timepoints for plasma collection to enable longitudinal monitoring of the development of the chronic stress phenotype.

Additional directions in chronic stress research

Previous studies of chronic stress have shown an increase in circulating phosphatidylcholine, but my work found a consistent trend toward the depletion of long-chain phosphatidylcholines under conditions of chronic stress. It has previously been observed that the administration of some phospholipid liposomes may inhibit the cortisol response. If true, then the depletion of endogenous phospholipids could also have an

influence on the binding of cortisol. This might provide an additional mechanism to explain the unexpected reduction in cortisol levels under conditions of chronic stress: If phospholipids are depleted in chronic stress, this could help to sensitize peripheral cells and tissues to cortisol so that an HPA axis response is effectively mounted even in response to very minimal changes in cortisol concentrations. This could help to account for how the symptoms of stress, such as increased heart rate, continue to be present even in patients with depressed baseline cortisol. Uniquely modulated phospholipid profiles in different tissues and structures might also enable certain parts of the cortisol response to be preserved while other (less adaptive) effects are abolished. Many prominent stress researchers have suggested that the down-regulation of the HPA axis observed in chronic stress represents a necessary tapering of the stress response to adapt to a stressful environment. As an alternative, a phospholipid-mediated shift toward higher cortisol sensitivity would enable the rapid generation of stress responses even under chronically stressful conditions without the adverse effects of excessive cortisol exposure. This hypothesis would be exciting to explore in future work.

Bibliography

[1] Djuric, Z., Bird, C. E., Furumoto-Dawson, A., Rauscher, G. H., *et al.*, Biomarkers of Psychological Stress in Health Disparities Research. *The Open Biomarkers Journal* 2008, *1*, 7-19.

[2] Baum, A., Garofalo, J. P., Yali, A. M., Socioeconomic Status and Chronic Stress: Does Stress Account for SES Effects on Health? *Annals of the New York Academy of Sciences* 2006, *896*, 131-144.

[3] Koob, G. F., Alcoholism: allostasis and beyond. *Alcoholism: Clinical and Experimental Research* 2003, *27*, 232-243.

[4] Evans, G. W., Schamberg, M. A., Childhood poverty, chronic stress, and adult working memory. *Proceedings of the National Academy of Sciences* 2009, *106*, 6545-6549.

[5] Gianaros, P. J., Jennings, J. R., Sheu, L. K., Greer, P. J., Prospective reports of chronic life stress predict decreased grey matter volume in the hippocampus. *Neuroimage* 2007, *35*, 795-803.

[6] Goertzel, B. N., Pennachin, C., de Souza Coelho, L., Allostatic load is associated with symptoms in chronic fatigue syndrome patients. *Pharmacogenomics* 2006, *7*, 485-494.

[7] Kapczinski, F., Vieta, E., Andreazza, A. C., Frey, B. N., Allostatic load in bipolar disorder: implications for pathophysiology and treatment. *Neuroscience and Biobehavioral Reviews* 2008, *32*, 675-692.

[8] Karlamangla, A. S., Singer, B. H., Greendale, G. A., Increase in epinephrine excretion is associated with cognitive decline in elderly men: MacArthur studies of successful aging. *Psychoneuroendocrinology* 2005, *30*, 453-460.

[9] Espie, C. A., Insomnia: conceptual issues in the development, persistence, and treatment of sleep disorder in adults. *Annual review of psychology* 2002, *53*, 215-243.

[10] McEwen, B. S., Mood disorders and allostatic load. *Biological psychiatry* 2003, *54*, 200-207.

[11] Juster, R. P., McEwen, B. S., Lupien, S. J., Allostatic load biomarkers of chronic stress and impact on health and cognition. *Neuroscience & Biobehavioral Reviews* 2010, *35*, 2-16.

[12] Vitaliano, P. P., Scanlan, J. M., ZHANG, J., A path model of chronic stress, the metabolic syndrome, and coronary heart disease. *Psychosomatic Medicine* 2002, *64*, 418-435.

[13] Przewłocki, R., Lasoń, W., Ho llt, V., Silberring, J., Herz, A., The influence of chronic stress on multiple opioid peptide systems in the rat: pronounced effects upon dynorphin in spinal cord. *Brain research* 1987, *413*, 213-219.

[14] Dhabhar, F. S., Acute stress enhances while chronic stress suppresses skin immunity: the role of stress hormones and leukocyte trafficking. *Annals of the New York Academy of Sciences* 2000, *917*, 876-893.

[15] Glaser, R., Sheridan, J., Malarkey, W. B., Chronic stress modulates the immune response to a pneumococcal pneumonia vaccine. *Psychosomatic Medicine* 2000, *62*, 804-807.

[16] Sabbah, W., Watt, R. G., Sheiham, A., Effects of allostatic load on the social gradient in ischaemic heart disease and periodontal disease: evidence from the Third National Health and Nutrition Examination Survey. *Journal of Epidemiology & Community Health* 2008, *62*, 415-420.

[17] Lundberg, U., Stress Responses in Low‐Status Jobs and Their Relationship to Health Risks: Musculoskeletal Disorders. *Annals of the New York Academy of Sciences* 1999, *896*, 162-172.

[18] Goodman, E., McEwen, B. S., Huang, B., Social inequalities in biomarkers of cardiovascular risk in adolescence. *Psychosomatic Medicine* 2005, *67*, 1.

[19] Allsworth, J. E., Weitzen, S., Boardman, L. A., Early age at menarche and allostatic load: data from the Third National Health and Nutrition Examination Survey. *Annals of epidemiology* 2005, *15*, 438-444.

[20] Crimmins, E. M., Kim, J. K., Poverty and biological risk: The earlier "aging" of the poor. *Journal of Gerontology. Series A, biological Sciences and Medical Sciences* 2009, *64*, 286-292.

[21] Chrousos, G. P., The role of stress and the hypothalamic-pituitary-adrenal axis in the pathogenesis of the metabolic syndrome: neuro-endocrine and target tissue-related causes. *International Journal of Obesity & Related Metabolic Disorders* 2000, *24*, S50-55.

[22] Kiecolt-Glaser, J. K., Preacher, K. J., *Proceedings of the National Academy of Sciences* 2003.

[23] Bagchi, M., Milnes, M., Williams, C., Balmoori, J., Ye, X., Acute and chronic stress-induced oxidative gastrointestinal injury in rats, and the protective ability of a novel grape seed proanthocyanidin extract. *Nutrition research* 1999, *19*, 1189-1199.

[24] Karlamangla, A. S., Singer, B. H., Reduction in allostatic load in older adults is associated with lower all-cause mortality risk: MacArthur studies of successful aging. *Psychosomatic Medicine* 2006.

[25] Lozano, R., Naghavi, M., Foreman, K., Lim, S., Shibuya, K., Global and regional mortality from 235 causes of death for 20 age groups in 1990 and 2010: a systematic analysis for the Global Burden of Disease Study 2010. *The Lancet* 2013.

[26] Walker, F., Jones, K., Zouikr, I., Patience, M., Understanding 'stress x microglial interactions' in stroke-induced secondary neurodegeneration: A major opportunity for the preservation of viable brain tissue. *Brain* 2015, *49*, e19-e20.

[27] Henderson, K. M., Clark, C. J., Lewis, T. T., Aggarwal, N. T., Psychosocial distress and stroke risk in older adults. *Stroke* 2013.

[28] Selye, H., The Evolution of the Stress Concept: The originator of the concept traces its development from the discovery in 1936 of the alarm reaction to modern therapeutic …. *American Scientist* 1973, *61*, 692-699.

[29] Sapolsky, R. M., Romero, L. M., Munck, A. U., How do glucocorticoids influence stress responses? Integrating permissive, suppressive, stimulatory, and preparative actions 1. *Endocrine reviews* 2000, *21*, 55-89.

[30] Fuchs, E., Flügge, G., Chronic social stress: effects on limbic brain structures. *Physiology & Behavior* 2003, *79*, 417-427.

[31] Kirschbaum, C., Pirke, K. M., Hellhammer, D. H., The 'Trier Social Stress Test'–a tool for investigating psychobiological stress responses in a laboratory setting. *Neuropsychobiology* 1993, *28*, 76-81.

[32] Sapolsky, R. M., *Why zebras don't get ulcers: The acclaimed guide to stress, stress-related diseases, and coping-now revised and updated*, Holt, Henry & Company, Inc 2004.

[33] Morelli, F., Burton, P. A., *Conference proceedings - U.S. Army Research Laboratory* 2004.

[34] Roozendaal, B., Stress and memory: opposing effects of glucocorticoids on memory consolidation and memory retrieval. *Neurobiology of learning and memory* 2002, *78*, 578-595.

[35] McEwen, B. S., Central effects of stress hormones in health and disease: Understanding the protective and damaging effects of stress and stress mediators. *European journal of pharmacology* 2008, *583*, 174-185.

[36] Sapolsky, R. M., Uno, H., Rebert, C. S., Hippocampal damage associated with prolonged glucocorticoid exposure in primates. *The Journal of Neuroscience* 1990, *10*, 2897-2902.

[37] Bagdy, G., Calogero, A. E., Aulakh, C. S., Szemeredi, K., Long-term cortisol treatment impairs behavioral and neuroendocrine responses to 5-HT1 agonists in the rat. *Neurobiology of Disease* 1989, *50*, 241-247.

[38] Stalder, T., Tietze, A., Steudte, S., Alexander, N., *et al.*, Elevated hair cortisol levels in chronically stressed dementia caregivers. *Psychoneuroendocrinology* 2014, *47*, 26-30.

[39] Steudte, S., Stalder, T., Dettenborn, L., Klumbies, E., *et al.*, Decreased hair cortisol concentrations in generalised anxiety disorder. *Psychiatry research* 2011, *186*, 310-314.

[40] De Vente, W., Olff, M., Van Amsterdam, J. G. C., Kamphuis, J. H., Emmelkamp, P. M. G., Physiological differences between burnout patients and healthy controls: blood pressure, heart rate, and cortisol responses. *Occupational and environmental medicine* 2003, *60 Suppl 1*, i54-61.

[41] Steudte, S., Kirschbaum, C., Gao, W., Alexander, N., Hair cortisol as a biomarker of traumatization in healthy individuals and posttraumatic stress disorder patients. *Biological psychiatry* 2013, *74*, 639-646.

[42] Kumari, M., Badrick, E., Chandola, T., Adam, E. K., Cortisol secretion and fatigue: associations in a community based cohort. *Psychoneuroendocrinology* 2009, *34*, 1476-1485.

[43] Andersen, J. P., Silver, R. C., Stewart, B., Koperwas, B., Psychological and physiological responses following repeated peer death. *PLoS ONE* 2013, *8*, e75881.

[44] Steudte-Schmiedgen, S., Stalder, T., Schönfeld, S., Hair cortisol concentrations and cortisol stress reactivity predict PTSD symptom increase after trauma exposure during military deployment. *Psychoneuroendocrinology* 2015, *59*, 123-133.

[45] Uschold-Schmidt, N., Nyuyki, K. D., Füchsl, A. M., Chronic psychosocial stress results in sensitization of the HPA axis to acute heterotypic stressors despite a reduction of adrenal in vitro ACTH responsiveness. *Psychoneuroendocrinology* 2012, *37*, 1676-1687.

[46] Schalinski, I., Elbert, T., Steudte-Schmiedgen, S., Kirschbaum, C., The Cortisol Paradox of Trauma-Related Disorders: Lower Phasic Responses but Higher Tonic Levels of Cortisol Are Associated with Sexual Abuse in Childhood. *PLoS ONE* 2015, *10*, e0136921.

[47] Lovell, B., Moss, M., Wetherell, M. A., Perceived stress, common health complaints and diurnal patterns of cortisol secretion in young, otherwise healthy individuals. *Hormones and behavior* 2011, *60*, 301-305.

[48] Childs, J. H., Stoeber, J., Do you want me to be perfect? Two longitudinal studies on socially prescribed perfectionism, stress and burnout in the workplace. *Work & Stress* 2012, *26*, 347-364.

[49] Zhou, Z., Zhu, G., Hariri, A. R., Enoch, M. A., *et al.*, Genetic variation in human NPY expression affects stress response and emotion. *Nature* 2008.

[50] Li-Tempel, T., Larra, M. F., Sandt, E., The cardiovascular and hypothalamus-pituitary-adrenal axis response to stress is controlled by glucocorticoid receptor sequence variants and promoter …. *Clinical Epigenetics* 2016, *8*, 12.

[51] Bernard, H. R., Killworth, P., Kronenfeld, D., The problem of informant accuracy: The validity of retrospective data. *Annual review of anthropology* 1984, *13*, 495-517.

[52] Yoshiuchi, K., Yamamoto, Y., Application of ecological momentary assessment in stress-related diseases. *BioPsychoSocial Medicine* 2008, *2*, 13.

[53] Bibb, J., Baker, F. A., McFerran, K. S., A critical interpretive synthesis of the most commonly used self-report measures in Australian mental health research. *Australasian Psychiatry* 2016.

[54] Wippert, P. M., Honold, J., Wang, V., Assessment of chronic stress: comparison of hair biomarkers and allostatic load indices. *Psychology Research* 2014, *4*, 517-524.

[55] Wynne, C., What are animals? Why anthropomorphism is still not a scientific approach to behavior. *Comparative Cognition & Behavior Reviews* 2007, *2*, 125-135.

[56] Hogg, S., A review of the validity and variability of the elevated plus-maze as an animal model of anxiety. *Pharmacology Biochemistry and Behavior* 1996, *54*, 21-30.

[57] Willner, P., Validity, reliability and utility of the chronic mild stress model of depression: a 10-year review and evaluation. *Psychopharmacology* 1997, *134*, 319-329.

[58] File, S. E., Hyde, J., Can social interaction be used to measure anxiety? *British journal of pharmacology* 1978, *62*, 19–12.

[59] Benatar, M., Lost in translation: treatment trials in the SOD1 mouse and in human ALS. *Neurobiology of Disease* 2007, *26*, 1-13.

[60] Mak, I. W., Evaniew, N., Ghert, M., Lost in translation: animal models and clinical trials in cancer treatment. *American journal of translational research* 2014, *6*, 114-118.

[61] Psychogios, N., Hau, D. D., Peng, J., Guo, A. C., Mandal, R., The human serum metabolome. *PLoS ONE* 2011, *6*, e16957.

[62] Wishart, D. S., Lewis, M. J., Morrissey, J. A., Flegel, M. D., The human cerebrospinal fluid metabolome. *Journal of Chromatography B* 2008, *871*, 164-173.

[63] Bouatra, S., Aziat, F., Mandal, R., Guo, A. C., Wilson, M. R., The human urine metabolome. *PLoS ONE* 2013, *8*, e73076.

[64] Goldsmith, P., Fenton, H., Morris-Stiff, G., Ahmad, N., Metabonomics: a useful tool for the future surgeon. *Journal of Surgical Research* 2010, *160*, 122-132.

[65] Manolio, T. A., Collins, F. S., Cox, N. J., Goldstein, D. B., Finding the missing heritability of complex diseases. *Nature* 2009.

[66] Hirschhorn, J. N., Daly, M. J., Genome-wide association studies for common diseases and complex traits. *Nature Reviews Genetics* 2005, *6*, 95-108.

[67] Bory, C., Boulieu, R., Chantin, C., Mathieu, M., Diagnosis of alcaptonuria: Rapid analysis of homogentisic acid by HPLC. *Clinica Chimica Acta* 1990, *189*, 7-11.

[68] Wang, Y., Xiao, Z., Liu, X., Berk, M., Venlafaxine modulates depression-induced behaviour and the expression of Bax mRNA and Bcl-xl mRNA in both hippocampus and myocardium. *Human psychopharmacology* 2011, *26*, 95-101.

[69] Brown, E. M., Wlodarska, M., Willing, B. P., Vonaesch, P., *et al.*, Diet and specific microbial exposure trigger features of environmental enteropathy in a novel murine model. *Nature Communications* 2015, *6*, 1-16.

[70] Eckle, T., Hartmann, K., Bonney, S., Reithel, S., Adora2b-elicited Per2 stabilization promotes a HIF-dependent metabolic switch crucial for myocardial adaptation to ischemia. *Nature Medicine* 2012, *18*, 774-782.

[71] Bahado-Singh, R. O., Akolekar, R., Mandal, R., Dong, E., *et al.*, Metabolomics and first-trimester prediction of early-onset preeclampsia. *Journal of Maternal-Fetal and Neonatal Medicine* 2012, *25*, 1840-1847.

[72] Ravanbakhsh, S., Liu, P., Bjordahl, T. C., Mandal, R., Accurate, fully-automated NMR spectral profiling for metabolomics. *PLoS ONE* 2015.

[73] Ghini, V., Saccenti, E., Tenori, L., Assfalg, M., Allostasis and resilience of the human individual metabolic phenotype. *Journal of proteome research* 2015, *14*, 2951-2962.

[74] Han, J., Datla, R., Chan, S., Borchers, C. H., Mass spectrometry-based technologies for high-throughput metabolomics. *Bioanalysis* 2009, *1*, 1665-1684.

[75] Zhou, B., Xiao, J. F., Tuli, L., Ressom, H. W., LC-MS-based metabolomics. *Molecular BioSystems* 2012, *8*, 470-481.

[76] Michalski, A., Damoc, E., Lange, O., Denisov, E., Ultra high resolution linear ion trap Orbitrap mass spectrometer (Orbitrap Elite) facilitates top down LC MS/MS and versatile peptide fragmentation modes. *Molecular & Cellular Proteomics* 2012, *11*, O111.013698.

[77] Xiao, J. F., Zhou, B., Ressom, H. W., Metabolite identification and quantitation in LC-MS/MS-based metabolomics. *Trends in Analytical Chemistry* 2012, *32*, 1-14.

[78] Witbracht, M. G., Van Loan, M., Adams, S. H., Keim, N. L., Laugero, K. D., Dairy Food Consumption and Meal-Induced Cortisol Response Interacted to Influence Weight

Loss in Overweight Women Undergoing a 12-Week, Meal-Controlled, Weight Loss Intervention. *Journal of Nutrition* 2013, *143*, 46-52.

[79] Bartels, M., de Geus, E., Kirschbaum, C., Sluyter, F., Heritability of daytime cortisol levels in children. *Behavior genetics* 2003.

[80] Weckesser, L. J., Plessow, F., Pilhatsch, M., Do venepuncture procedures induce cortisol responses? A review, study, and synthesis for stress research. *Psychoneuroendocrinology* 2014, *46*, 88-99.

[81] Shaw, J., Brown, R., Heinrich, P., Dunn, S., Doctors' experience of stress during simulated bad news consultations. *Patient education and counseling* 2013, *93*, 203-208.

[82] Braig, S., Grabher, F., Ntomchukwu, C., The Association of Hair Cortisol with Self‐Reported Chronic Psychosocial Stress and Symptoms of Anxiety and Depression in Women Shortly after Delivery. *Paediatric and Perinatal Epidemiology* 2015, *[Epub ahead of print]*.

[83] Inder, W. J., Dimeski, G., Russell, A., Measurement of salivary cortisol in 2012–laboratory techniques and clinical indications. *Clinical endocrinology* 2012, *77*, 645-651.

[84] Grass, J., Kirschbaum, C., Miller, R., Gao, W., Sweat-inducing physiological challenges do not result in acute changes in hair cortisol concentrations. *Psychoneuroendocrinology* 2015, *53*, 108-116.

[85] Dettenborn, L., Tietze, A., Kirschbaum, C., Stalder, T., The assessment of cortisol in human hair: associations with sociodemographic variables and potential confounders. *Stress: The International Journal on the Biology of Stress* 2012, *15*, 578-588.

[86] Russell, E., Kirschbaum, C., Toward standardization of hair cortisol measurement: results of the first international interlaboratory round robin. *Therapeutic drug monitoring* 2015, *37*, 71-75.

[87] Gao, W., Stalder, T., Foley, P., Rauh, M., Deng, H., Quantitative analysis of steroid hormones in human hair using a column-switching LC–APCI–MS/MS assay. *Journal of Chromatography B* 2013, *298*, 1-8.

[88] Stalder, T., Steudte, S., Alexander, N., Miller, R., Gao, W., Cortisol in hair, body mass index and stress-related measures. *Biological Psychology* 2012, *90*, 218-223.

[89] Stalder, T., Steudte, S., Miller, R., Skoluda, N., Intraindividual stability of hair cortisol concentrations. *Psychoneuroendocrinology* 2012, *37*, 602-610.

[90] Allen, A. P., Kennedy, P. J., Cryan, J. F., Dinan, T. G., Biological and psychological markers of stress in humans: Focus on the Trier Social Stress Test. *Neuroscience & Biobehavioral Reviews* 2014, *38*, 94-124.

[91] Anacker, C., O'Donnell, K. J., Meaney, M. J., Early life adversity and the epigenetic programming of hypothalamic-pituitary-adrenal function. *Dialogues Clin Neurosci* 2014, *16*, 321-333.

[92] Anacker, C., Pariante, C. M., Can adult neurogenesis buffer stress responses and depressive behaviour? *Molecular psychiatry* 2012, *17*, 9-10.

[93] Everly, J., G S, Lating, J. M., *A clinical guide to the treatment of the human stress response*, Springer-Verlag, New York 2012.

[94] Campbell, J., Ehlert, U., Acute psychosocial stress: does the emotional stress response correspond with physiological responses? *Psychoneuroendocrinology* 2012, *37*, 1111-1134.

[95] Monteiro, S., Roque, S., de Sá-Calçada, D., An efficient chronic unpredictable stress protocol to induce stress-related responses in C57BL/6 mice. *Frontiers in psychiatry* 2015.

[96] Bertola, A., Mathews, S., Ki, S. H., Wang, H., Gao, B., Mouse model of chronic and binge ethanol feeding (the NIAAA model). *Nature Protocols* 2013, *8*, 627-637.

[97] Guan, S.-z., Liu, J.-w., Fang, E. F., Ng, T. B., *et al.*, Chronic unpredictable mild stress impairs erythrocyte immune function and changes T-lymphocyte subsets in a rat model of stress-induced depression. *Environmental Toxicology and Pharmacology* 2014, *37*, 414-422.

[98] Mateus-Pinheiro, A., Patrício, P., Alves, N. D., The Sweet Drive Test: refining phenotypic characterization of anhedonic behavior in rodents. *Frontiers in psychiatry* 2014, *8*.

[99] Liu, W., Zhou, C., Corticosterone reduces brain mitochondrial function and expression of mitofusin, BDNF in depression-like rodents regardless of exercise preconditioning. *Psychoneuroendocrinology* 2012, *37*, 1057-1070.

[100] Ortolani, D., Garcia, M. C., Melo-Thomas, L., Spadari-Bratfisch, R. C., Stress-induced endocrine response and anxiety: the effects of comfort food in rats. *Stress: The International Journal on the Biology of Stress* 2014, *17*, 211-218.

[101] Zhu, X., Hao, X., Luo, J., Min, S., *et al.*, Propofol inhibits inflammatory cytokine-mediated glutamate uptake dysfunction to alleviate learning/memory impairment in depressed rats undergoing …. *Brain research* 2015, *1595*, 101-109.

[102] Biala, G., Pekala, K., Boguszewska-Czubara, A., Behavioral and Biochemical Interaction Between Nicotine and Chronic Unpredictable Mild Stress in Mice. *Molecular neurobiology* 2016, 1-18.

[103] Sharma, H. R., Thakur, M. K., Correlation of ERα/ERβ expression with dendritic and behavioural changes in CUMS mice. *Physiology & Behavior* 2015, *145*, 71-83.

[104] Yang, C. R., Bai, Y. Y., Ruan, C. S., Zhou, H. F., *et al.*, Enhanced aggressive behaviour in a mouse model of depression. *Neurotoxicity Research* 2015, *27*, 129-142.

[105] Li, J., Wijffels, G., Yu, Y., Nielsen, L. K., *et al.*, Altered Fatty Acid Metabolism in Long Duration Road Transport: An NMR-based Metabonomics Study in Sheep. *Journal of Proteome Research* 2011, *10*, 1073-1087.

[106] Wohleb, E. S., Hanke, M. L., Corona, A. W., β-Adrenergic receptor antagonism prevents anxiety-like behavior and microglial reactivity induced by repeated social defeat. *The Journal of Neuroscience* 2011, *31*, 6277-6288.

[107] Wang, X., Zhao, T., Qiu, Y., Su, M., *et al.*, Metabonomics Approach to Understanding Acute and Chronic Stress in Rat Models †. *Journal of Proteome Research* 2009, *8*, 2511-2518.

[108] Grippo, A. J., Beltz, T. G., Johnson, A. K., Behavioral and cardiovascular changes in the chronic mild stress model of depression. *Physiology & Behavior* 2003, *78*, 703-710.

[109] Hansen, Å. M., Larsen, A. D., Rugulies, R., Garde, A. H., Knudsen, L. E., A Review of the Effect of the Psychosocial Working Environment on Physiological Changes in Blood and Urine. *Basic & Clinical Pharmacology & Toxicology* 2009, *105*, 73-83.

[110] Lovell, B., Moss, M., Wetherell, M., The psychosocial, endocrine and immune consequences of caring for a child with autism or ADHD. *Psychoneuroendocrinology* 2012, *37*, 534-542.

[111] Irie, M., Asami, S., Nagata, S., Ikeda, M., *et al.*, Psychosocial factors as a potential trigger of oxidative DNA damage in human leukocytes. *Japanese journal of cancer research : Gann* 2001, *92*, 367-376.

[112] Martin, F.-P. J., Rezzi, S., Peré-Trepat, E., Kamlage, B., *et al.*, Metabolic Effects of Dark Chocolate Consumption on Energy, Gut Microbiota, and Stress-Related Metabolism in Free-Living Subjects. *Journal of Proteome Research* 2009, *8*, 5568-5579.

[113] Liu, X. J., Zhou, Y. Z., Li, Z. F., Cui, J., Li, Z. Y., Anti-depressant effects of Xiaoyaosan on rat model of chronic unpredictable mild stress: a plasma metabonomics study based on NMR spectroscopy. *Journal of Pharmacy and Pharmacology* 2012, *64*, 578-588.

[114] Zhang, W., Liu, S., Cai, H., Chronic unpredictable mild stress affects myocardial metabolic profiling of SD rats. *Journal of Pharmaceutical and Biomedical Analysis* 2012, *70*, 534-538.

[115] Zhou, Y.-Z., Zheng, X.-Y., Liu, X.-J., Li, Z.-Y., *et al.*, Metabonomic Analysis of Urine from Chronic Unpredictable Mild Stress Rats Using Gas Chromatography–Mass Spectrometry. *Chromatographia* 2012, *75*, 157-164.

[116] Denenberg, V. H., Critical periods, stimulus input, and emotional reactivity: A theory of infantile stimulation. *Psychological Review* 1964, *71*, 335-351.

[117] Francis, D., Nongenomic Transmission Across Generations of Maternal Behavior and Stress Responses in the Rat. *Science* 1999, *286*, 1155-1158.

[118] Weaver, I. C. G., Cervoni, N., Champagne, F. A., D'Alessio, A. C., *et al.*, Epigenetic programming by maternal behavior. *Nature Neuroscience* 2004, *7*, 847-854.

[119] McGowan, P. O., Sasaki, A., D'Alessio, A. C., Dymov, S., *et al.*, Epigenetic regulation of the glucocorticoid receptor in human brain associates with childhood abuse. *Nature Neuroscience* 2009, *12*, 342-348.

[120] Oberlander, T. F., Weinberg, J., Papsdorf, M., Grunau, R., *et al.*, Prenatal exposure to maternal depression, neonatal methylation of human glucocorticoid receptor gene (NR3C1) and infant cortisol stress responses. *Epigenetics* 2014, *3*, 97-106.

[121] Tyrka, A. R., Price, L. H., Marsit, C., Walters, O. C., Carpenter, L. L., Childhood Adversity and Epigenetic Modulation of the Leukocyte Glucocorticoid Receptor: Preliminary Findings in Healthy Adults. *PLoS ONE* 2012, *7*, e30148.

[122] Liu, D., Maternal Care, Hippocampal Glucocorticoid Receptors, and Hypothalamic-Pituitary-Adrenal Responses to Stress. *Science* 1997, *277*, 1659-1662.

[123] Razin, A., CpG methylation, chromatin structure and gene silencing---a three-way connection. *The EMBO Journal* 1998, *17*, 4905-4908.

[124] Klengel, T., Pape, J., Binder, E. B., Mehta, D., The role of DNA methylation in stress-related psychiatric disorders. *Neuropharmacology* 2014, *80*, 115-132.

[125] Meaney, M. J., Szyf, M., Seckl, J. R., Epigenetic mechanisms of perinatal programming of hypothalamic-pituitary-adrenal function and health. *Trends in molecular medicine* 2007, *13*, 269-277.

[126] Labonté, B., Yerko, V., Gross, J., Mechawar, N., *et al.*, Differential Glucocorticoid Receptor Exon 1B, 1C, and 1H Expression and Methylation in Suicide Completers with a History of Childhood Abuse. *Biological psychiatry* 2012, *72*, 41-48.

[127] Radtke, K. M., Schauer, M., Gunter, H. M., Ruf-Leuschner, M., *et al.*, Epigenetic modifications of the glucocorticoid receptor gene are associated with the vulnerability to psychopathology in childhood maltreatment. *Translational Psychiatry* 2015, *5*, e571-577.

[128] Li, Z., Vance, D. E., Thematic Review Series: Glycerolipids. Phosphatidylcholine and choline homeostasis. *The Journal of Lipid Research* 2008, *49*, 1187-1194.

[129] Cole, L. K., Vance, J. E., Vance, D. E., Phosphatidylcholine biosynthesis and lipoprotein metabolism. *Biochimica et Biophysica Acta (BBA) - Molecular and Cell Biology of Lipids* 2012, *1821*, 754-761.

[130] Exton, J. H., Signaling through phosphatidylcholine breakdown. *Journal of Biological Chemistry* 1990, *265*, 1-4.

[131] Parks, J. S., Gebre, A. K., Long-chain polyunsaturated fatty acids in the sn-2 position of phosphatidylcholine decrease the stability of recombinant high density lipoprotein apolipoprotein A-I and the activation energy of the lecithin:cholesterol acyltransferase reaction. *Journal of lipid research* 1997, *38*, 266-275.

[132] Mozzi, R., Porcellati, G., Conversion of phosphatidylethanolamine to phosphatidylcholine in rat brain by the methylation pathway. *FEBS Letters* 1979, *100*, 363-366.

[133] Kanehisa, M., Sato, Y., Kawashima, M., Furumichi, M., Tanabe, M., KEGG as a reference resource for gene and protein annotation. *Nucleic acids research* 2016, *44*, D457-D462.

[134] Voelker, D. R., Kennedy, E. P., Cellular and enzymic synthesis of sphingomyelin. *Biochemistry* 1982, *21*, 2753-2759.

[135] Moser, D., Molitor, A., Kumsta, R., Tatschner, T., *et al.*, The glucocorticoid receptor gene exon 1-F promoter is not methylated at the NGFI-A binding site in human hippocampus. *World Journal of Biological Psychiatry* 2007, *8*, 262-268.

[136] Broadhurst, D. I., Kell, D. B., Statistical strategies for avoiding false discoveries in metabolomics and related experiments. *Metabolomics* 2006, *2*, 171-196.

[137] Joosten, E., Homocysteine, vascular dementia and Alzheimer's disease. *Clinical chemistry and laboratory medicine* 2001, *39*.

[138] Cavalca, V., Cighetti, G., Bamonti, F., Loaldi, A., Oxidative stress and homocysteine in coronary artery disease. *Clinical Chemistry* 2001, *47*, 887-892.

[139] Templar, J., Kon, S. P., Milligan, T. P., Newman, D. J., Raftery, M. J., Increased plasma malondialdehyde levels in glomerular disease as determined by a fully validated HPLC method. *Nephrology, dialysis, transplantation : official publication of the European Dialysis and Transplant Association - European Renal Association* 1999, *14*, 946-951.

[140] Pasupathi, P., Chandrasekar, V., Kumar, U. S., Evaluation of oxidative stress, antioxidant and thyroid hormone status in patients with diabetes mellitus. *Journal of Medicine* 2009, *10*.

[141] Halliwell, B., Free radicals and vascular disease: how much do we know? *BMJ* 1993, *307*.

[142] Kesavulu, M. M., Rao, B. K., Giri, R., Vijaya, J., Lipid peroxidation and antioxidant enzyme status in Type 2 diabetics with coronary heart disease. *Diabetes research and ...* 2001, *53*, 33-39.

[143] Tsaluchidu, S., Cocchi, M., Tonello, L., Puri, B. K., Fatty acids and oxidative stress in psychiatric disorders. *BMC Psychiatry* 2008, *8*, S5.

[144] Dalle-Donne, I., Biomarkers of Oxidative Damage in Human Disease. *Clinical Chemistry* 2006, *52*, 601-623.

[145] Bhattacharyya, A., Chattopadhyay, R., Mitra, S., Crowe, S. E., Oxidative Stress: An Essential Factor in the Pathogenesis of Gastrointestinal Mucosal Diseases. *Physiological Reviews* 2014, *94*, 329-354.

[146] Aliev, G., Priyadarshini, M., P Reddy, V., Grieg, N. H., *et al.*, Oxidative Stress Mediated Mitochondrial and Vascular Lesions as Markers in the Pathogenesis of Alzheimer Disease. *Current medicinal chemistry* 2014, *21*, 2208-2217.

[147] Niranjan, R., The Role of Inflammatory and Oxidative Stress Mechanisms in the Pathogenesis of Parkinson's Disease: Focus on Astrocytes. *Molecular neurobiology* 2014, *49*, 28-38.

[148] Matsumoto, K., Yobimoto, K., Huong, N., Abdel-Fattah, M., Psychological stress-induced enhancement of brain lipid peroxidation via nitric oxide systems and its modulation by anxiolytic and anxiogenic drugs in mice. *Brain research* 1999, *839*, 74-84.

[149] Srikumar, R., Parthasarathy, N. J., Manikandan, S., Narayanan, G. S., Sheeladevi, R., Effect of Triphala on oxidative stress and on cell-mediated immune response against noise stress in rats. *Molecular and Cellular Biochemistry* 2006, *283*, 67-74.

[150] Fontella, F. U., Siqueira, I. R., Vasconcellos, A. P. S., Tabajara, A. S., *et al.*, Repeated Restraint Stress Induces Oxidative Damage in Rat Hippocampus. *Neurochemical Research* 2005, *30*, 105-111.

[151] Manikandan, S., Padma, M. K., Srikumar, R., Jeya Parthasarathy, N., *et al.*, Effects of chronic noise stress on spatial memory of rats in relation to neuronal dendritic alteration and free radical-imbalance in hippocampus and medial prefrontal cortex. *Neuroscience Letters* 2006, *399*, 17-22.

[152] Adachi, S., Kawamura, K., Takemoto, K., Oxidative Damage of Nuclear DNA in Liver of Rats Exposed to Psychological Stress. *Cancer Research* 1993, *53*.

[153] Ng, F., Berk, M., Dean, O., Bush, A. I., Oxidative stress in psychiatric disorders: evidence base and therapeutic implications. *The International Journal of Neuropsychopharmacology* 2008, *11*, 851-876.

[154] Sivoňová, M., Žitňanová, I., Hlinčíková, L., Škodáček, I., *et al.*, Oxidative Stress in University Students during Examinations. *Stress: The International Journal on the Biology of Stress* 2004, *7*, 183-188.

[155] Aschbacher, K., O'Donovan, A., Wolkowitz, O. M., Dhabhar, F. S., *et al.*, Good stress, bad stress and oxidative stress: Insights from anticipatory cortisol reactivity. *Psychoneuroendocrinology* 2013, *38*, 1698-1708.

[156] Zafir, A., Banu, N., Induction of oxidative stress by restraint stress and corticosterone treatments in rats. *Indian journal of biochemistry & biophysics* 2009, *46*, 53-58.

[157] Berk, M., Kapczinski, F., Andreazza, A. C., Dean, O. M., Pathways underlying neuroprogression in bipolar disorder: Focus on inflammation, oxidative stress and neurotrophic factors. *Neuroscience and Biobehavioral Reviews* 2011, *35*, 804-817.

[158] Wiswedel, I., Gardemann, A., Storch, A., Peter, D., Schild, L., Degradation of phospholipids by oxidative stress—Exceptional significance of cardiolipin. *Free Radical Research* 2010, *44*, 135-145.

[159] Halliwell, B., Whiteman, M., Measuring reactive species and oxidative damage in vivoand in cell culture: how should you do it and what do the results mean? *British journal of pharmacology* 2004, *142*, 231-255.

[160] Baron, C. P., Bro, R., Skibsted, L. H., Andersen, H. J., Direct measurement of lipid oxidation in oil in water emulsions using multiwavelength derivate UV spectroscopy. *Journal of Agricultural and Food Chemistry* 1997, *45*, 1741– 1745.

[161] Wheatley, R. A., Some recent trends in the analytical chemistry of lipid peroxidation. *Trends in Analytical Chemistry* 2000, *10*, 617.

[162] Moselhy, H. F., Reid, R. G., Yousef, S., Boyle, S. P., A specific, accurate, and sensitive measure of total plasma malondialdehyde by HPLC. *The Journal of Lipid Research* 2013, *54*, 852-858.

[163] Pilz, J., Meineke, I., Gleiter, C. H., Measurement of free and bound malondialdehyde in plasma by high-performance liquid chromatography as the 2,4-dinitrophenylhydrazine derivative. *Journal of chromatography. B, Biomedical sciences and applications* 2000, *742*, 315-325.

[164] Mateos, R., Lecumberri, E., Ramos, S., Goya, L., Bravo, L., Determination of malondialdehyde (MDA) by high-performance liquid chromatography in serum and liver as a biomarker for oxidative stressApplication to a rat model for hypercholesterolemia and evaluation of the effect of diets rich in phenolic antioxidants from fruits. *Journal of Chromatography B* 2005, *827*, 76-82.

[165] Sim, A. S., Salonikas, C., Naidoo, D., Wilcken, D. E. L., Improved method for plasma malondialdehyde measurement by high-performance liquid chromatography using methyl malondialdehyde as an internal standard. *Journal of chromatography. B, Analytical technologies in the biomedical and life sciences* 2003, *785*, 337-344.

[166] Grotto, D., Santa Maria, L. D., Boeira, S., Valentini, J., *et al.*, Rapid quantification of malondialdehyde in plasma by high performance liquid chromatography–visible detection. *Journal of Pharmaceutical and Biomedical Analysis* 2007, *43*, 619-624.

[167] Yeo, H. C., Helbock, H. J., Chyu, D. W., Ames, B. N., Assay of malondialdehyde in biological fluids by gas chromatography-mass spectrometry. *Analytical biochemistry* 1994, *220*, 391-396.

[168] Kawai, S., Fuchiwaki, T., Higashi, T., Tomita, M., High-performance liquid chromatographic determination of malonaldehyde using p-nitrophenylhydrazine as a derivatizing reagent. *Journal of Chromatography A* 1990, *514*, 29-35.

[169] Yao, X., Afonso, C., Fenselau, C., Dissection of proteolytic 18O labeling: endoprotease-catalyzed 16O-to-18O exchange of truncated peptide substrates. *Journal of Proteome Research* 2003, *2*, 147-152.

[170] Kerr, D. C. R., Zava, D. T., Piper, W. T., Saturn, S. R., *et al.*, Associations between vitamin D levels and depressive symptoms in healthy young adult women. *Psychiatry research* 2015, *227*, 46-51.

[171] Frandsen, T., Pareek, M., Hansen, J., Nielsen, C., Vitamin D supplementation for treatment of seasonal affective symptoms in healthcare professionals: a double-blind randomised placebo-controlled trial. *BMC Research Notes* 2014, *7*, 528.

[172] Rondanelli, M., Trotti, R., Opizzi, A., Solerte, S. B., Relationship among nutritional status, pro/antioxidant balance and cognitive performance in a group of free-living healthy elderly. *Minerva Medica* 2007, *98*, 639-645.

[173] Del Rio, D., Stewart, A. J., Pellegrini, N., A review of recent studies on malondialdehyde as toxic molecule and biological marker of oxidative stress. *Nutrition, Metabolism and Cardiovascular Diseases* 2005, *15*, 316-328.

[174] Shin, H.-S., Jung, D.-G., Sensitive Analysis of Malondialdehyde in Human Urine by Derivatization with Pentafluorophenylhydrazine then Headspace GC–MS. *Chromatographia* 2009, *70*, 899-903.

[175] Cighetti, G., Debiasi, S., Paroni, R., Allevi, P., Free and total malondialdehyde assessment in biological matrices by gas chromatography-mass spectrometry: what is needed for an accurate detection. *Analytical Biochemistry* 1999, *266*, 222-229.

[176] Lee, S. M., Cho, Y. H., Lee, S. Y., Jeong, D. W., *et al.*, Urinary Malondialdehyde Is Associated with Visceral Abdominal Obesity in Middle-Aged Men. *Mediators of Inflammation* 2015, *2015*, 524291.

[177] Yerlikaya, F. H., Toker, A., Çiçekler, H., Arıbaş, A., The association of total sialic acid and malondialdehyde levels with metabolic and anthropometric variables in obesity. *Biotechnic and Histochemistry* 2015, *90*, 31-37.

[178] Bengesser, S. A., Lackner, N., Birner, A., Fellendorf, F. T., *et al.*, Peripheral markers of oxidative stress and antioxidative defense in euthymia of bipolar disorder-Gender and obesity effects. *Journal of Affective Disorders* 2014, *172C*, 367-374.

[179] Hong, Y. L., Yeh, S. L., Chang, C. Y., Hu, M. L., Total plasma malondialdehyde levels in 16 Taiwanese college students determined by various thiobarbituric acid tests and an improved high-performance liquid chromatography-based method. *Clinical Biochemistry* 2000, *33*, 619-625.

[180] Rygula, R., Abumaria, N., Flügge, G., Fuchs, E., *et al.*, Anhedonia and motivational deficits in rats: Impact of chronic social stress. *Behavioural brain research* 2005, *162*, 127-134.

[181] Raab, A., Dantzer, R., Michaud, B., Mormede, P., Behavioural, physiological and immunological consequences of social status and aggression in chronically coexisting resident-intruder dyads of male rats. *Physiology & Behavior* 1986, *36*, 223-228.

[182] Kudryavtseva, N. N., Bakshtanovskaya, I. V., Koryakina, L. A., Social model of depression in mice of C57BL/6J strain. *Pharmacology Biochemistry and Behavior* 1991, *38*, 315-320.

[183] Albonetti, M. E., Farabollini, F., Social stress by repeated defeat: effects on social behaviour and emotionality. *Behavioural brain research* 1994, *62*, 187-193.

[184] Van de Poll, N. E., De Jonge, F., Van Oyen, H. G., Aggressive behaviour in rats: Effects of winning or losing on subsequent aggressive interactions. *Behavioural Processes* 1982, *7*, 143-155.

[185] Rodgers, R. J., Cole, J. C., Anxiety enhancement in the murine elevated plus maze by immediate prior exposure to social stressors. *Physiology & Behavior* 1993, *53*, 383-388.

[186] Keeney, A., Jessop, D. S., Harbuz, M. S., Marsden, C. A., *et al.*, Differential Effects of Acute and Chronic Social Defeat Stress on Hypothalamic-Pituitary-Adrenal Axis Function and Hippocampal Serotonin Release in Mice. *Journal of Neuroendocrinology* 2006, *18*, 330-338.

[187] Chao, H. M., Blanchard, D. C., Blanchard, R. J., The Effect of Social Stress on Hippocampal Gene Expression. *Molecular and Cellular Neuroscience* 1993, *4*, 543-548.

[188] Tornatzky, W., Miczek, K. A., Long-term impairment of autonomic circadian rhythms after brief intermittent social stress. *Physiology & Behavior* 1993, *53*, 983-993.

[189] Beden, S. N., Brain, P. F., Studies on the effect of social stress on measures of disease resistance in laboratory mice. *Aggressive Behavior* 1982, *8*, 126-129.

[190] Boissy, A., Fear and Fearfulness in Animals on JSTOR. *Quarterly Review of Biology* 1995, *70*, 165-191.

[191] Russo, S. J., Murrough, J. W., Han, M.-H., Charney, D. S., Nestler, E. J., Neurobiology of resilience. *Nature Publishing Group* 2012, *15*, 1475-1484.

[192] Golden, S. A., Covington, H. E., Berton, O., Russo, S. J., A standardized protocol for repeated social defeat stress in mice. *Nature Protocols* 2011, *6*, 1183-1191.

[193] Anacker, C., Scholz, J., O'Donnell, K. J., Neuroanatomic Differences Associated with Stress Susceptibility and Resilience. *Biological psychiatry* 2015.

[194] Chambers, M. C., Maclean, B., Burke, R., Amodei, D., *et al.*, A cross-platform toolkit for mass spectrometry and proteomics. *Nature Biotechnology* 2012, *30*, 918-920.

[195] Smith, C. A., Maille, G. O., Want, E. J., Qin, C., *et al.*, METLIN: A Metabolite Mass Spectral Database. *Therapeutic drug monitoring* 2005, *27*, 747.

[196] Giera, M., Lingeman, H., Niessen, W. M. A., Recent Advancements in the LC- and GC-Based Analysis of Malondialdehyde (MDA): A Brief Overview. *Chromatographia* 2012, *75*, 433-440.

[197] Cutler, R. G., Kelly, J., Storie, K., Pedersen, W. A., *et al.*, Involvement of oxidative stress-induced abnormalities in ceramide and cholesterol metabolism in brain aging and Alzheimer's disease. *Proceedings of the National Academy of Sciences* 2004, *101*, 2070-2075.

[198] Eriksson, T., Carlsson, A., Adrenergic influence on rat plasma concentrations of tyrosine and tryptophan. *Life sciences* 1982, *30*, 1465-1472.

[199] Cowen, P. J., Parry-Billings, M., Newsholme, E. A., Decreased plasma tryptophan levels in major depression. *Journal of Affective Disorders* 1989, *16*, 27-31.

[200] Huang, A., Fuchs, D., Widner, B., Glover, C., *et al.*, Serum tryptophan decrease correlates with immune activation and impaired quality of life in colorectal cancer. *British Journal of Cancer* 2002, *86*, 1691-1696.

[201] Foster, M. T., Social defeat increases food intake, body mass, and adiposity in Syrian hamsters. *AJP: Regulatory, Integrative and Comparative Physiology* 2005, *290*, R1284-R1293.

[202] Reber, S. O., Obermeier, F., Straub, H. R., Falk, W., Neumann, I. D., Chronic Intermittent Psychosocial Stress (Social Defeat/Overcrowding) in Mice Increases the Severity of an Acute DSS-Induced Colitis and Impairs Regeneration. *Endocrinology* 2006, *147*, 4968-4976.

[203] Denery, J. R., Nunes, A. A. K., Dickerson, T. J., Characterization of Differences between Blood Sample Matrices in Untargeted Metabolomics. *Analytical Chemistry* 2010, *83*, 1040-1047.

[204] Monteiro, M. S., Carvalho, M., Bastos, M. L., Guedes de Pinho, P., Metabolomics Analysis for Biomarker Discovery: Advances and Challenges. *Current medicinal chemistry* 2013, *20*, 257-271.

[205] De Iorio, M., Daviglus, M. L., Holmes, E., Stamler, J., Opening up the 'Black Box': Metabolic phenotyping and metabolome-wide association studies in epidemiology. *Journal of clinical epidemiology* 2010, *63*, 970-979.

[206] Oliveira, T. G., Chan, R. B., Bravo, F. V., Miranda, A., *et al.*, The impact of chronic stress on the rat brain lipidome. *Molecular psychiatry* 2015, *21*, 80-88.

[207] Tworoger, S. S., Poole, E. M., Armaiz Pena, G., Kubzansky, L., *et al.*, Abstract LB-180: Metabolomic changes in response to chronic stress in healthy mice. *Cancer Research* 2015, *75*, LB-180-LB-180.

[208] Faria, R., Santana, M. M., Aveleira, C. A., Simões, C., *et al.*, Alterations in phospholipidomic profile in the brain of mouse model of depression induced by chronic unpredictable stress. *Neuroscience* 2014, *273*, 1-11.

[209] Liu, X., Zheng, P., Zhao, X., Zhang, Y., *et al.*, Discovery and Validation of Plasma Biomarkers for Major Depressive Disorder Classification Based on Liquid Chromatography–Mass Spectrometry. *Journal of Proteome Research* 2015, *14*, 2322-2330.

[210] Ni, Y., Su, M., Lin, J., Wang, X., *et al.*, Metabolic profiling reveals disorder of amino acid metabolism in four brain regions from a rat model of chronic unpredictable mild stress. *FEBS Letters* 2008, *582*, 2627-2636.

[211] Yin, D., Tuthill, D., Mufson, R. A., Shi, Y., Chronic restraint stress promotes lymphocyte apoptosis by modulating CD95 expression.. *Journal of Experimental Medicine* 2000, *191*, 1423-1428.

Appendix I

XCMS commands for analyzing QTOF data

The following is an example of the commands used to analyze untargeted Waters QTOF-MS data by running the XCMS package in a local copy of R software. Negative and positive ion mode data must be analyzed separately. Items in square brackets would be replaced with the specified information. The settings shown here are those used for analysis of the untargeted data collected by QTOF-MS in Chapter 1 of this thesis. They may not be suitable for data collected using other MS configurations.

---

1. Convert raw spectra to CDF using Databridge.

2. Place spectra into folders corresponding to the groups to be compared (e.g., High, Low). Place the two group folders into a single overarching folder.

3. Open R and Load required packages (Biobase, Multtest)

4. Select data to be analyzed

```
File> Change Dir> Data> [Folder name] > library(xcms)
```

4. Peak detection

```
[Folder name]<- xcmsSet(method="matchedFilter", ppm=10,
snthresh=5, mzCenterFun="mean", integrate=2, mzdiff=0.02,
fitgauss=TRUE)
```

4. Retention time correction

```
[Folder name]<- retcor([Folder name], method="obiwarp",
profStep=0.5)
```

5. Peak grouping

```
[Folder name 2] <-group([Folder name], bw=5, mzwid=0.025,
minfrac=0.5)
```

6. Retention time correction (second round)

```
[Folder name 2] <-retcor([Folder name 2], family="s",
plottype="m")
```

7. Peak grouping (second round)

```
[Folder name 2] <- group([Folder name 2], bw=5)
```

8. Peak integration

```
[Folder name 3] <-fillPeaks([Folder name 2])
```

9. Group comparison

```
reporttab <-diffreport([Folder name 3], "[subfolder containing
group 1]", "[subfolder containing group 2]", "example",500)
```

XCMSOnline settings for analyzing Orbitrap data

Please see below the specific methods and settings used to perform data processing and multigroup statistical analysis of Orbitrap full-scan MS data using XCMS online. Negative and positive ion mode data were analyzed separately.

Negative ion mode settings:

```
------------------------------------------------------------------------
XCMSOnline  version  2.0.1
XCMS        version  1.41.1
CAMERA      version  1.22.0
------------------------------------------------------------------------
General parameters
       polarity    negative
       retention time format   minutes
      Parameter ID:  136      JOBID:  10922782. Feature detection
       method : centWave
       ppm   3
       snthr       20
       peakwidth   6 75
       mzdiff      0.05
       prefilter peaks   4
       prefilter intensity     25000
       noise       15000
       Feature detection results :
Group2_2_Neg.mzXML       [Meaney_Group2_NEG ]      -->  1689  Features.
Group2_1_Neg.mzXML       [Meaney_Group2_NEG ]      -->  1641  Features.
Group2_3_Neg.mzXML       [Meaney_Group2_NEG ]      -->  1835  Features.
Group2_4_Neg.mzXML       [Meaney_Group2_NEG ]      -->  1750  Features.
Group2_5_Neg.mzXML       [Meaney_Group2_NEG ]      -->  1887  Features.
Group2_6_Neg.mzXML       [Meaney_Group2_NEG ]      -->  1874  Features.
Group2_8_Neg.mzXML       [Meaney_Group2_NEG ]      -->  1853  Features.
Group1_3_Neg.mzXML       [Meaney_NEG_Group1]       -->  1804  Features.
Group1_1_Neg.mzXML       [Meaney_NEG_Group1]       -->  1690  Features.
Group1_2_Neg.mzXML       [Meaney_NEG_Group1]       -->  1689  Features.
Group1_4_Neg.mzXML       [Meaney_NEG_Group1]       -->  1762  Features.
Group1_6_Neg.mzXML       [Meaney_NEG_Group1]       -->  1827  Features.
Group1_8_Neg.mzXML       [Meaney_NEG_Group1]       -->  2086  Features.
Group3_1_Neg.mzXML       [Meaney_Group3_NEG]       -->  1741  Features.
Group3_3_Neg.mzXML       [Meaney_Group3_NEG]       -->  1760  Features.
Group3_4_Neg.mzXML       [Meaney_Group3_NEG]       -->  1926  Features.
Group3_6_Neg.mzXML       [Meaney_Group3_NEG]       -->  1848  Features.
Group3_7_Neg.mzXML       [Meaney_Group3_NEG]       -->  1698  Features.
Group3_5_Neg.mzXML       [Meaney_Group3_NEG]       -->  1785  Features.

3. Retention time correction
       method : obiwarp
       profStep    1
4. Grouping
       method : density
       bw    5
       mzwid       0.025
```

```
       minfrac     0.3
       minsamp     1
5. FillPeaks
6. Diffreport
       classes     Meaney_Group2_NEG
       classes     Meaney_NEG_Group1
       classes     Meaney_Group3_NEG
       statistical test        ANOVA parametric
       statistics.threshold.pvalue   0.01
       statistics.diffReport.value   into
Finished Running Statistical tests
7. Additional Plots & Statistics
      Running mummichog
      Printing heatmaps
      Printing MDS plot
      Printing static PCA and Select Scaling plot
8. Annotation (isotopes & adducts)
       featureAnnotation.CAMERA.annotate   isotopes
       featureAnnotation.CAMERA.mzabs      0.015
       featureAnnotation.CAMERA.ppm        5
       featureAnnotation.CAMERA.sigma      6
       featureAnnotation.CAMERA.perfwhm    0.6
       featureAnnotation.CAMERA.maxcharge        3
       featureAnnotation.CAMERA.maxiso     4
       featureAnnotation.CAMERA.intensity        into
9. Putative ID's (METLIN)
       identification.METLIN.ppm     5
       identification.METLIN.adducts       M-H, M+Cl
```

Positive ion mode settings:

```
-------------------------------------------------------------------------
-
XCMSOnline  version  2.0.1
XCMS        version  1.41.1
CAMERA      version  1.22.0
-------------------------------------------------------------------------
-
General parameters
       polarity    positive
       retention time format   minutes
      Parameter ID:  18672    JOBID:  10923842. Feature detection
       method : centWave
       ppm   3
       snthr       25
       peakwidth   6 75
       mzdiff      0.05
       prefilter peaks   4
       prefilter intensity     60000
       noise       50000
       Feature detection results :
Group2_1_pos.mzXML       [Susceptible_Pos]         -->  3707  Features.
Group2_4_pos.mzXML       [Susceptible_Pos]         -->  3883  Features.
Group2_2_pos.mzXML       [Susceptible_Pos]         -->  3884  Features.
Group2_3_pos.mzXML       [Susceptible_Pos]         -->  4124  Features.
Group2_5_pos.mzXML       [Susceptible_Pos]         -->  4275  Features.
Group2_6_pos.mzXML       [Susceptible_Pos]         -->  4071  Features.
Group2_8_pos.mzXML       [Susceptible_Pos]         -->  4373  Features.
Group1_2_pos.mzXML       [Control_Pos_remove8]     -->  3976  Features.
Group1_1_pos.mzXML       [Control_Pos_remove8]     -->  4765  Features.
Group1_5_pos.mzXML       [Control_Pos_remove8]     -->  3604  Features.
Group1_3_pos.mzXML       [Control_Pos_remove8]     -->  4049  Features.
Group1_4_pos.mzXML       [Control_Pos_remove8]     -->  4709  Features.
Group1_6_pos.mzXML       [Control_Pos_remove8]     -->  3747  Features.
      Group3_2_pos.mzXML       [Resilient_Pos]     -->  3628  Features.
      Group3_3_pos.mzXML       [Resilient_Pos]     -->  3470  Features.
      Group3_5_pos.mzXML       [Resilient_Pos]     -->  3800  Features.
      Group3_4_pos.mzXML       [Resilient_Pos]     -->  4146  Features.
      Group3_6_pos.mzXML       [Resilient_Pos]     -->  4167  Features.
      Group3_7_pos.mzXML       [Resilient_Pos]     -->  3385  Features.
3. Retention time correction
       method : obiwarp
       profStep    1
4. Grouping
       method : density
       bw    5
       mzwid       0.025
       minfrac     0.3
       minsamp     1
5. FillPeaks
6. Diffreport
       classes     Susceptible_Pos
```

```
       classes     Control_Pos_remove8
       classes     Resilient_Pos
       statistical test        ANOVA parametric
       statistics.threshold.pvalue   0.01
       statistics.diffReport.value   into
Finished Running Statistical tests
7. Additional Plots & Statistics
      Running mummichog
      Printing heatmaps
      Printing MDS plot
      Printing static PCA and Select Scaling plot
8. Annotation (isotopes & adducts)
       featureAnnotation.CAMERA.annotate   isotopes
       featureAnnotation.CAMERA.mzabs      0.015
       featureAnnotation.CAMERA.ppm        5
       featureAnnotation.CAMERA.sigma      6
       featureAnnotation.CAMERA.perfwhm    0.6
       featureAnnotation.CAMERA.maxcharge        3
       featureAnnotation.CAMERA.maxiso     4
       featureAnnotation.CAMERA.intensity        into
9. Putative ID's (METLIN)
       identification.METLIN.ppm     5
       identification.METLIN.adducts       M+H
```